From the Institute of Human Genetics
Theoretical Medicine and Biomedical Sciences
Faculty of Medicine
Saarland University, Homburg/Saar

A Sperm microRNA Panel for Assessing Male Subfertility and Predicting Assisted Reproductive Outcomes

Dissertation
for the degree of Doctor of Medicine (Dr. med.)
Faculty of Medicine
at
SAARLAND UNIVERSITY
2026

Submitted by:
Haidar Haidar
Date of Birth: November 2, 1988
Place of Birth: Damascus, Syria
Homburg 2026

Tag der Promotion: 10.08.2026

Dekan: Univ.-Prof. Dr. med. dent. Matthias Hannig

Berichterstatter: PD Dr. Masood Abu-Halima

Professor Dr. Martina Sester

I hereby declare in lieu of oath that I have prepared this dissertation independently and without improper assistance, that I have not used sources other than those indicated, and that all passages quoted from published or unpublished works have been indicated as such.

Homburg 19.01.2026
Haidar Haidar

Table of Contents

List of Tables

List of Figures

List of Abbreviations

Abbreviation	Expanded Name
ABP	Androgen-binding protein
AGO	Argonaute
ART	Assisted reproductive technologies
AUC	Area under the curve
AZF	Azoospermia factor
bp	Base pairs
CBAVD	Congenital bilateral absence of the vas deferens
CeRA	Center of Reproductive Medicine and Andrology
CFTR	Cystic fibrosis transmembrane conductance regulator
CRISP2	Cysteine-rich secretory protein 2
DNAH1	Dynein axonemal heavy chain 1
DPY19L2	Dpy-19 like 2
ESR1	Estrogen receptor 1
FDR	False discovery rate
FGFR1	Fibroblast growth factor receptor 1
FSH	Follicle-stimulating hormone
FSHR	Follicle-stimulating hormone receptor
GA	Germ cell arrest
GnRH	Gonadotropin-releasing hormone
HMMR	Hyaluronan mediated motility receptor
HPG axis	Hypothalamic-pituitary-gonadal axis
HSC70	Heat shock cognate 70 kDa protein
HSP90	Heat shock protein 90
HSPA1B	Heat shock protein family A member 1B
IBT	Immunobead test
ICSI	Intracytoplasmic sperm injection
IVF	In vitro fertilization
LH	Luteinising hormone
MA	Mixed atrophy
MAR	Mixed antiglobulin reaction
miRNA	MicroRNA
MMAF	Multiple morphological abnormalities of the sperm flagella
ncRNA	Non-coding RNA
NGS	Next-generation sequencing
NOA	Non-obstructive azoospermia
OAT	Oligoasthenoteratozoospermia
PABPC	Poly(A)-binding protein cytoplasmic
PCOS	Polycystic ovary syndrome
PFKFB4	6-Phosphofructo-2-kinase/fructose-2,6-bisphosphatase 4
piRNA	PIWI-interacting RNA
Pol II	RNA polymerase II
pre-miRNA	Precursor microRNA
pri-miRNA	Primary microRNA
PRM1	Protamine 1
PRM2	Protamine 2

RHOX	Reproductive homeobox genes
RISC	RNA-induced silencing complex
ROS	Reactive oxygen species
RT-qPCR	Reverse transcription quantitative polymerase chain reaction
SCO	Sertoli cell-only syndrome
snoRNA	Small nucleolar RNA
snRNA	Small nuclear RNA
SNV	Single nucleotide variant
SPATA6	Spermatogenesis associated 6
sRNA-seq	Small RNA sequencing
SYCP3	Synaptonemal complex protein 3
TEX11	Testis expressed 11
TEX15	Testis expressed 15
TNRC6	Trinucleotide repeat-containing 6
TRUS	Transrectal ultrasound
TSS	Transcription start site
TURED	Transurethral resection of the ejaculatory ducts
USP9Y	Ubiquitin specific peptidase 9 Y-linked
WES	Whole-exome sequencing
WGS	Whole-genome sequencing
WHO	World health organization

Summary

Sperm quality, which is primarily determined by morphology, motility, and concentration, is crucial to male fertility and has a significant impact on the results of assisted reproductive technologies (ART). Even while regular semen analysis is still a common clinical method, it is not always able to identify underlying molecular issues that might jeopardize fertilization or the development of the embryo. The increasing volume of research indicates that sperm-borne microRNAs (miRNAs) represent important components of spermatogenesis and sperm function, and their changed expression may provide more information than conventional metrics. The purpose of this research was to employ quantitative reverse transcription PCR (RT-qPCR) to assess the potential use of certain sperm miRNAs as biomarkers in an ART environment and to determine if they are linked to semen quality, embryo development, and pregnancy outcomes.

There were 85 male partners in this validation investigation who were part of couples receiving fertility therapy. A variety of semen quality and spermatogenic impairment were represented in the purified sperm samples, which were processed in accordance with World Health Organization (WHO) criteria. Using RT-qPCR, we measured specific miRNAs and investigated the relationship between their expression and biochemical pregnancy, live birth outcomes, hormonal indicators, semen characteristics, and embryo morphology.

Higher sperm concentration, progressive motility, and normal morphology are characteristics of higher-quality semen, which have been repeatedly linked to better embryo development. Poorer embryo grades were more prevalent as semen quality decreased, while couples with top-grade embryos (Grade 1) often had samples with exceptional sperm motility and morphology. This trend is consistent with reports that sperm characteristics affect embryo survival and fertilization competency, even in techniques like intracytoplasmic sperm injection (ICSI) that omit certain functional stages.

The findings of RT-qPCR indicated that three miRNAs, including hsa-miR-15b-5p, hsa-miR-19a-5p, and hsa-miR-20a-5p, were especially informative. Lower

sperm concentration, a larger percentage of immotile sperm, and decreased sperm motility and morphology were all substantially correlated with increased expression of these miRNAs. These miRNA levels corresponded with a number of clinical indicators: reduced expression was found in instances that led to successful clinical pregnancies and live births, while higher expression was observed in samples associated with lower β-hCG levels or worse pregnancy outcomes. The pattern of embryonic development was comparable. Sperm samples connected to G1 embryos often had lower expression levels of these miRNAs, while samples linked to G2 (Grade 2) embryos typically had greater expression levels. This implies that early development may be impacted by sperm with dysregulated miRNA expression.

With area under the curve (AUC) values ranging from 0.71 to 0.76, each miRNA demonstrated modest diagnostic accuracy for IVF outcomes when evaluated for predictive significance. An AUC of 0.75 was obtained by a combined model that included all three miRNAs, suggesting that they may together provide significant insights into the probability of treatment effectiveness. All things considered, our results support the concept that sperm miRNAs may identify aspects of sperm activity that are not discernible from traditional semen analysis alone. The three discovered miRNAs (hsa-miR-15b-5p, hsa-miR-19a-5p, and hsa-miR-20a-5p) clearly correlate with embryo development and pregnancy outcomes and appeared to represent underlying spermatogenic or functional abnormalities. Therefore, measuring them might be useful for determining male fertility or planning ART therapy.

This research concludes that some sperm miRNAs detected by RT-qPCR might be helpful indicators of the quality of semen and its potential for reproduction. Higher levels of hsa-miR-15b-5p, hsa-miR-19a-5p, and hsa-miR-20a-5p were associated with lower embryo quality, poorer semen parameters, and a lower likelihood of pregnancy and live birth. MiRNA analysis may enhance the capacity to detect mild male-factor infertility and improve ART prognosis when included in current diagnostic processes

Zusammenfassung

Die Qualität der Spermien, insbesondere hinsichtlich Konzentration, Motilität und Morphologie, spielt eine entscheidende Rolle für die männliche Fertilität und beeinflusst maßgeblich den Erfolg assistierter Reproduktionstechniken (ART). Die routinemäßige Samenanalyse liefert zwar grundlegende diagnostische Informationen, erfasst jedoch nicht immer molekulare Störungen, die die Befruchtung oder die frühe Embryonalentwicklung beeinträchtigen können. In den letzten Jahren hat sich gezeigt, dass spermiengetragene Mikro-RNAs (miRNAs) wichtige Hinweise auf den Zustand der Spermatogenese und die Funktionalität der Spermien geben können. Veränderungen ihrer Expression könnten zusätzliche Informationen über die männliche Fertilität liefern, die über klassische Samenparameter hinausgehen. Ziel dieser Arbeit war es daher, zu untersuchen, ob bestimmte miRNAs in Spermien mit Samenqualität, Embryonalentwicklung und Schwangerschaftsverlauf assoziiert sind, und zu prüfen, ob sie sich als Biomarker im ART-Kontext eignen. Die Analyse erfolgte mittels quantitativer RT-PCR (RT-qPCR).

In die Validierungsstudie wurden 85 männliche Partner von Paaren eingeschlossen, die sich einer Fruchtbarkeitsbehandlung unterzogen. Die Spermien wurden gemäß WHO-Richtlinien aufgereinigt und deckten ein breites Spektrum an Samenqualitäten ab. Anschließend wurde die Expression ausgewählter miRNAs mittels RT-qPCR bestimmt und in Beziehung zu Samenparametern, Hormonprofilen, Embryoqualität, biochemischer Schwangerschaft und Lebendgeburten gesetzt.

Wie erwartet zeigte sich, dass eine höhere Samenqualität – insbesondere höhere Konzentration, bessere progressive Motilität und ein größerer Anteil normal geformter Spermien – eng mit einer besseren Embryoqualität verknüpft war. Top-Embryonen (G1) stammten überwiegend aus Proben mit höherer Motilität und Morphologie, während schwächer entwickelte Embryonen häufiger mit eingeschränkten Samenparametern verbunden waren. Diese Beobachtungen decken sich mit bekannten Zusammenhängen zwischen Spermieneigenschaften und Befruchtungs- bzw. Entwicklungsfähigkeit, selbst bei Verfahren wie

Intracytoplasmatischen Spermieninjektion (ICSI), die einige funktionelle Hürden umgehen.

Die RT-qPCR-Analysen zeigten, dass drei miRNAs – hsa-miR-15b-5p, hsa-miR-19a-5p und hsa-miR-20a-5p – besonders aussagekräftig waren. Eine erhöhte Expression dieser miRNAs war deutlich mit reduzierter Motilität, schlechterer Morphologie, niedrigeren Spermienkonzentrationen und einem höheren Anteil unbeweglicher Spermien verbunden. Darüber hinaus spiegelten sich diese miRNA-Profile auch in klinischen Markern wider: hohe miRNA-Werte traten vermehrt bei Proben auf, die zu erniedrigten β-hCG-Werten oder ausbleibenden Schwangerschaften führten, während niedrige Expressionswerte bei erfolgreichen Behandlungen und Lebendgeburten vorkamen.

Auch die Embryoentwicklung zeigte klare Zusammenhänge. Spermienproben, die zur Entstehung von G1-Embryonen führten, wiesen in der Regel niedrigere Expressionsniveaus der drei miRNAs auf. Höhere Werte hingegen fanden sich häufiger bei Proben, die zu G2-Embryonen führten. Diese Ergebnisse deuten darauf hin, dass Fehlregulationen dieser miRNAs bereits frühe Entwicklungsprozesse beeinflussen könnten.

Bei der Bewertung ihres diagnostischen Potenzials zeigten die drei miRNAs jeweils eine moderate Vorhersagekraft für IVF-Ergebnisse, mit AUC-Werten zwischen 0,71 und 0,76. Ein kombiniertes Modell erreichte eine AUC von 0,75 und erwies sich damit als vielversprechend für eine mögliche klinische Anwendung.

Zusammengefasst sprechen die Ergebnisse dafür, dass spermiengetragene miRNAs wertvolle zusätzliche Informationen über die männliche Fruchtbarkeit liefern können, die in der klassischen Samenanalyse nicht sichtbar werden. Die identifizierten miRNAs – insbesondere hsa-miR-15b-5p, hsa-miR-19a-5p und hsa-miR-20a-5p scheinen Ausdruck zugrunde liegender funktioneller Einschränkungen zu sein und stehen in engem Zusammenhang mit Embryoqualität, Schwangerschaftsraten und Lebendgeburten. Eine Ergänzung der bestehenden Diagnostik durch die Analyse solcher miRNAs könnte helfen, subtile Störungen der

Spermatogenese früher zu erkennen und die Prognose bei ART-Behandlungen präziser einzuschätzen.

Insgesamt zeigt diese Arbeit, dass die Bestimmung ausgewählter miRNAs mittels RT-qPCR ein nützliches Werkzeug zur Bewertung der männlichen Fertilität darstellt. Erhöhte Spiegel der drei untersuchten miRNAs waren mit schlechteren Samenparametern, ungünstiger Embryoentwicklung und niedrigeren Erfolgsraten verbunden. Niedrigere Expression hingegen ging mit besseren reproduktiven Ergebnissen einher. Eine Integration miRNA-basierter Marker in die klinische Routine könnte dazu beitragen, Diagnostik und Behandlungsplanung bei Paaren mit unerfülltem Kinderwunsch weiter zu verbessern.

1. Introduction

1.1 Overview of Infertility

The World Health Organization (WHO) defines infertility as a couple's failure to conceive following a year of consistent, unprotected sexual activity [1]. This condition is a serious public health issue that impacts people's physical and mental well-being as well as couples' capacity to plan a family [1]. About 10-15% of couples worldwide experience infertility throughout their reproductive years, underscoring the need for early diagnosis and treatment [1-3]. Both male and female factors contribute to the complex etiology of infertility. Hormonal imbalance, genetic abnormalities, or lifestyle-related factors may cause infertility in both sexes. Common reasons in males include urogenital abnormalities, genital tract infections, and varicocele, which may be acquired or congenital [2,4]. Male infertility is diagnosed as idiopathic or unexplained in around 50% of instances, when the underlying reason is still unknown [5].

Endocrine diseases, age-related physiological reduction in fertility, or structural defects of the reproductive system are often linked to female infertility [6]. Depending on the person, fertility starts to fall after age 30 and more sharply around age 35. Uterine fibroids, endometriosis, polycystic ovarian syndrome (PCOS), and premature ovarian insufficiency are common reasons [6,7]. Men's and women's fertility is also greatly impacted by environmental contaminants, long-term stress, and poor lifestyle decisions, including cigarette smoking, poor diets, and physical inactivity [7].

A number of variables, including delayed family planning, greater exposure to environmental contaminants, elevated stress levels, and changes in lifestyle, are responsible for the growing incidence of infertility worldwide. Primary infertility, or the inability to conceive a first child, affects around one in eight couples, but secondary infertility, or the inability to conceive after a previous successful pregnancy, affects one in four [6,7].

A thorough assessment of both couples is necessary for an accurate diagnosis of infertility. Semen analysis, hormone profiling, and reproductive tract imaging are

among the diagnostic techniques used on men [2,3]. Ovulatory cycle monitoring, hormone level evaluations, and ultrasound imaging are frequently used diagnostic techniques in women [7]. Due to a broad spectrum of reasons for infertility, diagnostic workups are often complex and personalized. Depending on the exact reason, treatment options might include hormone therapy, lifestyle changes, surgery, and assisted reproductive technologies (ART), such as intrauterine insemination (IUI) or in vitro fertilization (IVF) [7].

Significant emotional and psychological stresses are also imposed by infertility. During the diagnosis and therapy phases, affected people often report feeling stressed, anxious, and depressed. Therefore, psychological assistance like counselling, peer support groups, and stress-reduction techniques should be included in comprehensive fertility treatment [7]. Research on the genetic, environmental, and molecular causes of infertility is still ongoing with the objective of improving treatment outcomes and diagnostic accuracy. When it comes to treating idiopathic infertility and finding biomarkers or genetic abnormalities, this kind of study has become essential.

1.2 Male Infertility

A complicated illness known as male infertility prevents a man from becoming pregnant with a female partner, even after engaging in frequent, unprotected sexual activity for at least a year. Genetic anomalies, illnesses, exposures to the environment, and lifestyle choices are some of the causes of this disorder [1]. Male infertility is mostly caused by genetic problems. Klinefelter syndrome (47,XXY karyotype), in which males with the condition have an extra X chromosome, is a well-known condition. These people often have gynecomastia (enlarged breast tissue), azoospermia (a lack of sperm in semen), and low testosterone levels, all of which seriously impair fertility [8]. Furthermore, androgen signaling may be disrupted by abnormalities in the AR (androgen receptor) gene, which would hinder normal sperm production [9].

Fertility is influenced by environmental and lifestyle variables in addition to genetics. Reduced sperm count, poor motility, and aberrant morphology have been

associated with excessive alcohol consumption, tobacco use, and heavy caffeine intake [10]. Sperm parameters are also adversely affected by recreational drug use, such as marijuana, anabolic steroids, and long-term use of several pharmaceuticals [11]. In addition, exposure to pesticides, chemicals, and radiation is related to decreased fertility [11]. The hypothalamic-pituitary-gonadal axis may be disrupted by psychological stress, which lowers testosterone levels and hinders spermatogenesis [12]. Furthermore, sperm DNA and cellular structures may be harmed by oxidative stress, which is an imbalance between reactive oxygen species (ROS) and the body's antioxidant defenses. This issue leads to decreased sperm function and viability [13].

Male infertility is caused by a number of illnesses that interfere with sperm transport or production. These include varicocele (enlarged scrotal veins), cryptorchidism (undescended testes), orchitis (testicular inflammation), or prostatitis (inflammation of the prostate), and cystic fibrosis [14,15]. The sperm's capacity to reach and fertilize the egg is also hindered by sperm transport abnormalities, which may be caused by congenital problems or structural blockages. Usually, there are two types of male infertility: primary and secondary. Men who have never led to pregnancy of their partners are considered to be in the primary infertile group, whereas those who have fathered children in the past but subsequently have infertility issues are considered to be in the secondary infertile group. Changes in lifestyle or health condition over time are often associated with secondary infertility [16].

About 40% of male infertility cases are caused by sperm production problems, making them the most common cause. These conditions include teratozoospermia (abnormal sperm morphology), oligospermia (low sperm concentration), and azoospermia [1,2]. Furthermore, sperm transport dysfunctions, which prevent sperm from reaching the ejaculate because of obstructions or anatomical abnormalities, occur in about 20% of instances [1,2]. Male infertility is diagnosed after a thorough clinical and laboratory assessment. Semen analysis, which evaluates sperm count, motility, and morphology, is the main method. Scrotal ultrasonography and hormonal tests (e.g., FSH, LH, and testosterone) are often utilized to identify underlying endocrine or anatomical problems. Genetic testing may be necessary in certain

circumstances, especially if disorders like cystic fibrosis or Klinefelter syndrome are suspected [12,16].

Surgical procedures like varicocele repair or testicular sperm extraction (TESE), hormone therapy for endocrine disorders, and assisted reproductive technologies (ART) like intracytoplasmic sperm injection (ICSI) in cases of severe sperm dysfunction are all possible treatments, depending on the specific etiology. To maximize reproductive health, lifestyle changes, including eliminating smoking, alcohol moderation, controlling weight, and reducing stress, are also advised. Additionally, antioxidant supplements—like those containing vitamins C and E—are frequently prescribed to reduce oxidative stress and enhance sperm quality [17].

1.3 Etiology of Male Infertility

Male infertility has an array of complicated reasons, including both acquired disorders and congenital defects. Anatomical deformities, endocrine dysfunctions, genetic abnormalities, and environmental exposures are major contributory factors (18). Idiopathic male infertility is the term used to describe the 60–70% of male infertility cases that cannot be explained despite significant advancements in diagnostics [18,19]. Although the exact processes are yet unknown, it is thought that a combination of environmental variables and genetic predisposition impairs reproductive function in these individuals.

Despite extensive clinical and laboratory testing, idiopathic male infertility indicates the lack of a discernible etiology. Recent research indicates that environmental stressors and mutations in fertility-related genes may impair spermatogenesis or testicular function in subtle, cumulative ways not yet detected by conventional diagnostics [19,20]. Approximately 4% of male infertility diagnoses are caused by known genetic factors such as Y chromosome microdeletions and Klinefelter syndrome (47,XXY karyotype) [21]. An extra X chromosome causes hypogonadism, low testosterone, and poor spermatogenesis in Klinefelter syndrome. Similarly, azoospermia or severe oligospermia are linked to microdeletions in the Y chromosome's azoospermia factor (AZF) regions because they disrupt genes essential for sperm production [21,22]. Due to the complexity of

gene–environment interactions, phenotypic heterogeneity, and a lack of adequate validation, regular clinical testing for the majority of the more than 100 genes linked to male infertility is still limited [23]. In reproductive genetics research, the creation of molecular markers for prompt and precise diagnosis remains the primary objective. Anomalies in sperm production, which may be roughly divided into quantitative and qualitative problems, are often linked to male infertility [24]. Understanding a specific kind of sperm abnormalities is essential for directing subsequent diagnostic procedures and selecting the best course of therapy.

1.3.1 Disorders Involving Sperm Function

Establishing the standard reference values for semen parameters is a prerequisite to comprehending the illnesses that may result from decreased sperm function. These values are outlined in the most recent version of the *Laboratory Manual for the Examination of Human Semen* published by the WHO [1], as shown in **Table 1**. When evaluating male reproductive potential, these criteria are essential, and deviations from them might be a sign of dysfunction.

Table 1. Comparative Overview of Semen Analysis Parameters

Parameter	Reference Value
Semen Volume	≥ 1.4 mL
pH	≥ 7.2
Sperm Concentration	≥ 16 million spermatozoa/mL
Total Sperm Number	≥ 39 million spermatozoa/ejaculate
Total Motility	≥ 42% motile spermatozoa
Progressive Motility	≥ 30% spermatozoa with forward progression
Sperm Morphology	≥ 4% normal forms
Sperm Vitality	≥ 54% live spermatozoa
Leukocyte Count	< 1 million/mL
Antisperm Antibodies (MAR/IBT)	< 50% spermatozoa with bound particles

— Abbreviations: MAR: Mixed Antiglobulin Reaction, IBT: Immunobead Test
— WHO Reference Standards (2021)

Once reference values for normal semen have been established, sperm function abnormalities that may lead to male infertility may be categorized. Clinicians can recognize and categorize functional sperm abnormalities that might lead to male infertility using these reference values.

These disorders include:

- **Aspermia**: Complete absence of ejaculate.
- **Azoospermia**: Complete absence of sperm in the ejaculate.
- **Oligozoospermia**: Sperm concentration below 16 million/mL.
- **Asthenozoospermia**: Reduced progressive motility, compromising the sperm's ability to reach and fertilize the oocyte.
- **Teratozoospermia**: Fewer than 4% of sperm exhibit normal morphology based on strict criteria.
- **Necrozoospermia**: A high proportion of non-viable or dead sperm cells.

It is noteworthy that mixed types of these diseases are often observed, especially in subfertile men. The examples involve:

- **Oligoasthenozoospermia** (low count and low motility),
- **Oligoasthenoteratozoospermia (OAT)**, a condition involving low sperm concentration, poor motility, and abnormal morphology.

A consistent and evidence-based method of diagnosing male infertility is made possible by the use of WHO-based semen reference standards. It facilitates clinical decision-making on further diagnostic tests and therapy planning, and it permits the classification of sperm abnormalities.

1.3.1.1 Sperm Morphology

A smooth, oval-shaped head that is around 5–6 µm long and 2.5–3.5 µm wide, with an acrosome covering 40–70% of the head surface, is the characteristic of a morphologically normal human spermatozoon. Slender and in line with the head, the midpiece is filled with mitochondria that drive motility. Usually consistent and uncoiled, the tail is around 10 times the length of the head and is in charge of the progressive movement [1,26]. As demonstrated in **Figure 1**, teratozoospermia, or deviations from normal morphology, may appear as anomalies in the head (e.g., amorphous, tapered, globozoospermia, macrocephaly), midpiece (e.g., bent, asymmetrical), or tail (e.g., coiled, multiple, short). These abnormalities, which include decreased motility, acrosome malfunction, poor chromatin packing, and

even higher rates of DNA fragmentation and aneuploidy, are linked to altered sperm function [26].

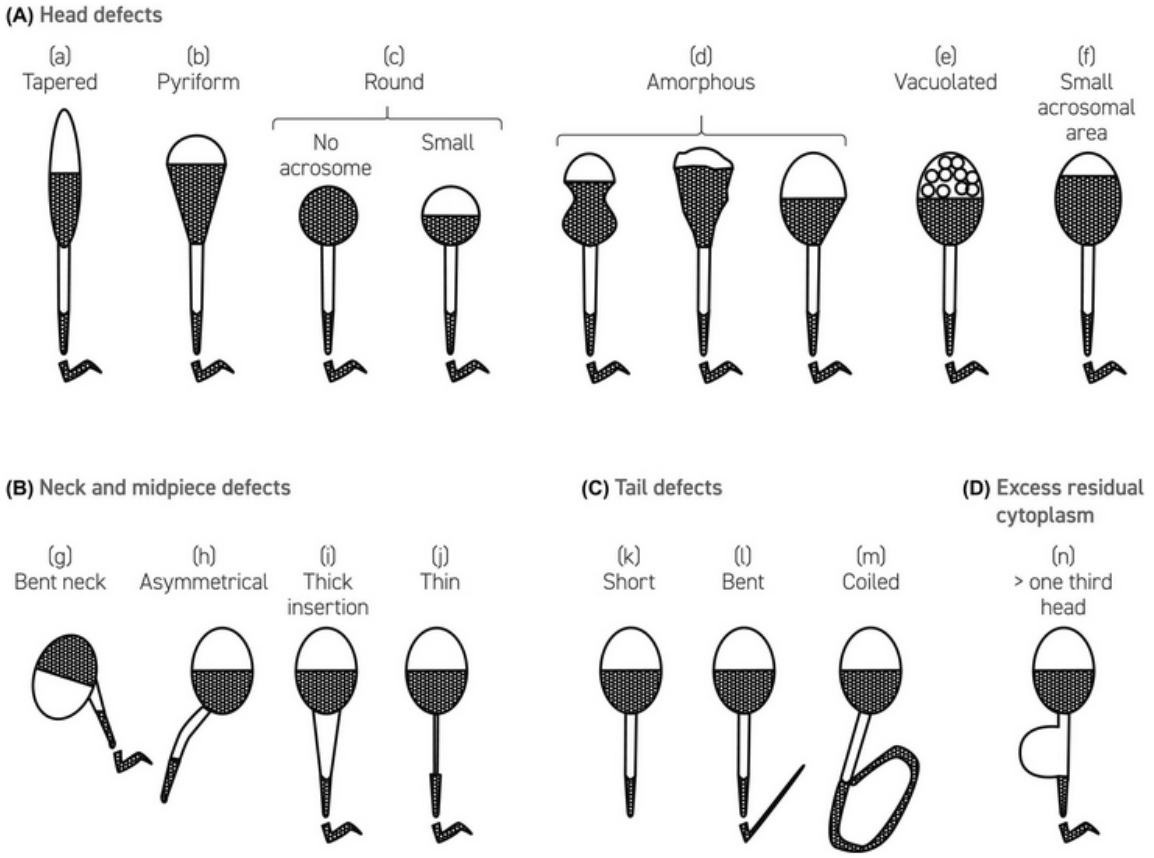

Figure 1. Illustrations of Abnormal Sperm Morphology Based on the WHO 6th Edition Criteria. Adapted from WHO Laboratory Manual for the Examination and Processing of Human Semen, 6th ed. Geneva: World Health Organization; 2021 [1].

Men who had less than 9% normal sperm forms (based on precise evaluation standards) were much more likely to have fertility issues, whereas those with levels over 12% were generally considered fertile, according to a major multicenter research including over 1,400 participants. Notably, morphology outperformed both sperm concentration and motility as diagnostic markers for identifying infertile men, outperforming all other conventional semen measures [27]. Given that morphological abnormalities may arise from genetic mutations, this issue emphasizes the significance of sperm morphology as a diagnostic marker as well as a possible signal of underlying spermatogenic or genetic problems.

1.3.1.2 Sperm Motility

Another important factor influencing male fertility is sperm motility, which measures the sperm's capacity to actively travel through the female reproductive system in order to reach and fertilize the oocyte. Forward, linear motion is referred to as progressive motility [1]. The flagellum, a highly specialized structure made up of microtubules organized in an axonemal pattern and driven by dynein arms that produce sliding forces, is mostly responsible for spermatozoa's motility [28]. The integrity of several structural and regulatory proteins is essential for proper flagellar activity. Reduced motility and male infertility have been associated with mutations in genes including *DNAH1*, which is important in axonemal structure, and *CATSPER*, which encodes calcium ion channels necessary for hyperactivation [29,30]. Additionally, low motility and poor fertilization outcomes are linked to morphological abnormalities of the midpiece or tail, including those observed in Multiple Morphological Abnormalities of the Sperm Flagella (MMAF) [26].

Asthenozoospermia is frequently observed in clinical practice and might result from environmental exposures, oxidative stress, infections, or genetic abnormalities [31]. Assessing sperm motility offers information regarding the molecular integrity and functional potential of the sperm cell, in addition to being a fundamental diagnostic metric in fertility evaluation.

1.3.2 Disorders Caused by Obstruction of the Ejaculatory Ducts

Male infertility is known to be significantly influenced by obstruction of the ejaculatory ducts, which may develop later in life or result from congenital defects [32]. This obstruction often causes anomalies in semen analysis, including oligospermia or azoospermia, and a noticeably decreased amount of semen. Additional observations include a lower seminal pH and the lack of fructose in the seminal fluid, both of which are linked to diminished fertility [32]. Obstruction may still impair fertility even if sperm production in the testes usually stays unaffected [33]. Infections of the ejaculatory ducts, vas deferens, or epididymis may also cause obstruction. Furthermore, surgical procedures like transurethral resection of the ejaculatory ducts (TURED) or congenital anomalies have been demonstrated to be contributory causes [33]. When hormonal assessments and

physical tests are normal, but semen analysis indicates anomalies, ejaculatory duct blockage should be evaluated as a probable cause of male infertility. A blockage of the ejaculatory duct is responsible for up to 5% of male infertility cases [34] and about 40% of cases with azoospermia [35].

Ejaculatory duct obstruction may be detected using a variety of diagnostic techniques. When obstruction is suspected, transrectal ultrasonography is regarded as the first diagnostic technique [36]. Vas deferens aspiration is one of the safe and efficient radiographic methods for verifying obstruction [37]. Following confirmation of the diagnosis, sperm may be directly used in assisted reproductive technologies like IVF and ICSI with the use of microsurgical sperm harvesting procedures [38].

1.3.3 Disorders Related to Spermatogenic Failure

Approximately 60% of instances of azoospermia are non-obstructive azoospermia (NOA), which may result from either intrinsic testicular malfunction or abnormal hormone control [35]. About 10% of male infertility instances are caused by primary testicular failure [39], which is defined by inherent abnormalities in the testes that hinder the generation of sperm. Elevated levels of follicle-stimulating hormone (FSH) and luteinizing hormone (LH) are usually detected. Another common cause of secondary testicular failure is congenital hypogonadotropic hypogonadism, which is characterized by small, undeveloped testes due to insufficient hypothalamic-pituitary axis activation [35]. The site of malfunction is usually used to categorize the etiology of NOA. Hormonal inadequacies that prevent testicular stimulation in spite of healthy testes are known as pre-testicular causes (secondary hypogonadism), and they are often brought on by anomalies in the pituitary or brain. On the other hand, intrinsic injury to the testes produces testicular causes (primary hypogonadism), which directly affects spermatogenesis [40]. A diagnostic protocol for assessing azoospermia is illustrated in **Figure 2**, emphasizing the procedures required to differentiate between obstructive and non-obstructive causes and directing future therapeutic care.

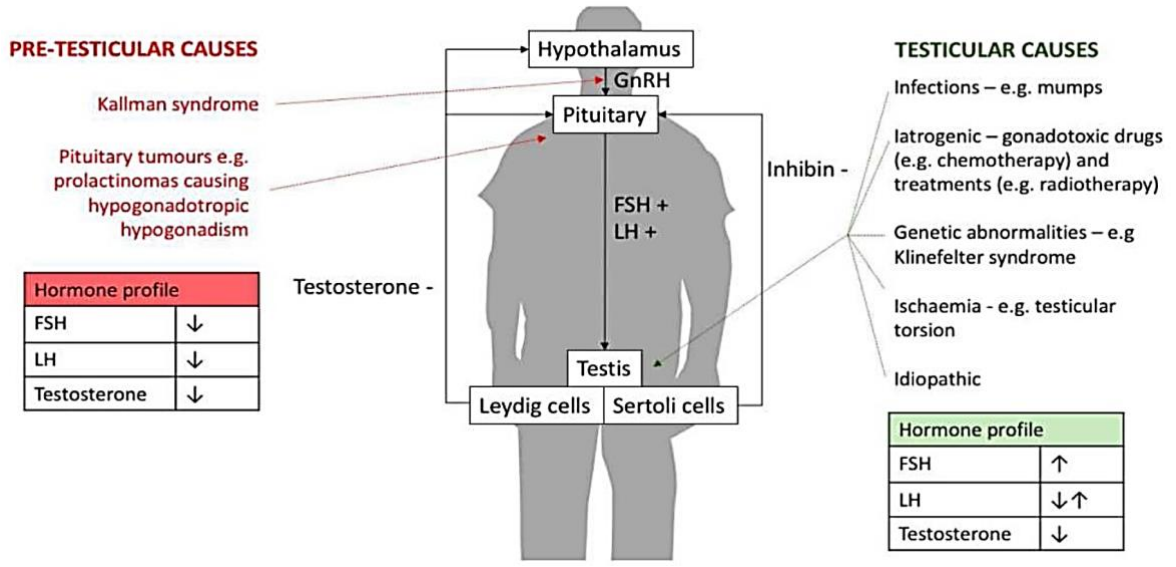

Figure 2. Etiological Factors and Hormonal Profiles in Non-Obstructive Azoospermia.
Adapted from Tharakan et al. [40]. Abbreviations: FSH – follicle-stimulating hormone; GnRH – gonadotropin-releasing hormone; LH – luteinising hormone.

Hypospermatogenesis, maturation arrest, or the presence of solely Sertoli cells in the seminiferous tubules are examples of pathological abnormalities [41-43]. Additionally, developmental anomalies, undescended testes (cryptorchidism), prominent varicoceles, and previous therapies like chemotherapy or radiation may cause NOA [35]. Men who appear with azoospermia need to be evaluated thoroughly, which includes a full assessment of their reproductive and general medical histories in addition to a rigorous physical examination. Prior surgical treatments, underlying medical problems, testicular volume and consistency, and the existence of varicoceles should all receive special consideration.

It is important to exclude other treatable disorders, including hormonal imbalances and anatomical obstacles, in order to make a diagnosis of NOA. Therefore, hormonal profiling is essential for identifying whether testicular dysfunction is attributable to a systemic condition or the result of an intrinsic testicular issue. Furthermore, the existence of complicated abnormalities like OAT syndrome or disorders like *necrospermia* (the presence of dead or immotile sperm) or *aspermia* may indicate defective spermatogenesis. However, as **Figure 3** illustrates, a significant percentage of patients continue to be idiopathic after thorough clinical assessment. According to clinical research, up to 72% of patients may eventually be categorized as idiopathic [25]. Genetic testing is advised to find

possible underlying genetic reasons for infertility when idiopathic hypergonadotropic hypogonadism is found **(Figure 3)** [21,44].

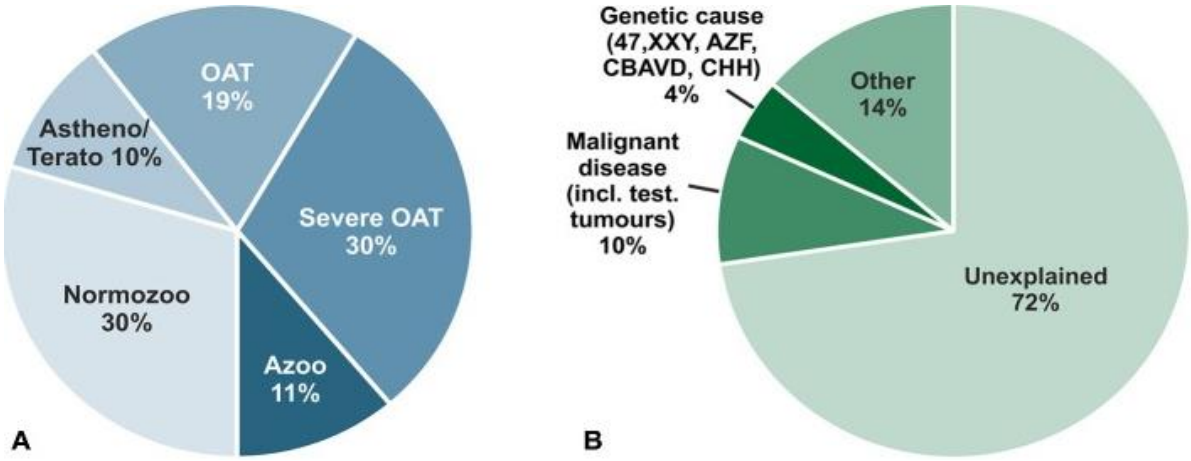

Figure 3. Diagnostic Distribution of Male Infertility Cases.
Data from 26,091 men in infertile couples attending the Center of Reproductive Medicine and Andrology (CeRA), Münster, over a 30-year period. (A) Descriptive diagnoses based on semen analysis. (B) Corresponding clinical diagnoses. Adapted from Tüttelmann et al. [21].

1.3.4 Disorders Due to Genetic Abnormalities

Male infertility has been determined to be mostly caused by genetics, especially in males who have severe spermatogenic failure, such as NOA or severe oligozoospermia [29]. Infertility is caused by a variety of environmental and endocrine factors, but chromosomal and monogenic genetic abnormalities are essential because they interfere with important phases of spermatogenesis, including meiosis, the production of sperm heads and tails, acrosome development, and chromatin condensation [29,45].

1.3.4.1 Chromosomal Abnormalities

As shown in **Figure 3**, chromosomal abnormalities are one of the most well-known genetic reasons for male infertility [21]. These include structural rearrangements like Y chromosome microdeletions, particularly in the AZFa, AZFb, and AZFc areas, as well as numerical anomalies like Klinefelter syndrome (47,XXY). Men with azoospermia typically have these deletions, which are linked to the loss of key genes required for spermatogenesis and usually result in total testicular failure [21,22,46,47]. Congenital bilateral absence of the vas deferens (CBAVD), which is often

brought on by abnormalities in the *CFTR* gene, is another important chromosomal disorder. This disorder, which is an instance of obstructive azoospermia, may manifest as a moderate indication of cystic fibrosis or occur independently [48].

1.3.4.2 Monogenic Causes of Male Infertility

Mutations in a single gene necessary for spermatogenesis or sperm function result in monogenic types of male infertility. These deficiencies are especially important for males who have isolated, severe, and specific sperm abnormalities. As described by Oud et al. (2019) [49], pre-testicular, testicular, and post-testicular origins may be used to broadly classify male infertility reasons, many of which have underlying genetic components.

1.3.4.2.1 Pre-testicular Causes

The hypothalamic-pituitary-gonadal axis is hindered by pre-testicular genetic abnormalities. The control of hormones is disrupted by mutations in genes including *FGFR1*, *NR5A1*, and *GNRH1*. A nuclear receptor involved in steroidogenesis and gonadal development is encoded by *NR5A1* (also called *SF-1*); mutations in this gene have been connected to hypospermatogenesis and combined gonadal dysfunction [50,51]. Additionally, *CYP21A2* or *CYP11B1* mutations may cause adrenal insufficiency linked to infertility.

1.3.4.2.2 Testicular Causes

Depending on the stage of spermatogenesis they impact, testicular genetic causes may be categorized. Meiotic recombination and synapsis depend on genes like *TEX11*, which is found on the X chromosome. Meiotic arrest and NOA may be brought on by *TEX11* loss-of-function mutations [52,53]. Similarly, idiopathic infertility has been related to mutations in the X-linked *RHOX* gene cluster, which codes for transcription factors important in germ cell development [54,55].

The genes linked to spermiogenesis, and sperm function include:

- ***AURKC***: Macrozoospermia, which is caused by mutations, is characterized by sperm that are unusually large-headed, have multiple flagella, and have abnormal chromatin condensation [56].

- ***DPY19L2***: Fertilization is hindered by globozoospermia, a condition in which round-headed sperm lack acrosomes [57].
- ***DNAH1* and other *DNAH* family genes:** These encode elements of the flagellar axoneme of sperm. Mutations result in MMAF and significantly decreased motility [58].
- ***CATSPER* gene family**: These encode calcium ion channels unique to sperm that are necessary for motility. Failure to fertilize and asthenozoospermia are linked to mutations [59].

1.3.4.3 Genetic Complexity and Future Directions

At least 78 genes have been conclusively connected to 92 different male infertility characteristics, according to Oud et al. (2019) [49]. These mutations demonstrate a variety of inheritance patterns, such as X-linked, Y-linked, autosomal dominant, and autosomal recessive. Some monogenic diseases are linked to syndromic presentations affecting the reproductive or endocrine systems, whereas many others result in syndromic abnormalities of the sperm.

Even while our knowledge of these genetic contributions is expanding, only a small percentage of genes have become relevant for clinical diagnosis. Although many potential genes have been identified, the majority are not validated for regular testing. The potential of whole-exome sequencing (WES) and whole-genome sequencing (WGS) to enhance diagnosis, genetic counseling, and individualized therapy is becoming more apparent as these technologies are incorporated into clinical processes.

1.4 Diagnostic Evaluation of Male Infertility

Semen analysis, which assesses sperm parameters using the WHO reference values, is often the first step in the diagnosis of male infertility [1]. A viable semen sample should have a volume of at least 1.4 mL, a sperm concentration of 16 million/mL, and a total sperm count of more than 39 million, under the most recent WHO recommendations. Furthermore, at least 4% of sperm should have normal morphology, 58% should be viable, progressive motility should reach 32%, and overall motility should surpass 40% [1,60].

Additional diagnostic techniques are used to identify underlying reasons when semen values fall below certain criteria. Assessing endocrine function is aided by a hormonal profile, which includes tests of FSH, LH, and testosterone. Spermatogenesis and sperm maturation may be impacted by abnormal hormone levels, which might indicate dysfunctions in the hypothalamic-pituitary-gonadal axis. Another useful method for identifying anatomical anomalies, such as varicocele, testicular masses, or epididymal obstruction, is scrotal ultrasonography. Genetic testing may be necessary in certain circumstances to detect chromosomal abnormalities, such as Y chromosome microdeletions and Klinefelter syndrome [1,24]. In order to improve diagnosis accuracy, advanced diagnostic techniques are being used more often in clinical evaluations, particularly in instances of infertility that cannot be explained. Reduced fertilization potential and embryo development are linked to sperm DNA fragmentation testing, which evaluates the integrity of the genetic material inside sperm cells. Furthermore, because of their involvement in sperm DNA damage and compromised function, indicators of oxidative stress, which indicate an imbalance between ROS and antioxidant defenses, are often assessed [61].

Genetic and molecular testing may identify underlying abnormalities when routine tests are not conclusive. For instance, studies demonstrate that integrating genetic testing with conventional diagnostic methods greatly increases the diagnosis rates of complicated infertility patients [25]. New diagnostic techniques concentrate on finding molecular indicators such as mRNA and miRNA expression patterns, epigenetic modifications, and mutations in spermatogenesis-related genes like *SYCP3* and *TEX11* [23,62,63]. It is expected that these developments would improve the accuracy of diagnoses and enable tailored treatment plans for infertile males, thereby boosting the effectiveness of ART.

1.5 Human Spermatogenesis

To determine the root causes of male infertility and differentiate between its various manifestations and contributing variables, a comprehensive grasp of spermatogenesis is necessary. As observed in **Figure 4**, human spermatogenesis is a multistage, extremely complicated process that takes place within the

seminiferous tubules of the testes. Primordial germ cells travel into the developing testes throughout embryonic development, where they develop into spermatogonia, which are immature germ cells. These cells remain inactive until puberty after settling inside two to three layers of the seminiferous tubule lining [64]. Spermatogonia start to divide by mitotic division at adolescence and gradually go through a number of distinct developmental phases before becoming sperm [64]. There are three main stages in the development of mature, haploid spermatozoa from diploid spermatogonial stem cells: spermatogonial proliferation, meiosis, and spermiogenesis [65,66]. Three fundamental phases include the generation of male gametes: meiosis, which involves genetic recombination and chromosomal reduction; mitosis, which involves the multiplication and differentiation of spermatogonia; and spermiogenesis, which involves the morphological change of sperm cells into functional sperm cells [64].

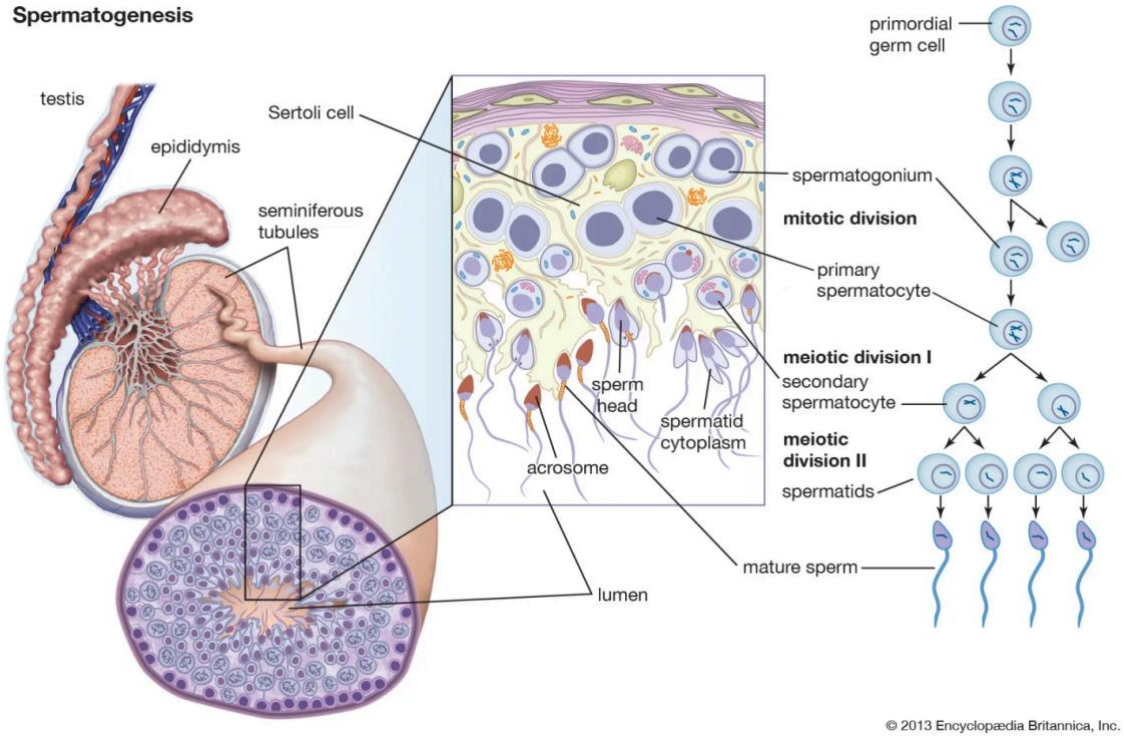

Figure 4. Schematic Representation of the Male Reproductive Tract and Spermatogenesis. Adapted from Encyclopaedia Britannica (© 2013 Encyclopaedia Britannica, Inc.), https://www.britannica.com [67].

Undifferentiated diploid spermatogonia, which are found along the basement membrane of the seminiferous epithelium, are the first stage of spermatogenesis. In order to maintain a stem cell pool and produce progenitor cells that will undergo meiosis, these cells divide mitotically [68]. The complete process of spermatogenesis takes around 74 days, and then the spermatozoa must travel via the epididymis for another 12 days before entering the ejaculate [69]. Previous research calculated this time to be 64 ± 8 days [70]; however, more recent histological models offer a twelve-stage acrosome-based categorization for human spermatogenesis, which improves alignment with model organisms and supports the updated schedule [71].

As demonstrated in **Figure 5**, the hypothalamic-pituitary-gonadal (HPG) axis tightly regulates endocrine regulation, which is essential to spermatogenesis. Gonadotropin-releasing hormone (GnRH), which is secreted by the hypothalamus, causes the anterior pituitary to produce LH and FSH [64,72]. FSH promotes Sertoli cells to improve their supporting roles, whereas LH stimulates Leydig cells to produce testosterone, which is necessary for the development of male germ cells [64,72]. To concentrate testosterone locally and preserve the blood-testis barrier, Sertoli cells produce androgen-binding protein (ABP). When testosterone is coupled to ABP, it exerts paracrine impacts on germ cells that facilitate maturation. Furthermore, Sertoli cells produce inhibin B, which contributes to hormonal control by providing negative feedback on FSH release [64,72].

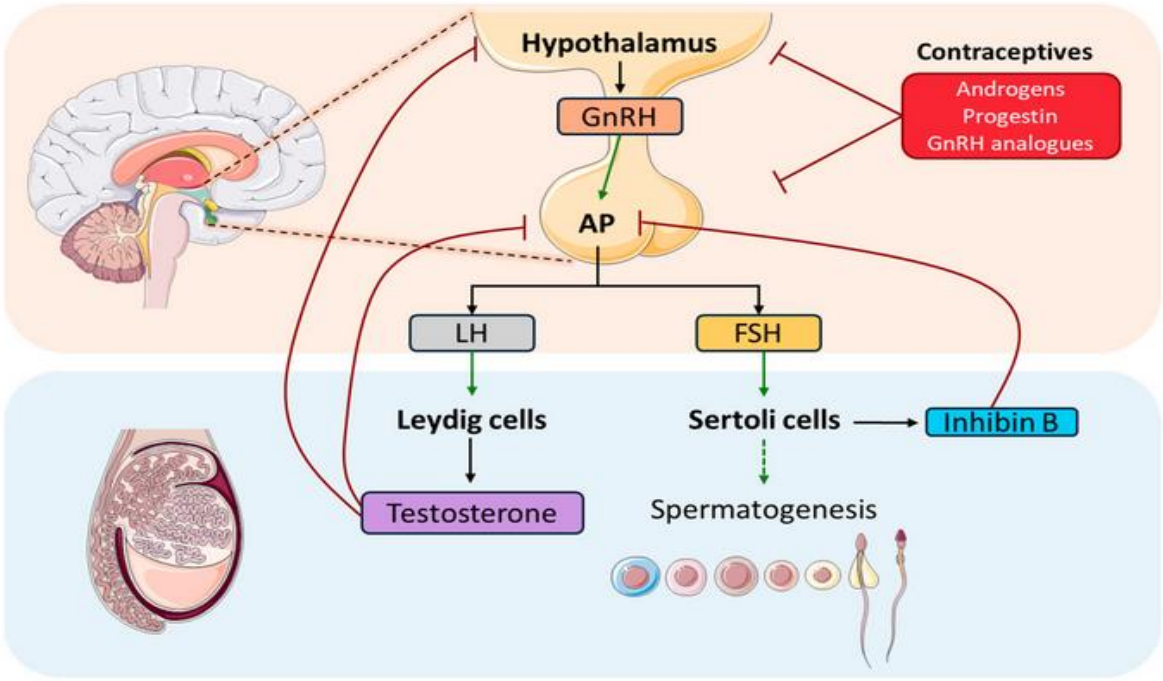

Figure 5. Endocrine Regulation of the Male Reproductive System.
Adapted from Servier Medical Art (https://smart.servier.com), licensed under CC BY 4.0 (https://creativecommons.org/licenses/by/4.0/) [73]. Abbreviations: FSH – follicle-stimulating hormone; GnRH – gonadotropin-releasing hormone; LH – luteinising hormone.

1.6 Spermatozoal RNAs

The primary purpose of spermatogenesis, which produces sperm, is to pass the paternal genetic material to the ovum. Although this seems simple, fertilization is impacted by a wide range of extrinsic environmental factors as well as intrinsic factors (e.g., DNA, RNA, and proteins) [74,75]. Mature spermatozoa have been shown to have a broad population of RNAs, despite the fact that these cells lack transcription [76]. The molecular history of sperm synthesis and maturation during spermatogenesis is reflected in these RNAs [77,78].

Furthermore, the majority of sperm RNAs are quite similar to those expressed in the testes [79]. The exact functions of these sperm and testicular transcripts in spermatogenesis and male infertility are still unknown, despite their thorough characterization. Male fertility may be influenced by transcriptional regulation during spermatogenesis [80].

Certain coding and non-coding RNAs (ncRNAs) are retained by sperm [81], which are essential to many biological processes and control gene expression at both the

transcriptional and post-transcriptional stages. The regulatory roles of the mRNA repertoire that sperm transfer to the oocyte during fertilization have been the subject of increasing amounts of research [75,76,82,83]. The whole scope of their activities in oocyte activation, fertilization, and embryonic development is still being studied, despite data indicating that sperm contain a distinct collection of RNAs with potential regulatory roles.

Until recently, ncRNAs were often believed to be merely the products of transcriptional "leakage," whereas small RNAs were written off as evolutionary remnants. Recent research, however, indicates that ncRNAs have an extensive variety of uses and may be divided into several groups according to their biological roles or size (**Figure 6**). It is increasingly evident than ever that ncRNAs are vital for both healthy physiological functions and disease mechanisms, and they play important functions in gene regulation [84]. **Figure 6** illustrates the extensive profiling of small RNAs in human sperm made possible by developments in biotechnology and bioinformatics [81]. Different intracellular and extracellular functions in gene regulation are demonstrated by each type of ncRNA. Among them, the study of miRNAs is a rapidly expanding area of molecular biology research [81].

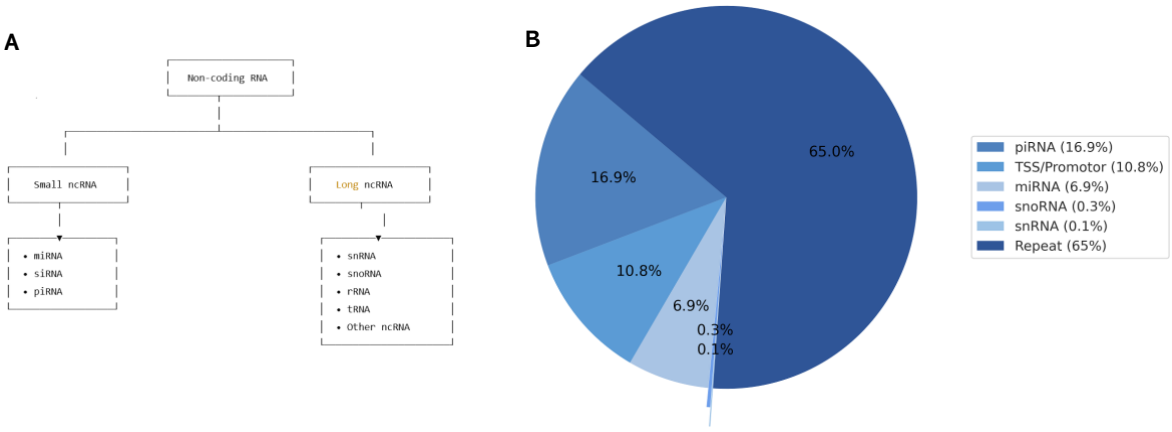

Figure 6. Classes and Characteristics of Non-Coding RNAs in Human Sperm**.**
(A) Classification of non-coding RNAs (ncRNAs) by length: small (<30 bp) vs. long (>200 bp). **(B)** Overview of various ncRNA classes identified in human sperm. Adapted from Krawetz et al. [81]. Abbreviations: piRNA – PIWI-interacting RNA; TSS – transcription start site; miRNA – microRNA; snoRNA – small nucleolar RNA; snRNA – small nuclear RNA.

1.6.1 Discovery and Regulatory Potential of miRNAs

By triggering the destruction of gene transcripts or preventing their translation, miRNAs are small, ~22-nucleotide non-coding RNAs that control gene expression post-transcriptionally [85]. They now play an essential part in controlling gene activation and fine-tuning a variety of cellular functions. Ambros and Ruvkun used the invertebrate model organism *Caenorhabditis elegans* to identify the first members of the miRNA family in 1993. This was a molecular biology discovery that brought ncRNAs back into prominence as important modulators of gene expression. Researchers discovered non-coding RNAs (ncRNAs) instead of protein-coding ones via the examination of the lin-4 and let-7 genes, which are involved in *C. elegans* development.

Since transcription factors and protein-dependent mechanisms have previously been linked to gene regulation, this was a surprising and groundbreaking discovery. Due to their sequence similarity, the RNAs reduced translation via RNA-RNA interactions with a motif identified in the 3′ untranslated region (3′UTR) of certain mRNAs [85-87]. After that, researchers discovered that let-7 is conserved in a number of species, including Homo sapiens, highlighting the significance of miRNAs in evolution [88]. Due to their conservation, miRNAs were fundamentally a part of the regulatory networks of multicellular organisms rather than a uniqueness of nematodes.

Since then, smaller RNAs with functions similar to those of lin-4 and let-7 have been discovered, suggesting a much wider range of post-transcriptional regulatory factors than initially believed [85,89]. These RNAs were referred to as "microRNAs" because of their smaller sizes, since their precise roles were not yet understood [85,89,90]. Databases that list these compounds expanded along with our understanding. A total of 2,654 mature human miRNAs are among the 38,589 entries from 271 species in the miRNA database miRBase as of 2018 (miRBase Release 22.1, http://www.mirbase.org/) [91]. The global endeavor to identify and describe the role of miRNAs in different species is demonstrated by this extensive list. An estimated 2,300 miRNAs have been functionally verified by 2019, of which

1,115 were identified in miRBase [92], demonstrating the size and complexity of this regulatory framework.

Individual miRNAs possess the capacity to control whole gene networks involved in development, immunity, and disease, and because a single miRNA may target hundreds of transcripts engaged in different biological processes, there is a great deal of potential for controlling gene expression. Due to their regulatory flexibility, miRNAs may function as molecular switches to either maintain homeostasis or contribute to disease states when their control is compromised. A number of diseases, including cancer, neurological conditions, and cardiovascular problems, may result from dysregulation of miRNA expression patterns [93]. Research on the processes and targets of miRNAs thereby advances our knowledge of the genesis of illness and validates their potential as diagnostic biomarkers [94,95].

1.6.2 Classification of miRNAs

Based on mutant phenotype, the let-7 and lin-4 miRNAs were identified, reflecting preliminary functional findings in *C. elegans* genetic investigations [85]. Since the majority of other miRNAs were unknown at the time of discovery, their names were assigned numerically in order of discovery [85,96]. As the research progressed, researchers used a variety of classification techniques to classify miRNAs according to their molecular characteristics. miRNAs may be categorized according to characteristics like target binding properties, biogenesis process, or sequence homology. Because miRNAs with similar seed sequences share both their target mRNAs and their regulatory activities, assigning miRNAs to families is very helpful. Certain miRNAs may have originated via gene duplication and functional diversification, as these families also happen to represent evolutionary affinities.

There are around 42% intergenic genes, which are found between genes that code for proteins, and some intragenic genes, which are found inside gene sequences. Introns, exons, and untranslated regions (in 3′UTRs and 5′UTRs) include intragenic miRNAs [97-99]. The fact that RNA Polymerase II transcribes most miRNAs is similar to that of protein-coding genes, suggesting a highly intricate interplay between coding and non-coding transcriptional processes [100-102].

1.6.3 Origin and Stability of miRNAs

The biogenesis of miRNAs and its mechanism of action is shown in **Figure 7**. RNA Polymerase II transcribes canonical miRNAs in the nucleus [103]. The precursor transcripts, also known as primary miRNAs (pri-miRNAs), have stem-loop or hairpin structures that result from self-complementary sequences [95]. Unlike mRNAs, these transcripts have a 5′ cap but do not need a 3′ poly(A) tail for stability or processing [103]. The microprocessor complex, which consists of Drosha and DGCR8, first comprises miRNA to produce a precursor miRNA (pre-miRNA) that is around 60–70 nucleotides long and has a distinctive 2-nucleotide 3′ overhang [104]. In a RAN-GTP-dependent manner, this pre-microRNA (pre-miRNA) is exported from the nucleus and identified by Exportin 5 [105].

A second enzyme called Dicer trims the terminal loop of the pre-miRNA when it enters the cytoplasm, resulting in the formation of a double-stranded RNA duplex with 3′ overhangs [106-108]. Molecular chaperones HSC70 and HSP90 catalyze this, using ATP to encourage structural alterations that are crucial for the duplex [109]. The guide strand is subsequently put into the RNA-induced silencing complex (RISC), whereas the passenger strand is removed and often destroyed [110]. The thermodynamic stability of the duplex ends, and the base identity at the 5′ end serve as guidance when selecting strands; Argonaute prefers phosphorylated adenine or uracil [111,112]. The mature miRNA drives the assembly of complementary target sequences when it is integrated into the RISC complex. The degradation of miRNAs at this region often requires specific processes like polyadenylation or trimming since they are quite persistent [113-115].

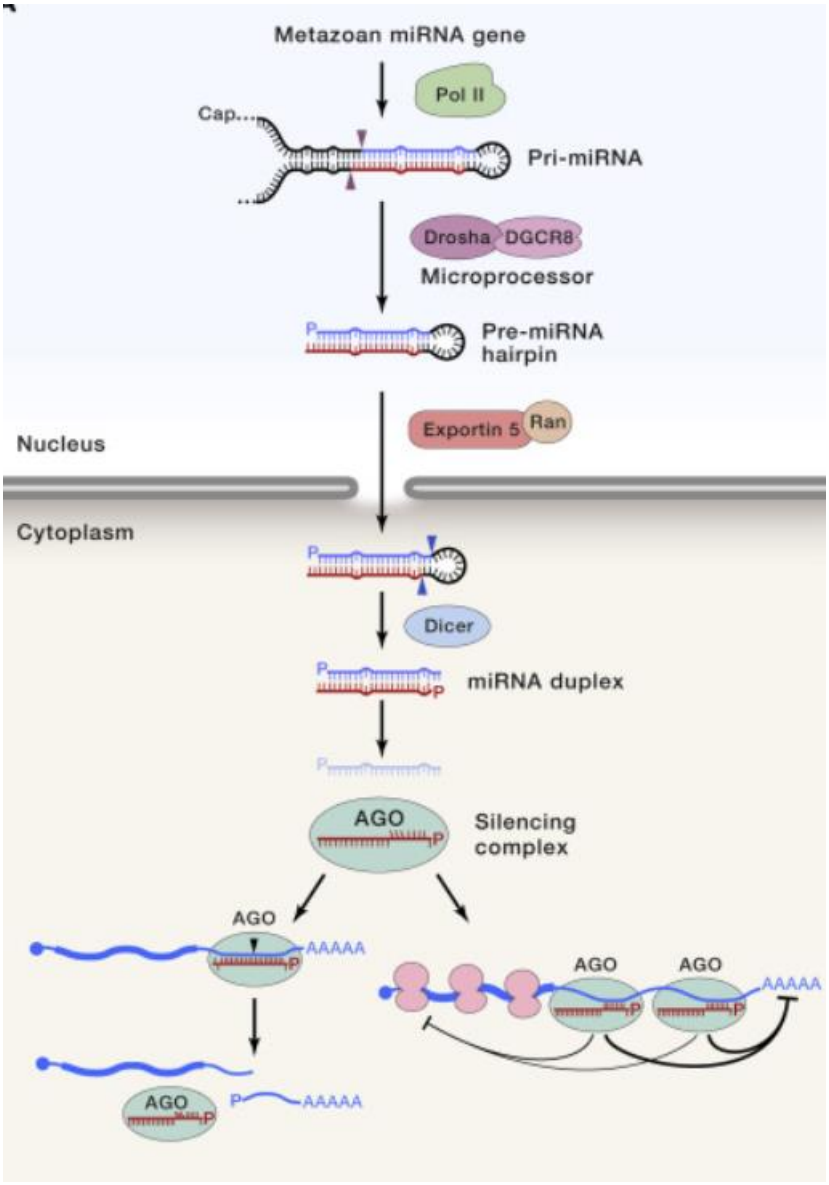

Figure 7. miRNA Biogenesis Pathway.
RNA polymerase II transcribes miRNAs as primary transcripts (pri-miRNAs), which Drosha processes in the nucleus to produce ~70 nt precursor miRNAs (pre-miRNAs). Dicer cleaves these after they are exported to the cytoplasm, creating around ~22 nt duplexes. Gene expression is controlled by the guide strand, which is integrated into the RISC complex. Adapted from Bartel [102]. Abbreviations: Pol II – RNA polymerase II; pri-miRNA – primary miRNA; pre-miRNA – precursor miRNA; AGO – Argonaute; miRNA – microRNA.

1.6.4 Identification of Targets and Regulatory Mechanisms of miRNAs

MiRNAs use two primary methods to carry out gene silencing [102]. Argonaute-directed direct endonucleolytic cleavage of the target transcript, which is made possible by virtually perfect base pairing, is usually what repression in plants entails [102,116,117]. However, miRNAs usually suppress gene expression in animal systems, particularly mammals, via processes that include mRNA degradation or translational repression. In mammals, miRNA-mediated repression usually involves the

recruitment of TNRC6, a scaffold protein with Argonaute binding capabilities. The poly(A) tail reduces as a result of TNRC6's engagement of poly(A)-binding proteins (PABPC) and deadenylase complexes, such as PAN2-PAN3 and CCR4-NOT [118,119].

Due to this, the mRNA becomes unstable, which in turn causes its decapping and degradation [102,120]. Additionally, via the helicase DDX6, which integrates the CCR4-NOT complex, the TNRC6 protein permits translational suppression [119]. The cellular environment dictates the decision between translation inhibition and degradation, with the latter option usually being the more frequent outcome [102,121,122]. The miRNA seed region, which consists of nucleotides 2–7 or 2–8, binds to complementary sites in the target mRNAs' 3′UTR to initiate target recognition [85,102]. The binding affinity may be increased by additional interaction, such as pairing at Position 8 or an adenosine opposite Position 1 [123]. Even while regions outside of the seed region, including nucleotides 13–16, are equally involved in APD determination, they only slightly increase repression by a small percentage of miRNAs, around 5% [85,102,124]. The first nucleotide of the miRNA is physically sequestered by the Argonaute protein, limiting its ability to interact [125]. Therefore, the middle of the seed region, nucleotides 2–5, is primarily involved in target binding and scanning [102,124].

1.7 Functions of miRNAs in Male Reproductive Health

1.7.1 Role of miRNAs in the Fertilization Process

It was discovered that 6.9% of the total ncRNA molecules in human spermatozoa were miRNAs [81]. These miRNAs can additionally alter the expression of some genes in the fertilized oocyte by moving from the sperm to the zygote [126], and can also influence the phenotype of the offspring [76,127,128]. Furthermore, it has been shown that the transfer of miRNAs from sperm to oocytes plays an important role in the early stages of embryonic development [76,82,83,129]. For instance, miR-430 targets a large inventory of maternally inherited mRNAs during zebrafish fertilization and early development [130]. Additionally, a set of miRNAs in mature mouse spermatozoa with potential mRNA targets in metaphase II oocytes was found by Amana et al. [127]. According to Liu et al., sperm miRNAs are transferred into the zygote during fertilization, and miR-34c is essential for the initial cell cleavage [131]. According to

recent research, miRNAs are released into IVF embryonic culture medium and exhibit variable abundance during embryonic cell cycles and genome activation. These results suggest that miRNAs play an essential role in embryonic developmental competence [132-136]. The idea that sperm contain a distinct collection of miRNAs with probable regulatory functions in fertilization is supported by current data, although little is known about the overall function of sperm-borne miRNAs, particularly with respect to their effects on oocyte activation, fertilization, and embryogenesis.

1.7.2 Functions of miRNAs in Spermatogenesis and Male Infertility

Regarding spermatogenesis, miRNAs are important for the development and generation of sperm in both somatic and germline cells. Even though a number of studies have examined deregulated miRNAs and/ or mRNAs in spermatogenesis, they have always focused solely on one aspect of the problem and ignored the effects of changed miRNA expression downstream [62,63,137]. In testicular tissue from NOA patients compared to controls, Lian et al. discovered 19 overexpressed and 154 underexpressed miRNAs [138]. Further research used next-generation sequencing (NGS) [139], reverse transcription quantitative polymerase chain reaction (RT-qPCR) [140,141], and microarrays to compare the amounts of miRNA in seminal plasma from NOA patients. When comparing seminal plasma from infertile men to fertile controls, Wang et al. found that the concentrations of seven miRNAs varied, with asthenozoospermic men having greater quantities and azoospermic patients having lower values [139]. Potential diagnostic markers of male infertility may be these miRNAs. Wu et al. discovered that infertile men had higher levels of let-7a and miR-19b than fertile controls, suggesting spermatogenic failure in oligozoospermia or idiopathic NOA [140]. In the seminal plasma of individuals with NOA, the same group subsequently discovered increased expressions of miR-7-1-3p, miR-429, and miR-141 [141]. Promising biomarkers for idiopathic male infertility were identified, including Let-7a, miR-19b, miR-7-1-3p, miR-429, and miR-141. Using miRNA microarrays, Liu et al. found 52 miRNAs that were differently expressed in fertile and infertile males [142].

Although it has been reported that a number of miRNAs are preferentially expressed in certain spermatogenic cell types, there have not been many functional studies on these miRNAs. For instance, in contrast to normozoospermic controls, oligoasthenozoospermic patients exhibit overexpression of *SEMG1* (*semenogelin 1*) at the mRNA and protein levels due to downregulation of miR-525-3p [143]. By attaching to its 3'UTR, miR-27a inhibits *CRISP2* (cysteine-rich secretory protein 2) and controls its production at the post-transcriptional stage [144], and reduced *CRISP2* protein, but not mRNA levels, are observed in asthenozoospermic individuals [145]. Heat shock protein 1B (*HSPA1B*), whose expression is negatively linked with miR-15a in sperm, is post-transcriptionally inhibited by miR-15a, which is also markedly reduced in varicocele patients [146].

1.7.3 Role of miRNAs in Extracellular Microvesicles and Exosomes

There is mounting evidence that a range of RNA species, including miRNAs, are carried by seminal microvesicles like exosomes. Vojtech et al. found that human semen exosomes have a unique miRNA complement that is probably involved in regulatory processes [147]. Microvesicles are linked to cellular regulatory processes and are released during ejaculation [148]. Exosomal miRNAs are prevalent in human seminal plasma, and variations in their levels have been linked to male infertility [149]. In particular, compared to fertile men, individuals with oligoasthenozoospermia had low levels of miR-15a and high levels of miR-1275 and miR-765. Notably, sperm, seminal plasma, and purified spermatozoa all included miRNAs that were differently expressed in microvesicles produced from seminal plasma, indicating a shared origin within the male reproductive system [139,141,142,150]. Functionally, it has been demonstrated that exosomal RNAs, such as miRNAs, promote intercellular communication and control gene expression via endocrine-like processes [148,151-153].

1.7.4 miRNAs as Candidate Biomarkers for Male Infertility

1.7.4.1 miRNA Profiling in Isolated Sperm and Testicular Tissue

Numerous profiling studies, including ours, have also found differently expressed miRNAs with established roles in spermatogenesis by comparing the miRNA expression profiles of infertile men and controls [154]. In testicular tissues from NOA males compared to men with normal spermatogenesis, 311 differently expressed

miRNAs were found by a thorough microarray and RT-qPCR investigation [155]. Changes in abundance of 46, 68, and 197 miRNAs were linked in this research to Sertoli cell-only (SCO) syndrome, mixed atrophy (MA), and germ cell arrest (GA), respectively. Notably, miR-129-3p, miR-517b, and members of the miR-34 and miR-449 families (miR-34b, miR-34c-5p, and miR-449a, miR-449b) were the most prominent miRNAs with substantial fold changes. Several miRNAs with altered abundance in comparison to normozoospermic controls were found in the sperm of males with asthenozoospermia and oligoasthenozoospermia, according to a comparable microarray research [150]. Men with oligoasthenozoospermia also had lower levels of miR-16, miR-449a, miR-15b, miR-34c-5p, and miR-34b, as well as substantially reduced levels of miR-1973, miR-122, and miR-34b [150].

All of the identified miRNAs (miR-122, miR-34c-5p, miR-34b, and miR-34b) demonstrated lower levels in sperm and testicular tissues of subfertile males, with the exception of miR-429, according to a validation experiment employing RT-qPCR [150,155,156]. Despite these findings, the precise roles of these miRNAs in spermatogenic failure remain unclear. Recent studies by Abu-Halima et al. clarified the regulatory roles of miR-23a-3p and miR-23b-3p with regard to their target genes in men who are infertile [157,158]. He verified their increase in oligoasthenozoospermic males and those with poor spermatogenesis using RT-qPCR. The inhibition of *TEX15*, *SPATA6*, *HMMR*, and *PFKFB4* by these miRNAs has been demonstrated using bioinformatics and Dual-Luciferase tests by him. This inhibition was eliminated by changes in the binding site at 3'UTR. Higher miRNA levels were linked to poor sperm count, motility, and morphology, whereas target gene expression was positively connected with these characteristics, according to correlation analysis [157,158].

1.7.4.2 miRNA Profiling of Seminal Plasma-Derived Exosomes

Extracellular microvesicles developed from seminal plasma are a potential non-invasive biomaterial for assessing male infertility, in addition to sperm and testicular tissues. We found that extracellular vesicles from both fertile and subfertile (i.e., oligoasthenozoospermic) males had a unique miRNA profile [159]. A total of 36 miRNAs were found to be differently expressed by microarray and RT-qPCR; 29

were downregulated, and seven were elevated in sub-fertile people. Thirty of them coincided with the isolated sperm's differently expressed miRNAs [150]. Furthermore, six miRNAs were unique to microvesicles: miR-4306, miR-483-5p, miR-100, miR-96, miR-93, and miR-28-5p [159]. Male fertility and reproductive health may be impacted by their alteration.

1.7.4.3 miRNA Profiling in Embryonic Culture Media

Three million children have been born as a result of ART worldwide [160]; however, only around 30% of ART cycles (IVF or ICSI) result in a successful pregnancy [161]. These errors cause a great deal of stress, which emphasizes the need for novel methods of diagnosis to find embryos with the greatest potential for development [162,163]. The procedure is limited by its nature, yet morphological examination is still the gold standard for sperm and embryo selection. During fertilization, sperm provide the oocyte with a variety of RNAs, including miRNAs [76,164], and miRNAs are crucial for development and fertilization [164]. Although few studies have measured miRNA concentrations in embryonic culture media, most have demonstrated that miRNA concentrations indicate embryo quality and developmental potential [132-136]. A total of 621 miRNAs were found in a recent research that used a microarray scan of the miRNome of embryonic culture medium after transfer [132]. Compared to 149 miRNAs in successful pregnancies, an average of 163 miRNAs were found in unsuccessful ones [132]. The miR-634 indicated a successful pregnancy outcome with 85% sensitivity and 71% accuracy. The most significant shift in abundance was observed for miR-29c-3p out of the 102 miRNAs that were differentially expressed. Reduced miRNA levels are probably caused by the fact that culture medium from excellent outcomes contained fewer extracellular vesicles (3.8×10^9/mL) than those from poor results (7.35×10^9/mL).

Subsequent investigation identified miRNAs in both sperm and embryonic media, including miR-19b-3p and let-7a-5p. Grades of embryos (Grades 1, 2, and 3) were associated with miRNA abundance. For instance, there were differences in miR-15a-5p and miR-320a between Grade 1 and 2 embryos, miR-21-5p between Grades 1 and 3, and miR-20a-5p between Grades 2 and 3. Successful pregnancy outcomes were favorably correlated with levels of miR-19b-3p abundance

(AUC^{Embryo} = 0.818; AUC^{Sperm} = 0.908). AUCs ranging from 0.753 to 0.855 indicated that the other miRNAs, miR-20a-5p, miR-21-5p, miR-15a-5p, and miR-320a, were predictive. This comprehensive investigation highlights the potential of miRNAs as biomarkers for improving ART success rates and explaining and diagnosing male infertility.

1.8 Aim of Thesis

The etiology of infertility varies greatly depending on the geographic, environmental, and social circumstances. It is a multifaceted global health condition. Although male infertility accounts for around 50% of all instances of infertility, little is known about its molecular mechanisms. With their critical functions in spermatogenesis, oocyte stimulation, fertilization, and early embryonic development, miRNAs are being recognized as important regulators of reproductive health.

Al Smadi and Haidar et al. discovered groups of differently expressed miRNAs in sperm with excellent motility and morphology using small RNA sequencing (sRNA-seq), in contrast to sperm with impaired motility and irregular morphology [165]. The screening cohort was used for this research, and **Table 2** shows the miRNAs that were differently expressed.

Table 2. Differentially Expressed miRNAs in Sperm With Normal vs. Impaired Motility and Morphology

MicroRNA	log2 Fold Change	p-value
hsa-miR-223-3p	-5.19	0.0001
hsa-miR-424-5p	-2.48	0.0003
hsa-miR-199a-5p	-2.59	0.0015
hsa-miR-199b-5p	-2.59	0.0015
hsa-miR-15a-5p	-1.37	0.0033
hsa-miR-15b-5p	-2.03	0.0072
hsa-miR-19a-5p	-1.94	0.0091
hsa-miR-106b-5p	-0.94	0.0098
hsa-miR-449b-5p	-2.10	0.0124
hsa-miR-149-5p	1.38	0.0196
hsa-miR-335-5p	-1.85	0.0196
hsa-miR-449a	-2.09	0.0218
hsa-miR-99a-5p	0.74	0.0280
hsa-miR-20a-5p	-0.76	0.0323
hsa-miR-16-5p	-1.12	0.0446
hsa-miR-146a-5p	-0.85	0.0480

— MiRNAs identified in the screening cohort using sRNA-seq, as indicated by [165]

— Adjusted p-value (FDR)

The primary objective of this thesis is to assess the biological and clinical importance of a panel of 16 miRNAs (as indicated in **Table 2**) in human sperm. The thesis specifically focuses on:

— Determine how many of 16 miRNAs are expressed in sperm samples from males with different infertility phenotypes, such as asthenozoospermia (A), oligoasthenospermia (OA), oligoasthenoteratozoospermia (OAT), and asthenoteratozoospermia (AT).

— Analyze the relationships between these miRNA expression levels and important semen characteristics such as sperm count, motility, and morphology, and consider if these miRNAs might be used as biomarkers to determine male infertility.

— Examine how sperm miRNA expression patterns relate to female hormone levels, embryo quality, and pregnancy outcomes (β-hCG and live birth) in ART to assess whether sperm-derived miRNAs may be used as predictors of ART success.

2. Materials and Methods

2.1 Materials

2.1.1 Consumables

Table 3 lists the consumable items utilized throughout the experiment, including all-purpose supplies and labware.

Table 3. Consumable Materials Used in Experiments

Description	Name / Type	Manufacturer
96-Well Plates	PCR® Microplate	Axygen Scientific, Inc.
Adhesive Tape	Parafilm	Bemis Company, Inc.
Barrier Tips	MultiGuard Barrier Tips Safeguard (10 µL)	Sorenson BioScience, Inc.
Falcon Tubes	Cellstar® Tubes (50 mL, 15 mL)	Greiner Bio-One GmbH
Gloves (light)	Rotiprotect® - Nitril Light	Carl Roth GmbH + Co. KG
Microfluidic Array	Dynamic Array™	Fluidigm/Standard BioTools
Nano Chip	RNA Nano Chips	Agilent Technologies, Inc.
Pipette Tips	Tips (10 µL, 20 µL, 200 µL, 1250 µL)	PEQLAB Biotechnologie
Pipettes	Cellstar® Pipettes (5 mL, 10 mL, 20 mL)	Greiner Bio-One GmbH
Tubes	General Purpose Tubes	SARSTEDT AG & Co. KG
Wipes	Precision Wipes	Kimberly-Clark Professional™

2.1.2 Chemicals

Table 4 provides an overview of the chemicals and reagents utilized, such as solvents, buffers, and RNA reagents.

Table 4. Chemicals and Reagents Utilized in the Study

Description	Manufacturer
2× Assay Loading Reagent	Fluidigm/Standard BioTools Inc.
20× GE Sample Reagent	Fluidigm/Standard BioTools Inc.
Chloroform	Sigma-Aldrich Co. LLC
Control Line Fluid	Fluidigm/Standard BioTools Inc.
Ethanol	Thermo Fisher Scientific Inc.
Glycogen	Thermo Fisher Scientific Inc.
Ham's F-10 Nutrient Mixture (F-10)	PAN-Biotech GmbH
Human Serum Albumin (HSA)	PAN-Biotech GmbH
Nuclease-Free Water (Ambion™)	Thermo Fisher Scientific Inc.
Penicillin G Sodium/Streptomycin Sulfate Solution	PAN-Biotech GmbH
PureSperm® Density Gradients	Nidacon International AB
QIAzol Lysis Reagent	QIAGEN GmbH
RNA 6000 Nano Reagents	Agilent Technologies, Inc.
TE buffer (pH 8.0)	Thermo Fisher Scientific Inc.

2.1.3 Kits

Table 5 lists the commercial kits used for reverse transcription, preamplification, qPCR analysis, and RNA isolation.

Table 5. Commercial Kits Employed in Analyses

Description	Manufacturer
96.96 Dynamic Array™ IFC	Fluidigm/Standard BioTools Inc.
miRNeasy® Micro Kit	Thermo Fisher Scientific Inc.
TaqMan™ MicroRNA Reverse Transcription Kit	Thermo Fisher Scientific Inc.
TaqMan™ PreAmp Master Mix (2×)	Thermo Fisher Scientific Inc.
TaqMan™ Universal PCR Master Mix, No AmpErase™ UNG	Thermo Fisher Scientific Inc.

2.1.4 Devices

Table 6 provides a summary of the tools and equipment utilized in the laboratory for preparing samples, quality control, and amplification processes.

Table 6. Laboratory Instruments and Devices Utilized in This Thesis

Description	Name / Model	Manufacturer
Bioanalyzer	2100 Bioanalyzer	Agilent Technologies, Inc.
Centrifuge	Centrifuge 5417 R	Eppendorf AG
Freezer	C585 Innova	New Brunswick Scientific
Heating Block	Test Tube Thermostat	Carl Roth GmbH + Co. KG
Ice Machine	Flake-Line	Wessamat Eismaschinenfabrik GmbH
IFC Controller Juno™	HX	Fluidigm/Standard BioTools Inc.
Makler Counting Chamber	SM-363	Sefi Medical Instruments Ltd.,
NanoDrop	NanoDrop 2000	Thermo Fisher Scientific Inc.
Real-Time PCR System	BioMark HD	Fluidigm/Standard BioTools Inc.
Shaker	Unimax 1010	Heidolph Instruments GmbH & Co.
Termalcycler	Biometra - TProfessional	Analytik Jena AG
Vortexer	VF2	IKA®-Werke GmbH & Co. KG
Water Bath	VWB 12	VWR International, LLC (part of

2.1.5 Assays

Table 7 provides a summary of the particular TaqMan™ MicroRNA Assays that were used.

Table 7. TaqMan™ MicroRNA Assays Used for miRNA Expression Analysis

Assay ID	Target miRNA	Manufacturer
002295	*hsa*-miR-223-3p	Thermo Fisher Scientific Inc.
000604	*hsa*-miR-424-5p	Thermo Fisher Scientific Inc.
000498	*hsa*-miR-199a-5p	Thermo Fisher Scientific Inc.
000500	*hsa*-miR-199b-5p	Thermo Fisher Scientific Inc.
000389	*hsa*-miR-15a-5p	Thermo Fisher Scientific Inc.
000390	*hsa*-miR-15b-5p	Thermo Fisher Scientific Inc.
002424	*hsa*-miR-19a-5p	Thermo Fisher Scientific Inc.
000442	*hsa*-miR-106b-5p	Thermo Fisher Scientific Inc.
001608	*hsa*-miR-449b-5p	Thermo Fisher Scientific Inc.
002255	*hsa*-miR-149-5p	Thermo Fisher Scientific Inc.
000546	*hsa*-miR-335-5p	Thermo Fisher Scientific Inc.
001030	*hsa*-miR-449a	Thermo Fisher Scientific Inc.
000435	*hsa*-miR-99a-5p	Thermo Fisher Scientific Inc.
000580	*hsa*-miR-20a-5p	Thermo Fisher Scientific Inc.
000391	*hsa*-miR-16-5p	Thermo Fisher Scientific Inc.
000468	*hsa*-miR-146a-5p	Thermo Fisher Scientific Inc.
000417	*hsa*-miR-30a-5p	Thermo Fisher Scientific Inc.
000437	*hsa*-miR-100-5p	Thermo Fisher Scientific Inc.
001093	RNU6B	Thermo Fisher Scientific Inc.

2.2 Methods

2.2.1 Subjects

The research procedure received ethical approval from the Saarland University Ethics Committees in Germany. The Institutional Review Board (IRB) of the Saarland Medical Association granted further approval (approval number Ha 195/11; updated in June 2021 and 2025). Prior to participation, each participant provided written informed consent. Research was carried out in compliance with applicable institutional procedures and the ethical principles outlined in the Declaration of Helsinki.

Through the examination of semen samples from 85 men—all of whom were the male partners in couples now undergoing ART therapy—the current study investigated male infertility. A documented history of infertility for at least 12 months of unprotected sexual activity was one of the specific clinical inclusionary criteria

used to select the patients. The 2021 WHO criteria, which describe male infertility based on fixed semen parameters—sperm concentration, motility, and morphology—were used for classification and assessment [1].

Oligospermia, asthenozoospermia, teratozoospermia, or any combination of these medical conditions were among the inappropriate semen profiles that the patients suffered from. To maximize comparative molecular and functional evaluation, the patients were divided into four diagnostic groups based on these clinical manifestations:

- Oligoasthenospermia (OA, *n* = 28)
- Asthenozoospermia (A, *n* = 35)
- Oligoasthenoteratozoospermia (OAT, *n* = 18)
- Asthenoteratozoospermia (AT, *n* = 4)

2.2.2 Sample Processing

While the sample was collected, all individuals were obligated to abstain from sexual activity for at least three days. Masturbation was used to collect semen samples, which were then placed in sterile containers and allowed to liquefy for around half an hour at 37°C. Volume, pH, viscosity, liquefaction duration, agglutination, sperm concentration, motility, viability, and morphology were all measured immediately upon liquefaction in accordance with WHO guidelines.

The samples underwent a typical sperm purification procedure after the first examination. To distinguish motile, morphologically normal spermatozoa from seminal plasma and debris, all samples were centrifuged at 500 × g for 20 minutes at room temperature after being overlaid over discontinuous 45%–90% PureSperm® density gradients. Ham's F-10 medium with 5 mg/mL of human serum albumin and 0.1 mg/mL of penicillin G/streptomycin sulfate was employed to wash the pellet twice. After that, 0.75 mL of the same medium was added to the suspension of purified sperm, and it was incubated for 45 minutes at 37°C. Following incubation, the supernatant was collected, and the concentration, motility, and lack of somatic contaminants of the spermatozoa were examined in a Makler counting chamber. It assisted in the selection of only healthy and high-quality spermatozoa for further cellular and molecular research.

2.2.3 Extraction of RNA from Sperm Samples

The miRNeasy® Micro Kit was utilized in accordance with the manufacturer's protocol, with some adjustments for the low RNA yield typical of spermatozoa, in order to extract total RNA, including small RNAs like miRNAs, from purified human sperm cells. Each sperm sample was first lysed in 350 µL of the kit's QIAzol® Lysis Reagent, a monophasic phenol-guanidine thiocyanate solution for effective cell lysis and RNase inactivation. For efficient homogenization, samples were gently combined and vortexed for seven minutes. After lysis, samples were allowed to dissociate nucleoproteins for five minutes at room temperature. Each tube was filled with 70 µL of chloroform for phase separation after homogenization and lysis. After a full 15-second vortex, the tubes were allowed to sit at ambient temperature for three minutes. Three layers were created after samples were centrifuged for 15 minutes at 4°C at 12,000 × g:

- Upper aqueous phase, containing total RNA, including miRNAs
- Interphase, containing genomic DNA and denatured proteins
- Lower organic phase, containing lipids and excess QIAzol reagent

To avoid cross-contamination from the interphase or organic phase, only the top aqueous layer (~200 µL) containing the RNA was carefully transferred to a fresh RNase-free microcentrifuge tube. For traceability, the original sample's work number was written on each tube. Moreover, 1.5 volumes of 100% ethanol (~300 µL) were pipetted into the aqueous phase and thoroughly mixed by pipetting in order to precipitate RNA and encourage its binding to the column membrane. After that, the mixture was added to the miRNeasy spin column within a collection tube.

Following the conventional centrifugation-based procedure, membrane-bound RNA was repeatedly washed with RWT Buffer (which contains guanidine salt to remove protein impurities) and RPE Buffer (which contains ethanol to remove salts and other impurities). In order to eliminate genomic DNA contamination, an extra DNase I digestion step was added in between the washes.

After centrifugation, the RNA was finally eluted in 14 µL of RNase-free water and transferred directly into fresh RNase-free tubes. The RNA samples were kept at -80°C until they were needed for qPCR and reverse transcription.

2.2.4 RNA Yield and Purity Measurement

A two-method approach was employed to quantify RNA yield, purity, and integrity: Microfluidic capillary electrophoresis using the Agilent 2100 Bioanalyzer and the Agilent RNA 6000 Nano Kit, as well as UV spectrophotometry using the NanoDrop® 2000.

2.2.4.1 UV-Spectrophotometric Quantitation and Purity Analysis

The NanoDrop® 2000, a micro-volume UV-Vis spectrophotometer employed for high-speed nucleic acid content measurement, was employed to measure the amount of RNA. The apparatus uses Beer-Lambert's law to determine the concentration of nucleic acid by measuring absorbance at the maximum wavelength of RNA, 260 nm. Approximately 40 µg/mL of RNA corresponds to an absorbance (A260) value of 1.

Absorbance at 280 nm, where protein contamination absorbs, and 230 nm, a phenol-sensitive region, as well as guanidinium salts and ethanol contamination, were also measured in order to determine the purity of the RNA sample. Analysis was carried out on two significant absorbance ratios:

- A260/A280, ideally between 1.8–2.0, with little protein contamination
- A260/A230, with ideal values >2.0, indicating minimal chemical or salt interference

The miRNeasy® Micro Kit's elution buffer, 1 µL RNase-free water, was employed to measure a blank read first, then the same amount was used to measure sample reads.

2.2.4.2 RNA Integrity Evaluated using Bioanalyzer

Using the Agilent RNA 6000 Nano Kit and the Agilent 2100 Bioanalyzer platform, the RNA structural integrity and fragmentation status were evaluated. Total RNA with sizes ranging from 25 to 500 ng/µL is properly quantified, sized, and given integrity

scores (RIN values) using the platform. First, the RNA Nano Gel-Dye Mix was made by mixing 1 µL of RNA Nano Dye Concentrate with 65 µL of filtered RNA Nano Gel Matrix, then centrifuging the mixture for 10 minutes at 13,000 × g. Before being loaded onto the chip, the mixture was shielded from light and allowed to settle at ambient temperature for half an hour. The RNA 6000 Ladder was aliquoted for use after being preheated for two minutes at 70°C and then rapidly chilled on ice. After setting up the chip priming station for the RNA test, 9 µL of the gel-dye mixture was pipetted into the priming well and then into the subsequent well.

Every sample (1 µL) was placed in the designated wells (positions 1–12), and the RNA ladder (1 µL) was placed in the designated ladder well. One microliter of RNA Nano Marker for chip balancing was added to the remaining wells. The sample-charged chip was put into the Bioanalyzer and run using the "Eukaryote Total RNA Nano Series II" procedure after being vortexed at 2,400 rpm for one minute. To provide a reliable assessment of RNA integrity, the system exhibited high-resolution electropherograms and gel-like images along with RNA Integrity Number (RIN) values ranging from 1 (highly degraded) to 10 (intact).

2.2.5 Reverse Transcription, Pre-Amplification, and Quantitative PCR for miRNA

A three-step reverse transcription (RT), preamplification, and real-time PCR procedure using TaqMan™-based chemistry was employed to quantify the levels of miRNA expression from sperm RNA. The manufacturer's step-by-step instructions for custom assay setup were followed.

2.2.5.1 Custom RT Primer Pool Preparation

A total of 17 single TaqMan™ MicroRNA Assays, each carrying a 5× stem-loop RT primer for a mature miRNA, were combined to develop pools of customized RT primers (see **Table 6**). A 1.5 mL microcentrifuge tube was filled with 7.5 µL of each of the 5×RT primers. This was combined with 607.5 µL of 1× TE buffer (pH 8.0) to create 750 µL.

As a consequence, each experiment in the pool had a final concentration of 0.05× RT primer. After a brief centrifugation and gentle vortexing, the primer pool mixture was aliquoted and kept at –20°C for up to two months.

2.2.5.2 Reverse Transcription

The TaqMan™ MicroRNA Reverse Transcription Kit was used to perform reverse transcription (RT). A 12 µL RT reaction was prepared on ice for every sample as follows:

- 6.00 µL of each RT primer pool (0.05× final concentration per primer)
- 0.30 µL dNTPs containing dTTP (100 mM)
- 3.00 µL MultiScribe™ Reverse Transcriptase (50 U/µL)
- 1.50 µL 10× RT buffer
- 0.19 µL RNase Inhibitor (20 U/µL)
- 1.01 µL nuclease-free water

Each reaction was gently mixed by inversion and then quickly centrifuged. In each well of a 96-well PCR plate, 3.0 µL of total RNA (containing 75 ng) was added. A total of 12 µL of ready RT reaction mixture was then added. RNA was substituted with nuclease-free water as a negative control. After sealing and inverting the plates to mix, they were centrifuged and left on ice for five minutes. The thermal cycler software described in **Table 8** was employed to carry out the RT.

Table 8. Thermal Cycler Program for Reverse Transcription

Step	Temperature	Time	Cycles
RT step 1	16 °C	2 minutes	40×
RT step 2	42 °C	1 minute	
RT step 3	50 °C	1 second	
Enzyme inactivation	85 °C	5 minutes	1×
Final hold	4 °C	∞	

For the preamplification process, completed RT reactions were stored at -20°C.

2.2.5.3 Preparation of Custom Preamplification Primer Pool

TaqMan™ PreAmp Master Mix (2×) was used for preamplification in order to increase the detection sensitivity of low-abundance miRNAs. In a 1.5 mL microcentrifuge tube, 5 µL of each of the 20× TaqMan® MicroRNA Assay was

combined to generate the preamplification primer pool. To achieve the final volume of 500 µL and 0.2 times the final concentration per test, 405 µL of 1× TE buffer (pH 8.0) was added. The pool was held at -20°C after being gently mixed and briefly spun.

2.2.5.4 Preamplification Reaction

A final volume of 11.26 µL was used for all preamplification processes, as follows:

- 6.25 µL TaqMan™ PreAmp Master Mix (2×)
- 1.88 µL custom preamplification primer pool
- 3.13 µL nuclease-free water

A volume of 1.37 µL of the reaction product was added to each well of a 96-well PCR plate after the reaction's components were firmly inverted to mix them and centrifuged. Thermal cycling was performed using the procedure described in **Table 9** after sealing, mixing, and a brief centrifugation.

Table 9. Thermal Cycler Program for Preamplification

Step	Temperature	Time	Cycles
Enzyme activation	95 °C	10 minutes	1×
Annealing	55 °C	2 minutes	1×
Extension	72 °C	2 minutes	1×
Denaturation	95 °C	15 seconds	12×
Anneal/Extend	60 °C	4 minutes	
Enzyme inactivation	99.9 °C	10 minutes	1×
Final hold	4 °C	∞	

2.2.5.5 Dilution of PreAmp Product

After amplification, the reactions were briefly centrifuged, and the result was diluted by adding 43 µL of 0.1× TE buffer (pH 8.0) to each well. After being sealed, the plates were flipped to mix, centrifuged, and stored at -20°C for up to a week or on ice for short-term usage.

2.2.5.6 Quantitative Real-Time PCR

The TaqMan™ Universal PCR Master Mix, No AmpErase™ UNG, and the 96.96 Dynamic Array™ Integrated Fluidic Circuit (IFC), running on the Biomark™ HD system, were used to perform quantitative real-time PCR (qPCR).

2.2.5.6.1 Priming and Preparation of the IFC

On the Juno™ System, the 96.96 IFC was primed. Before feeding the accumulators with 150 µL of control line fluid, the bottom protective film covering the IFC was carefully removed. To prime the IFC, the Juno "Prime 96.96 GE" script was executed. To avoid evaporation failure, it was ensured that every loading phase was finished within 60 minutes after priming.

2.2.5.6.2 Assay Preparation

The 10× assay mix used in each qPCR experiment was made by mixing:

- 2.5 µL of 20× TaqMan® Gene Expression Assay
- 2.5 µL 2× Assay Loading Reagent

With primer and probe final concentrations of 9 µM and 2 µM at 10× strength, respectively, this resulted in a final assay volume of 5.0 µL per inlet.

2.2.5.6.3 Sample Preparation and Pre-Mix

A total of 6 µL of reaction mix was created for each sample per IFC inlet. This included 1 µL of preamplified cDNA and 5 µL of sample pre-mix. RNase-free conditions were utilized to prepare the pre-mix:

- 2.5 µL of TaqMan™ Universal PCR Master Mix (2×)
- 0.25 µL of 20× GE Sample Loading Reagent
- 2.25 µL of preamplified cDNA

Before aliquoting, this pre-mix was centrifuged and vortexed for a short time. To attain the final amount of 6 µL per sample, 2.7 µL of the diluted preamplified cDNA was added to each aliquot. Prior to loading IFC, samples were centrifuged, vortexed, and placed on ice.

2.2.5.6.4 Loading and Thermal Cycling

Following the preparation of the assay and sample mixes, 5.0 µL of each assay mix and 6.0 µL of each sample mix were carefully pipetted into their corresponding IFC inlets without creating bubbles (only up to the first pipette stop). Equal amounts of 3.0 µL of assay loading reagent and water were added to the unused inlets, and 3.3 µL of sample mix and 2.7 µL of water were introduced for samples.

The assay and sample solutions were then loaded into the IFC's microfluidic channels using the "Load Mix 96.96 GE" script on the Juno system. The loaded IFC was placed straight into the Biomark™ HD system for fluorescence detection and thermal cycling.

2.2.5.6.5 PCR Program and Data Acquisition

The GE 96x96 Standard v1.pcl protocol was used for real-time amplification, using the parameters indicated in **Table 10**.

Table 10. Thermal Cycler Program for Quantitative PCR

Step	Temperature	Time	Cycles
Initial denaturation	95 °C	10 minutes	1×
Denaturation	95 °C	15 seconds	40×
Annealing/Extension	60 °C	1 minute	40×

FAM-MGB was employed as the detection chemical, while ROX served as the passive reference dye. To maximize images, auto exposure was turned on. Biomark™ Data Collection software was employed to gather and evaluate data after the run. Non-template controls (NTCs) were used in each qPCR run to assess for contamination and non-specific amplification, and each sample was performed in triplicate. Endogenous control miRNAs that are known to be stable in sperm RNA were employed to standardize the relative quantification (*Δ*Ct) of miRNA expression level.

2.3 Statistical Analysis

In order to analyze the miRNA expression levels and their correlation with reproductive and clinical factors, rigorous statistical analysis was carried out using R software (version 4.5.0) with the packages *ggplot2*, *tidyverse*, *dplyr*, *readxl*, *openxlsx*, *pROC*, *caret*, and *gridExtra*. The primary objectives were to quantify miRNA expression in 85 human samples, evaluate inter-individual differences, detect differential expression profiles, and quantify the potential diagnostic potential of some miRNAs for their correlation with fertility outcomes.

Using R software (version 4.5.0) and the packages *ggplot2*, *tidyverse*, *dplyr*, *readxl*, *openxlsx*, pROC, *caret*, and *gridExtra*, a thorough statistical analysis was

performed to examine the levels of miRNA expression and their relationship to reproductive and clinical variables. Quantifying miRNA expression in 85 human samples, assessing inter-individual variations, identifying differential expression patterns, and estimating the possible diagnostic value of certain miRNAs for their association with reproductive outcomes were the main objectives.

2.3.1 Data Normalization and Preprocessing

The Biomark™ HD equipment was employed to produce quantitative RT-qPCR data under strict manufacturer-recommended thermal cycling conditions. Before statistical modeling, miRNA expression levels were normalized to account for technical variability. Endogenous control genes, including RNU6B, hsa-miR-30a-5p, and hsa-miR-100-5p, were employed to standardize the expression levels of 16 miRNAs (listed in **Table 7**). Given their low coefficients of variation (CVs), which show little fluctuation in expression across the sample, these miRNA reference genes were chosen. The most consistently expressed gene was RNU6B (CV = 0.136), closely followed by hsa-miR-30a-5p (CV = 0.141) and hsa-miR-100-5p (CV = 0.155). To choose the most stable endogenous controls, the CV, or standard deviation to mean ratio, was computed for each potential reference miRNA.

3. Results

3.1 Study Population

3.1.1 Sample Characteristics and Semen Abnormalities Overview

The thesis comprised 85 male partners who were receiving infertility assessment; their ages ranged from 21 to 30 years, with a mean age of 25.33 ± 2.76 years, as shown in **Table 11**. The age distribution of the participants was remarkably comparable: 25 were between the ages of 21 and 23, 26 were between the ages of 24 and 26, and 34 were between the ages of 27 and 30.

With values ranging from 2 × 10^6/mL to 35 × 10^6/mL, the mean sperm concentration was 14.55 × 10^6/mL (±8.54). The mean of progressive motility (Types A+B) was 15.84% (±6.85), with values ranging from 2% to 28%. The majority of sperm were immotile (Type D), with a mean of 53.34% (±12.94), often as high as 85%, whereas non-progressive motility (Type C) averaged 30.82% (±9.45).

The mean of normal morphology was 5.35% (±2.99), with a range of 1% to 15%. Individuals 29, 34, 38, and 39 all had morphology scores of 1%, while individual 74 received the highest morphology score at 15%.

Table 11. Semen Analysis Parameters of Male Partners Undergoing Infertility Evaluation

Male ID	Age (Year)	Sperm Count (mil/mL)	Progressive Motility (Type A+B) %	Non-Progressive Motility (Type C) %	Immotile Sperm (Type D) %	Normal Morphology %
1	25	7	9	30	61	5
2	23	6	11	40	49	3
3	30	6	14	35	51	5
4	27	25	28	31	41	7
5	26	26	18	34	48	6
6	23	7	9	22	69	2
7	23	15	21	32	47	6
8	26	14	18	34	48	3
9	23	12	18	40	42	3
10	25	16	21	38	41	4
11	28	7	11	28	61	3
12	29	12	15	27	58	11
13	28	9	9	34	57	5
14	28	6	9	11	80	4
15	25	14	14	16	70	10
16	26	9	9	42	49	4
17	24	3	5	25	70	5

18	22	14	18	36	46	4
19	27	9	7	21	72	2
20	23	10	16	46	38	5
21	27	15	21	21	58	6
22	24	5	12	38	50	2
23	28	30	28	35	37	4
24	24	14	18	34	48	3
25	21	5	8	23	69	2
26	25	18	21	20	59	3
27	30	8	14	44	42	4
28	25	5	9	40	51	2
29	28	13	10	30	60	1
30	23	6	3	51	46	4
31	22	5	12	33	55	4
32	21	8	4	21	75	2
33	22	6	2	44	54	5
34	24	3	5	20	75	1
35	24	16	15	30	55	5
36	25	2	5	15	80	2
37	29	2	10	12	78	2
38	25	2	13	20	67	1
39	28	7	9	34	57	1
40	30	30	28	34	38	8
41	24	14	17	43	40	3
42	28	31	28	32	40	7
43	26	35	25	30	45	13
44	29	35	28	41	31	8
45	21	24	21	33	46	7
46	23	14	18	21	61	12
47	25	28	21	32	47	12
48	26	15	18	50	32	8
49	23	21	21	38	41	6
50	24	4	12	18	70	7
51	30	9	5	25	70	9
52	29	31	19	35	46	12
53	28	8	11	22	67	4
54	26	15	22	32	46	5
55	23	17	21	25	54	7
56	30	9	12	19	69	4
57	21	12	14	30	56	5
58	24	25	28	34	38	7
59	25	15	26	32	42	6
60	27	18	13	37	50	3
61	21	25	19	36	45	4
62	21	12	15	25	60	6
63	24	25	21	26	53	12
64	26	13	13	15	72	5
65	27	18	14	32	54	4
66	27	3	6	35	59	4
67	24	4	8	14	78	4
68	29	32	21	43	36	5
69	23	28	27	28	45	5
70	30	13	27	35	38	12
71	21	15	19	35	46	5

72	23	21	22	34	44	3
73	24	16	18	36	46	4
74	28	18	24	41	35	15
75	27	17	21	41	38	4
76	29	12	13	11	76	8
77	22	24	19	33	48	6
78	29	17	19	32	49	5
79	21	24	23	36	41	8
80	22	16	16	43	41	8
81	24	18	14	38	48	3
82	24	8	11	31	58	4
83	29	12	6	9	85	5
84	21	24	27	15	58	5
85	29	15	16	46	38	7
Mean (± SD)	**25.33** (± 2.76)	**14.55** (± 8.45)	**15.84** (± 6.85)	**30.82** (± 9.45)	**53.34** (± 12.94)	**5.35** (± 2.99)

— Total subjects: 85 male partners

— Values are presented as mean ± standard deviation (SD)

3.1.2 Classification Distribution of the Included Male Partners

According to WHO guidelines, the cohort was divided into four clinical groups based on combined abnormalities of semen parameters, as demonstrated in **Figure 8**. 35 people (41.2%) were diagnosed with asthenozoospermia (A), which was the most prevalent. Oligoasthenospermia (OA), which was reported in 28 people (32.9%), was the subsequent condition. A total of 18 people (21.2%) were found to have oligoasthenoteratozoospermia (OAT), which is characterized by concurrent abnormalities in sperm concentration, motility, and morphology. Asthenoteratozoospermia (AT), a smaller group, encompasses four individuals (4.7%).

According to the WHO threshold values:

— 44 participants (51.8%) had sperm concentrations below 15 × 10^6/mL

— 46 (54.1%) had progressive motility under 15%

— 21 (24.7%) exhibited normal morphology below 4%

All 18 subjects who were classified as OAT had concurrent impairments in all three criteria.

The most severe instances, including those of people 36–38, coupled with the lowest sperm quantities (2 × 10^6/mL) and significantly reduced motility and morphology. However, despite possessing poor motility (6%), individual 74 showed

the greatest morphology score (15%), while individuals 29,34, 38, and 39 exhibited the poorest overall morphology.

Immotile sperm fractions of over 70% were often observed, especially in individuals with asthenozoospermia. According to the statistics, the most common defect is a lack of motility, which often coexists with low sperm concentration and irregular morphology.

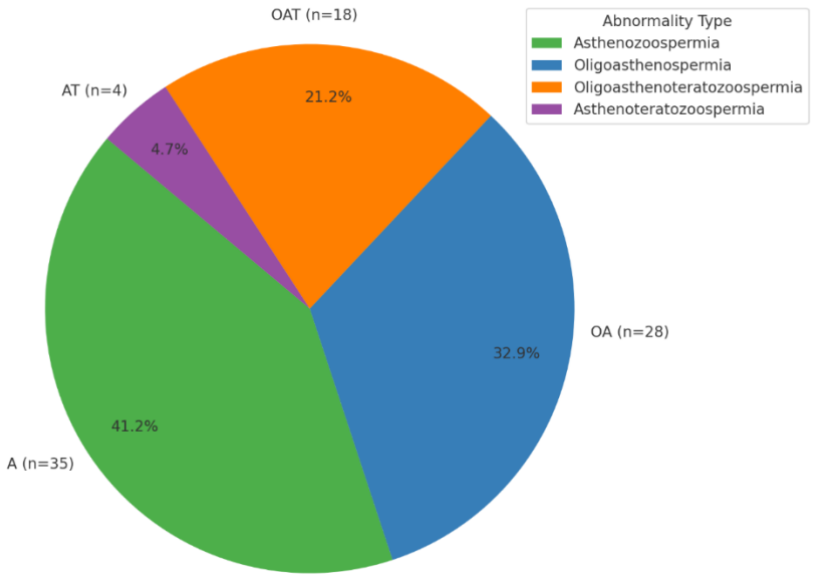

Figure 8. Classification of Semen Abnormalities in Males Included in This Study.
This pie chart, which is separated into four categories—asthenozoospermia (A), oligoasthenospermia (OA), oligoasthenoteratozoospermia (OAT), and asthenoteratozoospermia (AT)—shows the distribution of semen abnormality types among the male participants.

3.1.3 Hormone Levels and Pregnancy Outcomes Associated with Male Infertility

Table 12 provides data from male individuals receiving infertility therapy, with each record connected to the hormonal and clinical results of their corresponding female counterparts, as a successful pregnancy requires both couples. The β-hCG result, FSH and LH levels, embryo quality grade, and live birth outcome are all included in this table.

A consistent morphological grading system determined by cell symmetry and fragmentation was employed to classify the quality of the embryos (Grades G1–G4), with G1 being the best grade and G4 the lowest. Multiple embryos of the same grade

were transferred, as indicated by composite embryo grades (e.g., 2G1). The most often reported embryo quality was 2G1, especially in couples with favorable β-hCG results. Six couples received mixed-grade embryos (e.g., 1G1/1G2), while other embryo grades that were reported were 2G2, 1G2, 1G1/1G2, 2G3, 2G4, and 3G1.

A biochemical indicator of early pregnancy, the β-hCG result, was presented as either positive (n = 44; 51.8%) or negative (n = 41; 48.2%). Although other grades, such as 1G1/1G2, 3G1, and 2G2, were also noted, the majority of positive β-hCG instances were linked to 2G1 embryos. A broader spectrum of embryo grades, including all cases of 2G3 and 2G4 embryos, showed negative β-hCG values.

Among female partners, the range of FSH levels was 4.3 to 19.2 mIU/mL (mean: 11.27 ± 3.29 mIU/mL), while the range of LH levels was 4.9 to 26.8 mIU/mL (mean: 14.89 ± 5.47 mIU/mL).

The result of the live birth was classified as:

- Male singleton (one male infant)
- Female singleton (one female infant)
- Male twins, female twins, or male/female twins (based on recorded sex)
- “Not available (NA)” for cases without outcome records

Among the 44 couples that tested positive for β-hCG, 30 experienced live births, mostly after 2G1 embryos were transferred. Additionally, 3G1 or 1G1/1G2 embryos were linked to a few live births. In 61 instances (71.8%), live birth outcomes were not known. These included 20 positive cases with no follow-up and all β-hCG negative findings.

Table 12. Embryo Quality and Hormonal Profiles of Female Partners in Couples Undergoing Infertility Evaluation

Male ID	Embryo Grade	β-hCG Outcome	FSH (mIU/mL)	LH (mIU/mL)	Live Birth Outcome
1	2G1	Negative	7.2	9.3	NA
2	2G2	Negative	7.3	5.8	NA
3	1G1/1G2	Negative	5.5	8.6	NA
4	3G1	Negative	8.3	7.5	NA
5	2G2	Negative	7.4	4.9	NA

6	2G2	Negative	7.3	8.1	NA
7	2G2	Negative	8.4	6.4	NA
8	2G1	Negative	9.8	8.6	NA
9	2G1	Negative	7.0	8.5	NA
10	1G2	Negative	9.2	7.9	NA
11	2G1	Negative	12.0	11.8	NA
12	2G2	Negative	9.3	13.2	NA
13	2G2	Negative	10.4	11.7	NA
14	2G1	Negative	11.6	12.8	NA
15	1G2	Negative	15.8	12.4	NA
16	2G2	Negative	8.9	8.8	NA
17	2G2	Negative	10.2	13.1	NA
18	2G2	Negative	12.4	14.7	NA
19	2G1	Negative	13.3	10.2	NA
20	2G2	Negative	11.9	11.3	NA
21	2G2	Negative	4.6	10.6	NA
22	2G3	Negative	10.5	12.3	NA
23	2G1	Negative	8.7	8.5	NA
24	2G1	Negative	7.8	11.4	NA
25	2G2	Negative	8.3	7.7	NA
26	1G2	Negative	8.6	12.9	NA
27	2G2	Negative	9.4	8.8	NA
28	2G4	Negative	7.8	7.6	NA
29	2G4	Negative	9.1	8.7	NA
30	2G2	Negative	11.7	11.5	NA
31	2G2	Negative	8.5	12.7	NA
32	2G2	Negative	10.6	9.1	NA
33	1G1/1G2	Negative	12.7	8.3	NA
34	2G2	Negative	8.6	13.2	NA
35	2G2	Negative	4.3	14.8	NA
36	1G2	Negative	10.1	10.6	NA
37	2G2	Negative	9.4	12.2	NA
38	2G2	Negative	12.1	18.7	NA
39	2G3	Negative	6.3	6.3	NA
40	2G2	Negative	8.4	12.8	NA
41	2G2	Negative	12.6	10.5	NA
42	2G1	Positive	8.5	12.4	Male singleton
43	2G1	Positive	9.6	13.6	Male singleton
44	2G1	Positive	10.7	14.8	Male singleton
45	2G1	Positive	11.8	16.0	Male singleton
46	2G1	Positive	12.9	17.2	Male singleton
47	2G1	Positive	14	18.4	Male singleton
48	2G1	Positive	15.1	19.6	Male singleton
49	2G1	Positive	16.2	20.8	Male singleton
50	2G1	Positive	7.3	12.0	Male singleton
51	2G1	Positive	8.4	13.2	Male singleton
52	2G1	Positive	9.5	14.4	Male/Female twins
53	2G1	Positive	10.6	15.6	Female singleton
54	2G1	Positive	11.7	16.8	Female singleton

55	2G1	Positive	12.8	18.0	Female singleton
56	2G1	Positive	13.9	19.2	Female singleton
57	2G1	Positive	15.0	20.4	Female singleton
58	2G1	Positive	16.1	21.6	Female singleton
59	2G1	Positive	17.2	22.8	Female singleton
60	2G1	Positive	8.3	14.0	Female singleton
61	2G1	Positive	9.4	15.2	Female singleton
62	2G1	Positive	10.5	16.4	Female singleton
63	2G1	Positive	11.6	17.6	Female singleton
64	2G1	Positive	12.7	18.8	Female singleton
65	2G1	Positive	13.8	20	Male twins
66	2G1	Positive	14.9	21.2	Male twins
67	2G1	Positive	16	22.4	Male/Female twins
68	2G1	Positive	17.1	23.6	Female twins
69	2G1	Positive	18.2	24.8	Female twins
70	2G1	Positive	9.3	16	Female twins
71	2G1	Positive	10.4	17.2	Female twins
72	2G1	Positive	11.5	18.4	NA
73	2G1	Positive	12.6	19.6	NA
74	2G1	Positive	13.7	20.8	NA
75	2G1	Positive	14.8	22	NA
76	2G1	Positive	15.9	23.2	NA
77	2G1	Positive	17.0	24.4	NA
78	2G1	Positive	18.1	25.6	NA
79	2G1	Positive	19.2	26.8	NA
80	2G1	Positive	10.3	18	NA
81	2G1	Positive	11.4	19.2	NA
82	2G1	Positive	12.5	20.4	NA
83	2G1	Positive	13.6	21.6	NA
84	2G1	Positive	14.7	22.8	NA
85	2G1	Positive	15.8	24	NA
Mean (± SD)	-	-	**11.27** (± 3.29)	**14.89** (± 5.47)	-

- Total subjects: 85 male partners.
- Values are presented as mean ± standard deviation (SD).
- Abbreviations: Beta Human Chorionic Gonadotropin (β-hCG), Follicle-Stimulating Hormone (FSH), Luteinizing Hormone (LH), Grade 1 (G1), Grade 2 (G2), Grade 3 (G3), Grade 4 (G4), Not Available (NA)

3.2 Correlation of Sperm Quality with Embryo Grading Outcomes

We examined correlations between embryo grades and important semen characteristics, such as sperm count, progressive motility, and normal morphology, in order to investigate possible connections between semen quality and embryo development (**Tables 11** and **12**). Sperm count ($\times 10^6$/mL) and progressive motility (%) are shown in **Figure 9A**, stratified by embryo quality grades (G1–G4).

Spearman's correlation coefficient (*r*) across samples linked to G1 embryos was 0.800 ($p < 0.0001$, $n = 48$), suggesting a robust and statistically significant connection. Additionally, the connection continued to be substantial for G2 embryos ($r = 0.806$, $p < 0.0001$, $n = 33$). These results indicate that increased motility is consistently linked to higher sperm counts within both groups.

With increasing motility ranging from 2% to 28%, sperm concentrations associated with G1 embryos varied from 2 to 35 $\times 10^6$/mL. The sperm concentrations and motility in G2-associated samples, on the other hand, were intermediate, usually falling between those observed in the G1 and G3 groups. A boxplot of normal sperm morphology (%) across embryo grades can be seen in **Figure 9B**. While G2 morphology consistently remained around 7%, G1 embryo morphology results clustered between 6% and 8%.

The morphology of the G1 and G2 groups differed statistically significantly ($p = 0.0017$) according to pairwise comparisons. However, statistical analyses were not conducted for the G3 and G4 groups due to their small sample sizes in order to prevent reaching false results.

G3 embryos exhibited more fluctuating morphology values, sometimes falling below 6%. The lowest sperm concentrations (as low as 2 $\times 10^6$/mL), decreased motility (2% to 10%), and morphological values often below 5% were all related to G4 embryos, which also had a broader dispersion.

These results indicate that superior semen characteristics, especially sperm count, motility, and morphology, are often linked to higher-quality embryos.

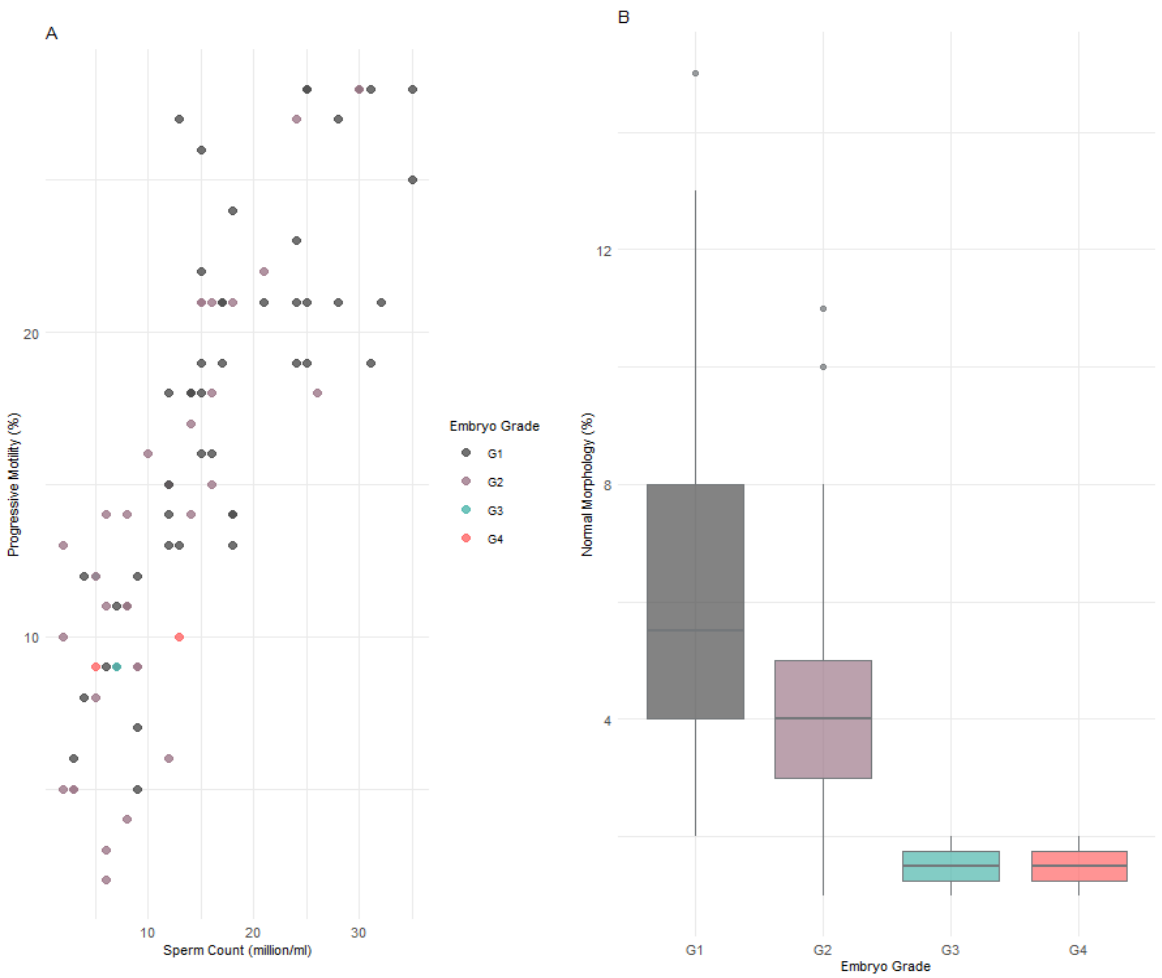

Figure 9. Relationship Between Semen Parameters and Embryo Quality Grades.
(A) Scatter plot of sperm concentration (×10⁶/mL) versus progressive motility (%), stratified by embryo grade (G1–G4). Strong positive correlations between Spearman's correlations for G1 and G2 suggest that higher sperm counts are linked to better-quality embryos' increased motility. **(B)** Boxplot of normal sperm morphology (%) by embryo grade. The morphology of G1 is much greater than that of G2, while the values of G3–G4 are lower and more variable. Because of the insufficient sample numbers, statistical comparisons for G3–G4 were not conducted. Mann–Whitney U test; $p < 0.05$.

3.3 Association Between Sperm Quality and β-hCG Pregnancy Outcome

Key sperm parameters were examined between couples with positive and negative β-hCG results in order to examine the connection between semen quality and pregnancy success. Individuals with positive β-hCG findings had a significantly higher sperm concentration (×10⁶/mL), progressive motility (%), and normal morphology (%), as demonstrated in **Figure 10**.

The range of sperm concentration was broad in both result groups, ranging from less than 5 to more than 30 $\times 10^6$/mL; however, the β-hCG positive group had a considerably higher median concentration ($p < 0.001$). In terms of progressive

motility, there was a more pronounced difference; those in the positive group tended to have values between 15% and 25%, while those in the negative group had motility that was often lower, frequently less than 10% ($p < 0.001$).

Similarly, the β-hCG positive group had higher values for normal sperm morphology, usually between 4% and 12%, whereas the negative group had lower and more variable morphology percentages, often below 4% ($p < 0.001$). These findings show that progressive motility and morphology are closely linked to pregnancy outcomes and sperm concentration, while sperm count, though more variable, contributes considerably.

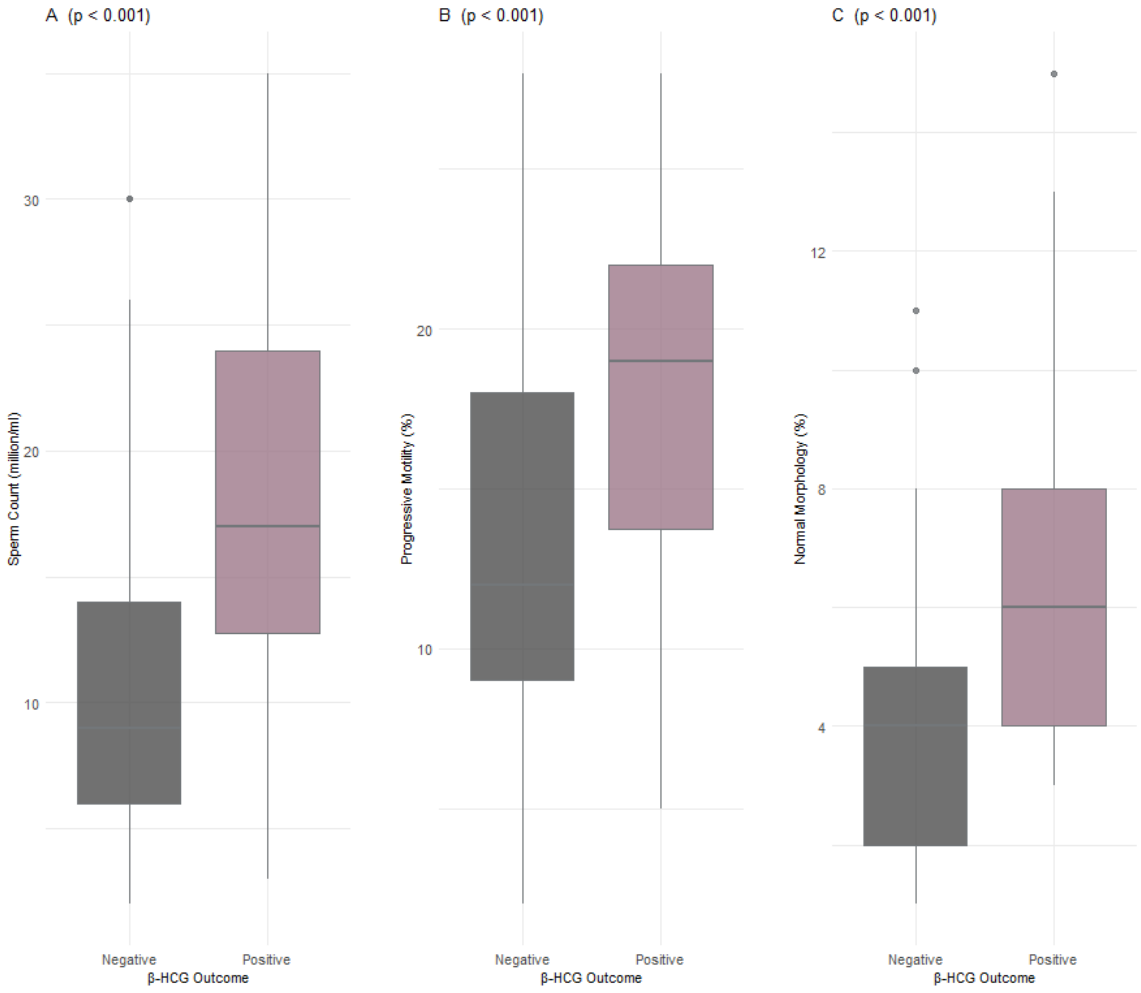

Figure 10. Association of Semen Parameters with β-hCG Outcomes.
(A) Sperm concentration (×10⁶/mL), **(B)** progressive motility (%), and **(C)** normal sperm morphology (%) were compared between individuals with negative and positive β-hCG outcomes. In the hCG-positive group, all measures were considerably higher, with increasing motility and morphology demonstrating clearer group separation and sperm concentration displaying more variability. The Mann-Whitney U test was used to determine statistical significance ($p < 0.001$).

3.4 Association of FSH and LH Levels with β-hCG Pregnancy Outcomes

Serum FSH and LH concentrations were compared across couples with positive and negative β-hCG values in order to investigate the association between female partner hormone levels and biochemical pregnancy outcomes (**Figure 11**). The distribution of FSH levels among those in the β-hCG positive group was narrow, with most values falling between approximately 4 and 8 mIU/mL, and a few rising slightly above 8 mIU/mL. FSH levels in the β-hCG negative group, on the other hand, exhibited more variation, ranging from approximately 4 to more than 10 mIU/mL, with a significant percentage with levels between 6 and 10 mIU/mL and a few individuals above 10 mIU/mL. LH showed a similar pattern: values in the positive group spanned between approximately 5 and 10 mIU/mL with little variation, whereas LH levels in the negative group were more widely distributed, ranging from approximately 5 to more than 15 mIU/mL. Interestingly, there were many higher outliers and a large number of patients in the negative group with LH levels ranging from 7 to 10 mIU/mL.

Comparisons showed that the β-hCG positive group had considerably lower levels of both FSH and LH ($p < 0.001$ for both hormones). These results imply that a lower chance of a successful pregnancy outcome may be linked to higher gonadotropin levels.

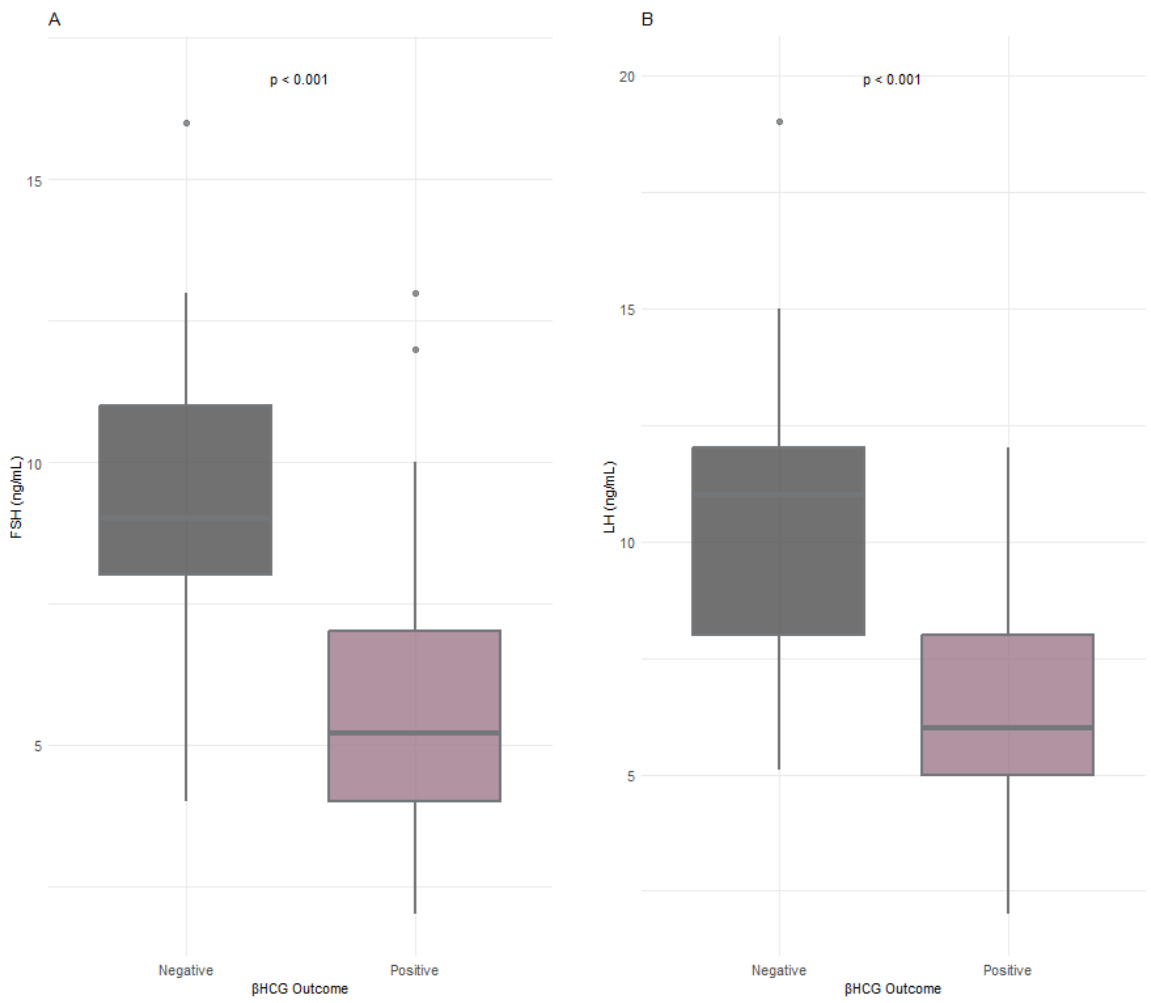

Figure 11. Association of hormonal parameters with β-hCG outcomes.
(A) Serum FSH levels (mIU/mL) and **(B)** serum LH levels (mIU/mL) presented as boxplots comparing β-hCG negative and positive outcome groups. FSH and LH concentrations were significantly lower in the β-hCG positive group ($p < 0.001$). The Mann-Whitney U test was used for statistical comparisons. A total of 85 samples were examined. Outliers, medians, and interquartile ranges are shown as separate data points in boxplots. A threshold of less than 0.05 for the adjusted *p*-value was used to evaluate statistical significance.

3.5 Association of Semen Parameters and Hormonal Levels by Birth Outcome

By comparing distributions between individuals with and without a documented live birth, the association between semen parameters, hormonal levels, and live birth outcomes was investigated (**Figure 12A–E**). Overall, the semen and hormonal profiles of couples who had a live birth were noticeably better. The birth result group had a significantly higher sperm count (×10⁶/mL) (**Figure 12A**), with values mostly lying between approximately 12 and 35 ×10⁶/mL. In contrast, the no-birth group had a wider range, with many instances dropping below approximately 5 ×10⁶/mL ($p < 0.001$). Similarly, for progressive motility (%) (**Figure 12B**), the birth group had

values that were generally in the range of approximately 15% to 25%, whereas the no-birth group had more dispersion as well as more frequent values below approximately 10% ($p = 0.0019$). The birth group had considerably greater normal sperm morphology (%) (**Figure 12C**), with the majority of samples clustering between approximately 6% and 8%, than the no-birth group, which had lower and more variable morphology values, many of which dropped below approximately 4% ($p < 0.001$).

The two groups were further distinguished by the hormonal profiles of their female spouses. While the levels in the no-birth group were more variable, often surpassing approximately 8 mIU/mL and sometimes surpassing approximately 15 mIU/mL ($p < 0.001$), the birth group's serum FSH concentrations (mIU/mL) (**Figure 12D**) varied narrowly between approximately 4 and 8 mIU/mL. The birth outcome group also had considerably lower blood LH levels (mIU/mL) (**Figure 12E**), with the majority of values falling between approximately 5 and 8 mIU/mL. The no-birth group, on the other hand, had a broader distribution, often recording values between approximately 7 and 10 mIU/mL, with outliers surpassing approximately 15 mIU/mL ($p < 0.001$).

These results indicate a strong correlation between successful live birth and lower gonadotropin levels and better sperm quality, as measured by several reproductive parameters.

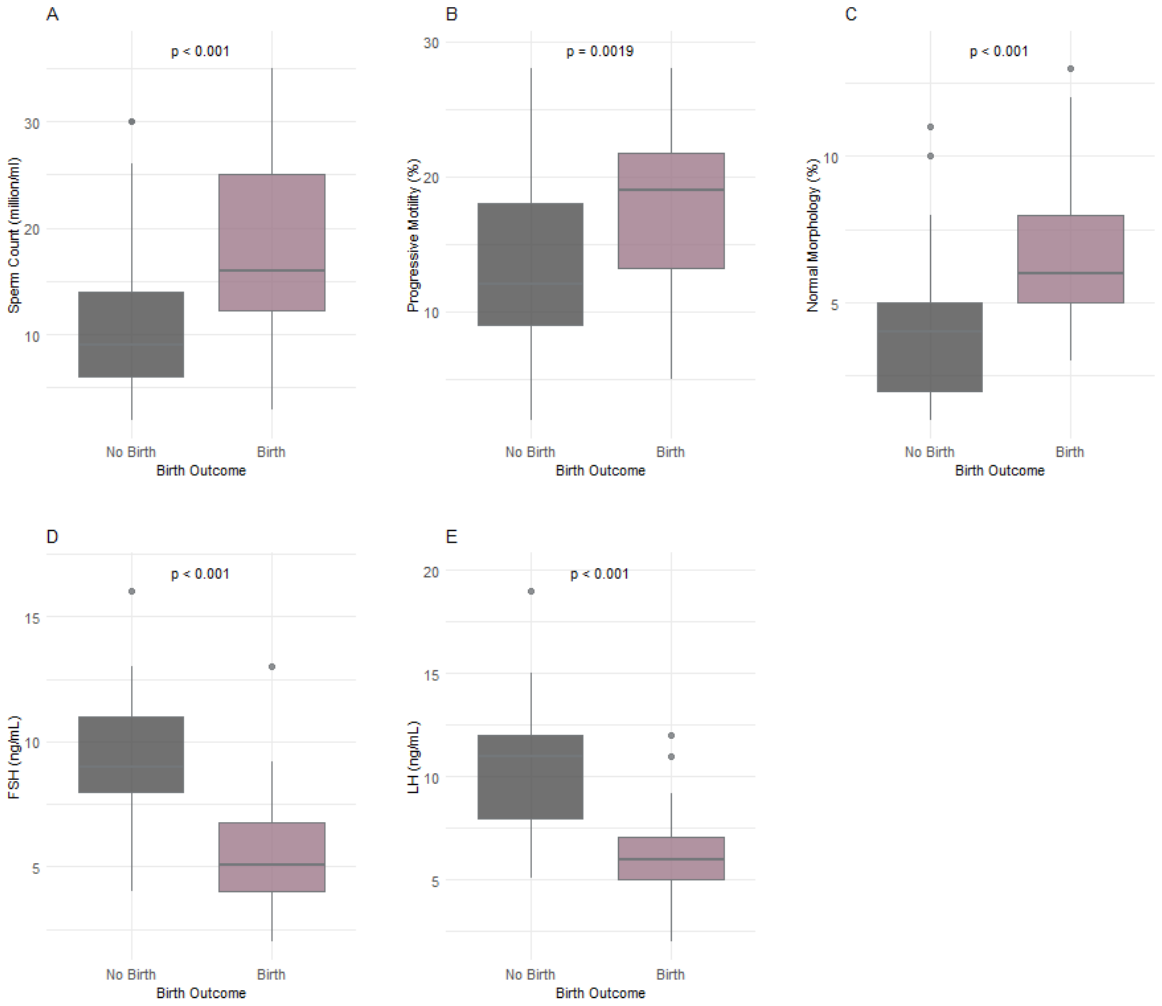

Figure 12. Association of Semen and Hormonal Parameters with Live Birth Outcomes.
(A) Sperm concentration (× 10^6/mL), **(B)** progressive motility (%), **(C)** normal morphology (%), **(D)** serum FSH levels (mIU/mL), and **(E)** serum LH levels (mIU/mL) presented as boxplots comparing individuals with and without a recorded live birth outcome. The birth group had considerably greater sperm count, motility, and morphology, but significantly lower levels of FSH and LH ($p < 0.001$ for all comparisons except motility, $p = 0.0019$). The Mann-Whitney U test was employed for statistical comparisons. In total, 85 samples were examined. Boxplots show outliers, interquartile ranges, and medians as separate points. A threshold of less than 0.05 for the adjusted *p*-value was used to evaluate statistical significance.

3.6 Expression Patterns of miRNAs in Relation to Age

We examined whether the age of male participants receiving infertility treatment was related to the expression levels of 16 selected miRNAs, as variables like age might affect miRNA expression. Each miRNA's expression levels were measured as *Δ*Ct, and their relationship to participant age was evaluated. Scatter plots for 16 distinct miRNAs, each demonstrating the correlation between expression levels and age, are shown in **Figure 13**. Distributional trends are presented by LOESS

regression lines, and each plot panel includes annotations for Spearman correlation coefficients (*r*) and their related p-values.

There was no statistically significant association between age and any of the miRNAs examined. For example, hsa-miR-106b-5p ($r = –0.06$, $p = 0.59$), hsa-miR-146a-5p ($r = –0.11$, $p = 0.33$), hsa-miR-149-5p ($r = –0.13$, $p = 0.25$), and hsa-miR-15a-5p ($r = 0.02$, $p = 0.85$) demonstrated weak and non-significant associations. Similarly, other miRNAs, including hsa-miR-15b-5p ($r = –0.01$, $p = 0.90$), hsa-miR-16-5p ($r = –0.09$, $p = 0.43$), hsa-miR-199a-5p ($r = –0.12$, $p = 0.31$), hsa-miR-199b-5p ($r = –0.14$, $p = 0.21$), and hsa-miR-19a-5p ($r = –0.16$, $p = 0.16$) showed negligible relationships with age as well.

Moreover, hsa-miR-20a-5p ($r = 0.00$, $p = 0.99$), hsa-miR-223-3p ($r = –0.17$, $p = 0.13$), and hsa-miR-335-5p ($r = –0.17$, p = 0.13) were in line with the general trend of non-significance. Similarly, hsa-miR-424-5p ($r = –0.07$, $p = 0.54$), hsa-miR-449a ($r = –0.12$, $p = 0.28$), hsa-miR-449b-5p ($r = –0.10$, $p = 0.37$), and hsa-miR-99a-5p ($r = –0.10$, $p = 0.40$) demonstrated non-significant correlation coefficients with no significant trends.

All relationships were not statistically significant and weak ($r \leq 0.17$), suggesting that age had no discernible impact on miRNA expression levels in this group. Age-related effects are thus unlikely to be the cause of the variations in miRNA expression demonstrated elsewhere in the thesis.

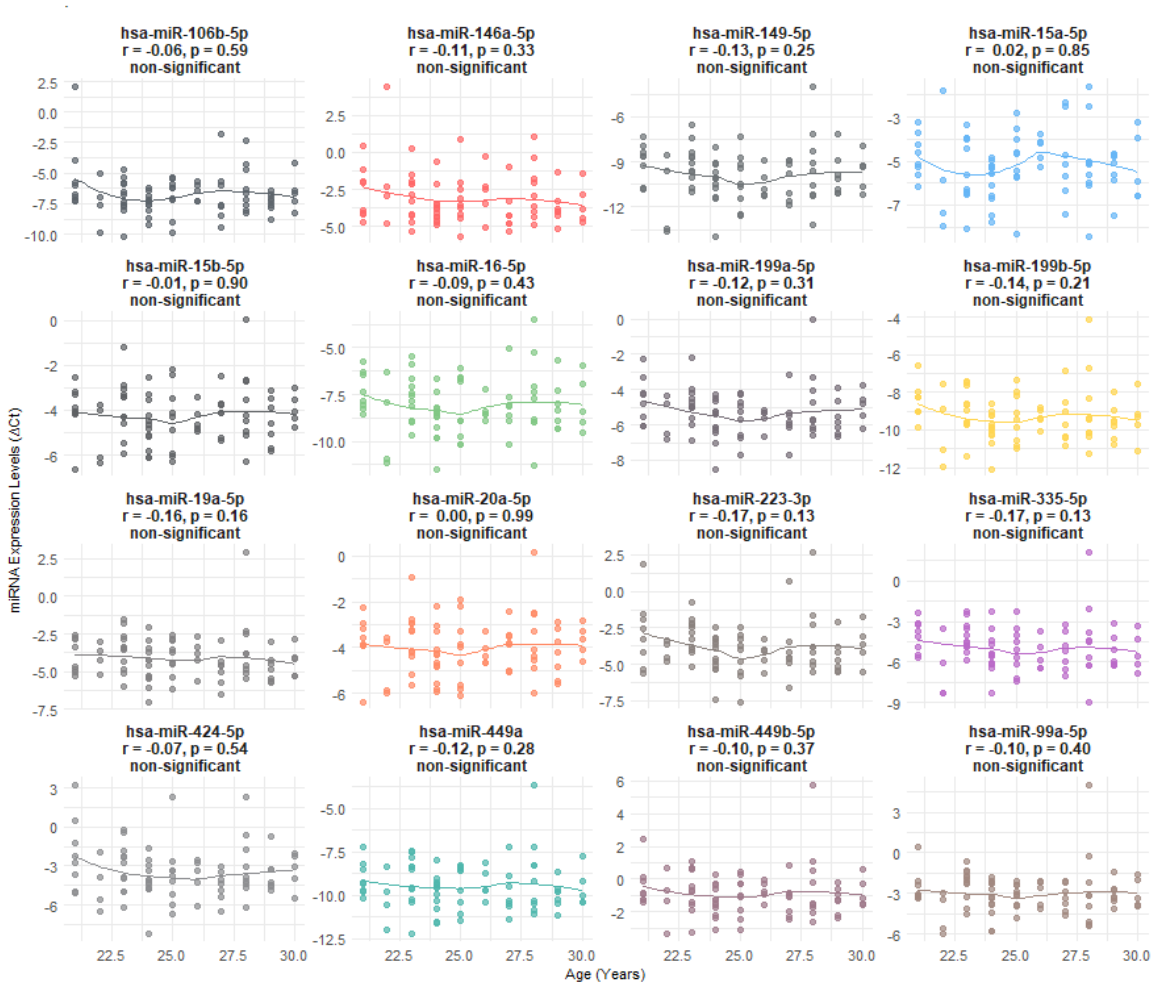

Figure 13. Association Between Age and the Expression of 16 Selected miRNAs.
Each dot represents a single subject in scatter plots that show the *Δ*Ct expression levels of 16 distinct miRNAs plotted against participant age (years). Age-specific expression patterns are demonstrated by LOESS regression lines. Each panel displays the corresponding p-values and Spearman correlation coefficients (*r*). There was no significant monotonic association between age and miRNA expression in this dataset, since all correlations were non-significant ($r \leq 0.17$). A threshold of less than 0.05 for the adjusted p-value was used to evaluate statistical significance.

3.7 Differential Expression of miRNAs Across Sperm Classification Groups

We analyzed *Δ*Ct expression levels among four sperm classification groups (OA, A, OAT, and AT) to determine if miRNA expression patterns vary across different sperm pathologies. The Kruskal–Wallis test and Benjamini–Hochberg correction were employed in the statistical analysis to limit the false discovery rate and account for multiple comparisons.

As observed in **Figure 14**, a number of miRNAs showed statistically significant differences in expression across the groups. With corrected *p*-values of 4.35×10^{-6}, hsa-miR-146a-5p and hsa-miR-19a-5p exhibited the most differences, indicating

substantial group-specific expression. Across the four sperm groups, these miRNAs demonstrated distinct expression stratification.

Hsa-miR-449b-5p (adjusted $p = 9.64 \times 10^{-6}$) and hsa-miR-199b-5p (adjusted $p = 2.14 \times 10^{-5}$) were two more miRNAs with considerable variation that frequently demonstrated intergroup differences. Similarly, hsa-miR-15b-5p and hsa-miR-20a-5p exhibited increased expression in certain sperm morphologies and were substantially different across groups (adjusted $p = 2.97 \times 10^{-5}$). Despite meeting the inclusion criterion, hsa-miR-99a-5p had the highest adjusted *p*-value (1.35×10^{-3}) among all substantially distinct miRNAs. Despite having a reduced effect size, the relationship was nonetheless statistically significant.

Different sperm groups demonstrated different expression patterns of numerous miRNAs, suggesting their potential use as molecular biomarkers for male infertility diagnosis.

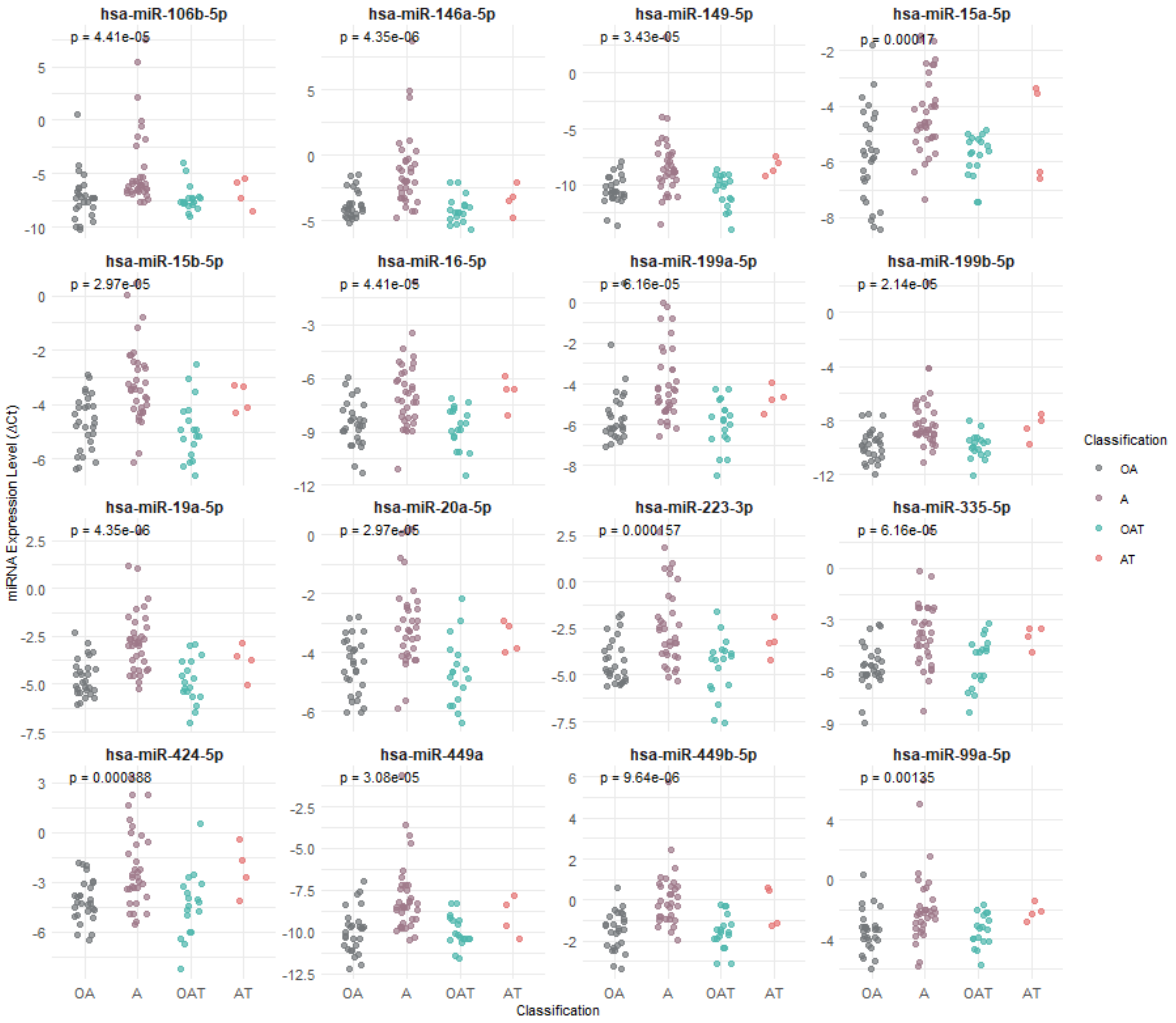

Figure 14. Expression Levels of miRNAs Across Four Sperm Classification Groups.
Dot plots displaying normalized *Δ*Ct values for 16 selected miRNAs across four sperm quality phenotypes: Asthenozoospermia (A, n = 35), Oligoasthenospermia (OA, n = 28), Oligoasthenoteratozoospermia (OAT, n = 18), and Asthenoteratozoospermia (AT, n = 4). To enhance visibility, each dot represents a single sample that has been jittered. *P*-values were corrected for multiple comparisons using the Benjamini–Hochberg method, and group-wise differences were examined using the Kruskal–Wallis test. Above each panel are the adjusted *p*-values. A threshold of less than 0.05 for the adjusted p-value was used to evaluate statistical significance.

3.8 miRNA Expression Levels Correlate with Basic Semen Parameters

A Spearman's rank correlation analysis was employed to investigate the link between miRNA expression and key semen quality indicators, such as sperm count, motility, morphology, and the percentage of immotile sperm. The strength and repeatability of the observed connections were highlighted by the derived correlation coefficients (*r*), which revealed similar patterns across datasets after being corrected for multiple comparisons.

3.8.1 Association Between miRNA Expression and Sperm Count

Spearman's correlation analysis was employed to correlate normalized *Δ*Ct expression data with sperm count values (million/mL) in order to explicitly investigate the association between miRNA expression and sperm concentration. The findings indicated an ongoing trend of statistically significant negative associations, suggesting that lower sperm counts were linked to increased expression levels of particular miRNAs.

Ten miRNAs showed significant negative relationships with sperm concentration, as shown in **Figure 15**, with correlation values ranging from $r = –0.614$ to $r = –0.704$. The strongest association was recognized for hsa-miR-19a-5p ($r = –0.704$, $p = 8.86 \times 10^{-13}$), followed by hsa-miR-449a ($r = –0.691$, $p = 2.78 \times 10^{-11}$) and hsa-miR-146a-5p ($r = –0.688$, $p = 6.1 \times 10^{-11}$).

Other miRNAs that demonstrated strong adverse relationships were hsa-miR-20a-5p ($r = –0.675$), hsa-miR-15a-5p ($r = –0.646$), hsa-miR-15b-5p ($r = –0.651$), hsa-miR-106b-5p ($r = –0.642$), and hsa-miR-149-5p ($r = –0.635$). Negative correlations were seen for hsa-miR-223-3p ($r = –0.615$) and hsa-miR-424-5p ($r = –0.614$), somewhat weaker but still substantial. After controlling for multiple comparisons, all found relationships remained highly significant, with *p*-values ranging from 10^{-9} to 10^{-13}.

These results imply that these miRNAs may serve as molecular markers of compromised spermatogenesis, as increased expression of these miRNAs is negatively correlated with sperm concentration.

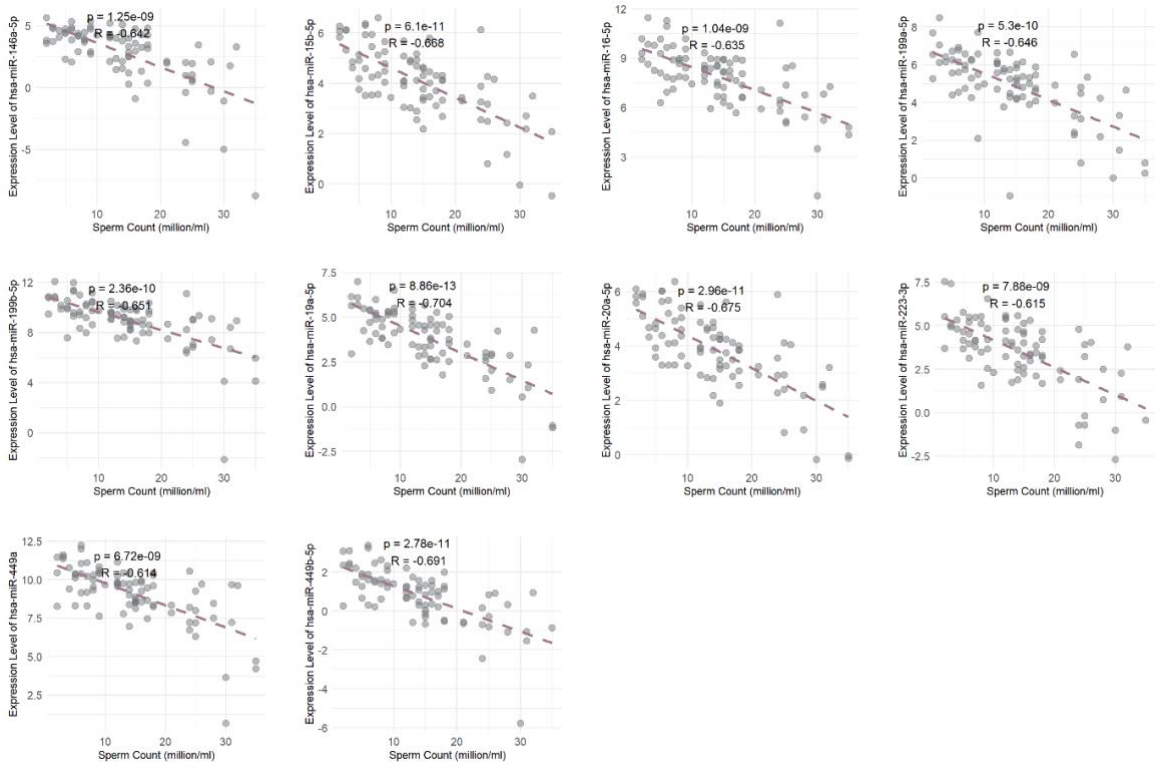

Figure 15. Correlation Between miRNA Expression and Sperm Count.
Scatter plots illustrating the inverse relationship between miRNA expression (*Δ*Ct values) and sperm concentration (× 10^6/mL) for ten selected miRNAs. A single sample (n = 85) is represented by each point, and the linear regression trend is shown by the dashed line. Only miRNAs having Spearman correlations (*r*, adjusted $p < 0.05$) that are statistically negative are shown. Strong, statistically significant associations are indicated by annotated correlation coefficients and *p*-values.

3.8.2 Association Between miRNA Expression and Progressive Sperm Motility

Using *Δ*Ct expression values from 85 semen samples, Spearman's rank correlation analysis was employed to examine the connection between miRNA expression and progressive sperm motility. The proportion of increasingly motile sperm and miRNA expression levels exhibited a continuous pattern of strong negative relationships, according to the results. All eight of the examined miRNAs exhibited statistically significant inverse relationships, as shown in **Figure 16**, with correlation coefficients (*r*) ranging from –0.751 to –0.827.

The greatest adverse relationship between these and progressive motility was shown by hsa-miR-449b-5p ($r = –0.827$, $p = 9.63 \times 10^{-20}$), followed by hsa-miR-424-5p ($r = –0.780$, $p = 2.26 \times 10^{-17}$), hsa-miR-20a-5p ($r = –0.766$, $p = 3.6 \times 10^{-16}$), and hsa-miR-199b-5p ($r = –0.764$, $p = 2.98 \times 10^{-16}$). Other miRNAs with strong inverse correlations involved hsa-miR-15b-5p ($r = –0.761$), hsa-miR-146a-5p ($r = –0.751$),

hsa-miR-18a-5p (*r* = –0.794), and hsa-miR-449a (*r* = –0.780). These findings demonstrate that progressive sperm motility significantly decreases as miRNA expression increases.

These results provide compelling evidence that decreased sperm motility corresponds to increased levels of these miRNAs. Their potential as molecular indicators of impaired sperm function, especially in motility-related male infertility, is supported by the consistency and intensity of these relationships.

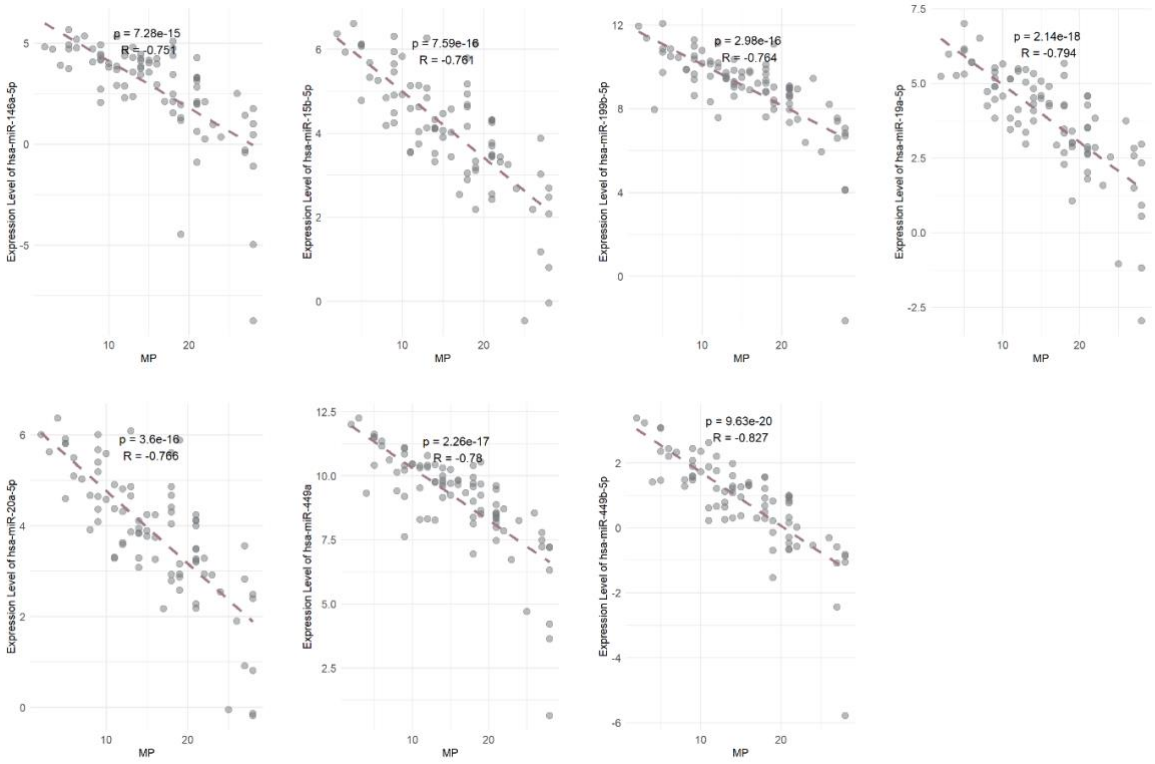

Figure 16. Correlation Between miRNA Expression and Progressive Sperm Motility.

Scatter plots depicting the expression levels (*Δ*Ct values) of eight selected miRNAs plotted against progressive sperm motility (MP, %) in 85 semen samples. A single sample is represented by each point, and the linear trend is shown by dashed lines. With adjusted *p*-values ≤ 0.05 and Spearman's correlation coefficients (*r*) ranging from –0.751 to –0.827, each correlation shown is statistically significant.

3.8.3 Association Between miRNA Expression and Immotile Sperm Percentage

Using *Δ*Ct values from 85 samples, Spearman's rank correlation analysis was used to investigate the link between miRNA expression levels and the percentage of immotile spermatozoa (IM). A continuous pattern of statistically significant positive

associations was found in the research, suggesting that higher expression levels of certain miRNAs are linked to a higher proportion of immotile sperm. **Figure 17** illustrates that the correlation coefficients (*r*) for each of the ten examined miRNAs ranged from 0.556 to 0.645, with adjusted *p*-values < 1×10^{-6}.

Among these, hsa-miR-15b-5p ($r = 0.636$, $p = 1.27 \times 10^{-9}$) and hsa-miR-20a-5p ($r = 0.645$, $p = 5.9 \times 10^{-10}$) demonstrated the strongest relationships with higher percentages of immotile sperm. Other miRNAs demonstrating similarly strong correlations involved hsa-miR-16-5p ($r = 0.587$), hsa-miR-19a-5p ($r = 0.578$), and hsa-miR-149-5p ($r = 0.564$). Additional miRNAs, including hsa-miR-223-3p ($r = 0.562$), and hsa-miR-424-5p ($r = 0.556$) also showed statistically significant positive relationships.

These results imply that a larger percentage of immotile spermatozoa may be a result of decreased sperm motility caused by increased expression of these miRNAs. Their potential use as molecular indicators of impaired spermatogenesis is supported by these expression patterns.

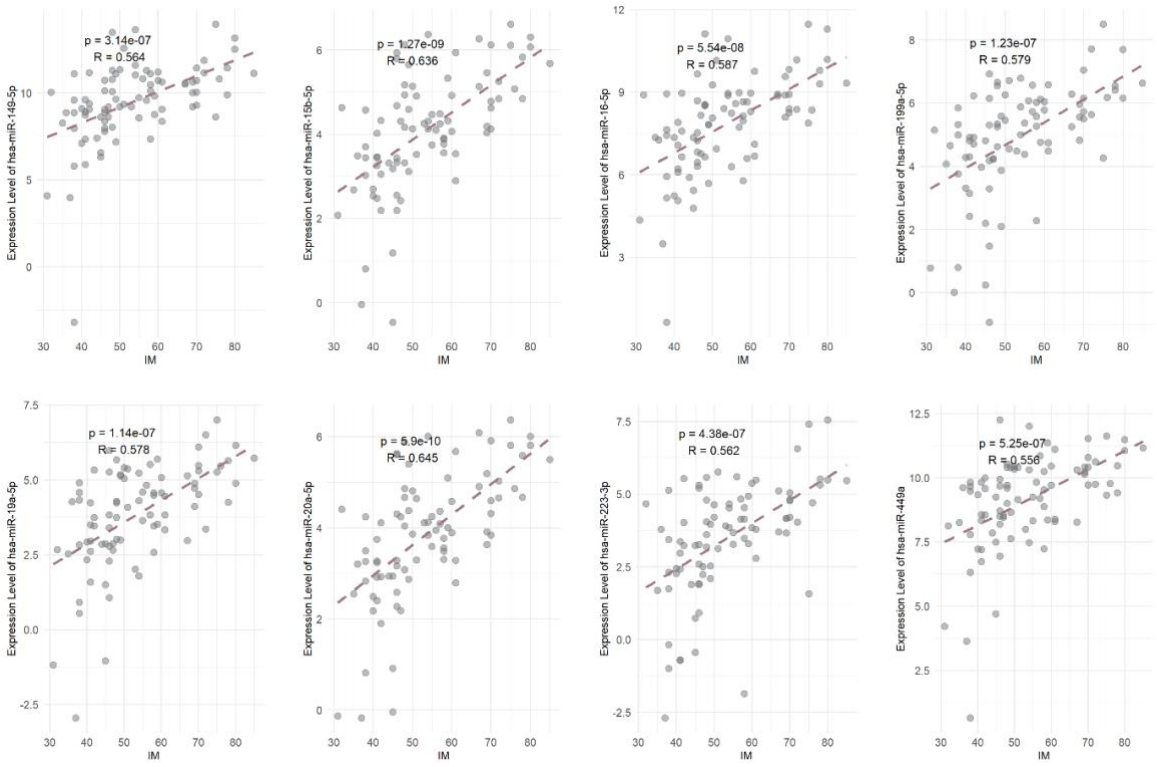

Figure 17. Correlation Between miRNA Expression and Immotile Sperm Percentage.
Scatter plots displaying the expression levels (*Δ*Ct values) of ten selected miRNAs plotted against immotile sperm percentage (IM, %) across 85 semen samples. The linear regression trend is shown by dashed lines, with each point representing a distinct sample. Spearman correlation coefficients (r) ≥ 0.556 and adjusted p-values ≤ 0.05 demonstrate that every correlation is statistically significant.

3.8.4 Association Between miRNA Expression and Sperm Morphology

Using *Δ*Ct values from 85 semen samples, Spearman's rank correlation analysis was employed to assess the association between miRNA expression and the percentage of morphologically normal spermatozoa. For each of the five miRNAs examined, the findings indicated modest but statistically significant negative associations between miRNA expression and normal morphology (**Figure 18**).

The correlation coefficients (r) ranged from –0.425 to –0.449, with adjusted p-values between 0.0003 and 0.0008. Specifically, hsa-miR-146a-5p (r = –0.449, p = 0.00038), hsa-miR-15b-5p (r = –0.444, p = 0.0004), and hsa-miR-19a-5p (r = –0.434, p = 0.0005) demonstrated the strongest adverse relationships with sperm morphology. Moreover, hsa-miR-20a-5p (r = –0.425, p = 0.0009) and hsa-miR-449b-5p (r = –0.442, p = 0.0007) showed statistically significant inverse relationships.

The continuously negative trends indicate that increased expression of these miRNAs may lead to less favorable sperm morphology, even if the strength of these relationships was not as strong as those demonstrated for sperm count and motility. These results confirm their significance as molecular markers of poor sperm quality.

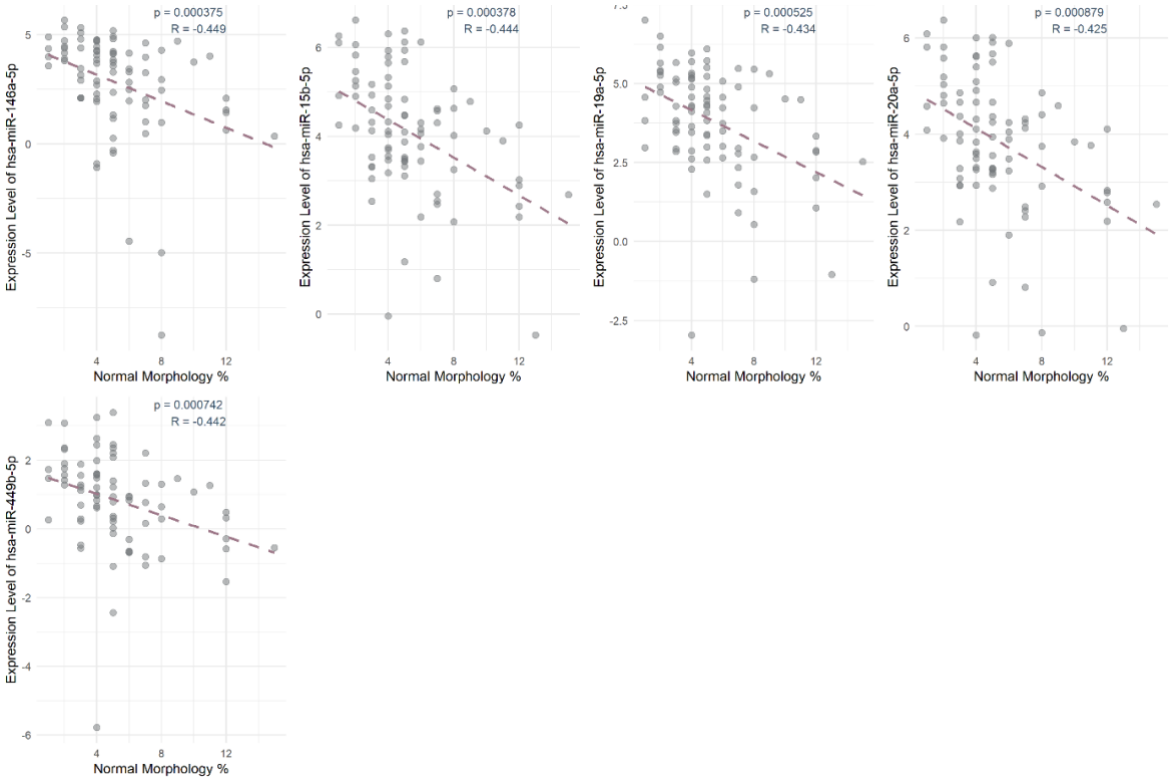

Figure 18. Correlation Between miRNA Expression and Normal Sperm Morphology.
Scatter plots displaying the inverse expression levels (*Δ*Ct values) of five selected miRNAs plotted against normal sperm morphology (%) across 85 semen samples. The dashed line represents the linear regression trend, whereas each dot represents a separate sample. Every miRNA shown had negative Spearman correlation coefficients (*r*) that were statistically significant, with adjusted *p*-values ≤ 0.05.

3.9 Correlation Between miRNA Expression Levels and Hormonal Parameters

3.9.1 Association Between miRNA Expression and Serum FSH Levels

Spearman's rank correlation analysis was applied to evaluate the association between circulating blood FSH concentrations and miRNA expression levels. All examined miRNAs exhibited statistically significant positive relationships with serum FSH levels, as demonstrated in **Figure 19**, with adjusted p-values less than 0.01 and correlation coefficients (*r*) ranging from 0.365 to 0.469.

The strongest relationships were seen for hsa-miR-15a-5p (r = 0.469, p = 0.0001), hsa-miR-20a-5p (r = 0.458, p = 0.0002), and hsa-miR-449b-5p (r = 0.438,

p = 0.0009). Additional robust relationships involved hsa-miR-449a (*r* = 0.439, p = 0.0035), hsa-miR-16-5p (*r* = 0.414, *p* = 0.0013), and hsa-miR-199b-5p (*r* = 0.403, *p* = 0.0021). It is noteworthy that hsa-miR-223-3p (*r* = 0.387, *p* = 0.0040), hsa-miR-335-5p (*r* = 0.373, *p* = 0.0081), hsa-miR-149-5p (*r* = 0.374, *p* = 0.0068), hsa-miR-15b-5p (*r* = 0.365, *p* = 0.0094), hsa-miR-18a-5p (*r* = 0.446, *p* = 0.0001), and hsa-miR-19a-5p (*r* = 0.388, *p* = 0.0041) demonstrated statistically significant relationships as well.

These results demonstrate a similar pattern linking increased serum FSH levels to greater miRNA expression, indicating that these miRNAs may be involved in the control or response to gonadotropic signaling.

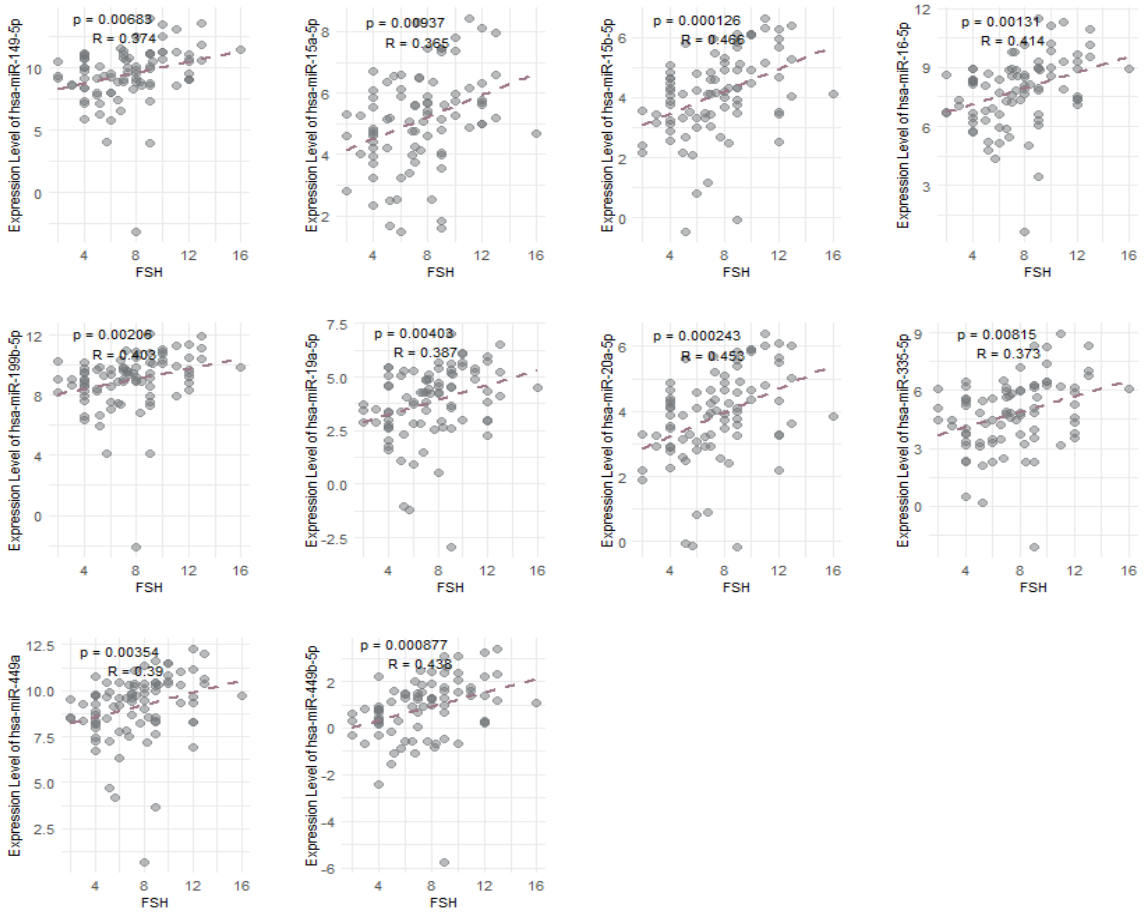

Figure 19. Correlation Between miRNA Expression and Serum Follicle-Stimulating Hormone (FSH) Concentrations.
Scatter plots demonstrating the correlation between serum FSH concentrations (mIU/mL) and miRNA expression levels (*Δ*Ct values) in 85 semen samples. Only miRNAs with statistically significant Spearman correlation coefficients (*r*) and adjusted *p*-values ≤ 0.05 are demonstrated. A single sample is represented by each point, and the linear trend is shown by the dashed line.

3.9.2 Association Between miRNA Expression and Serum LH Levels

The association between blood LH concentrations and the expression levels of particular miRNAs was assessed using Spearman's rank correlation analysis. LH levels and the expression of all three examined miRNAs demonstrated modest but statistically significant positive relationships, shown in **Figure 20**.

Among these, hsa-miR-15b-5p indicated the strongest relationship (r = 0.432, p = 0.00064), followed closely by hsa-miR-20a-5p (r = 0.425, p = 0.0009) and hsa-miR-19a-5p (r = 0.335, p = 0.0277). All three miRNAs exhibited statistically significant positive correlations, indicating a persistent pattern in which greater LH levels are related to increased miRNA expression, even if the degree of these connections was considerably smaller than that observed with FSH levels.

These results suggest that these miRNAs may be involved in LH-mediated pathways or serve as biomarkers for changes in the activity of the hypothalamic-pituitary-gonadal axis.

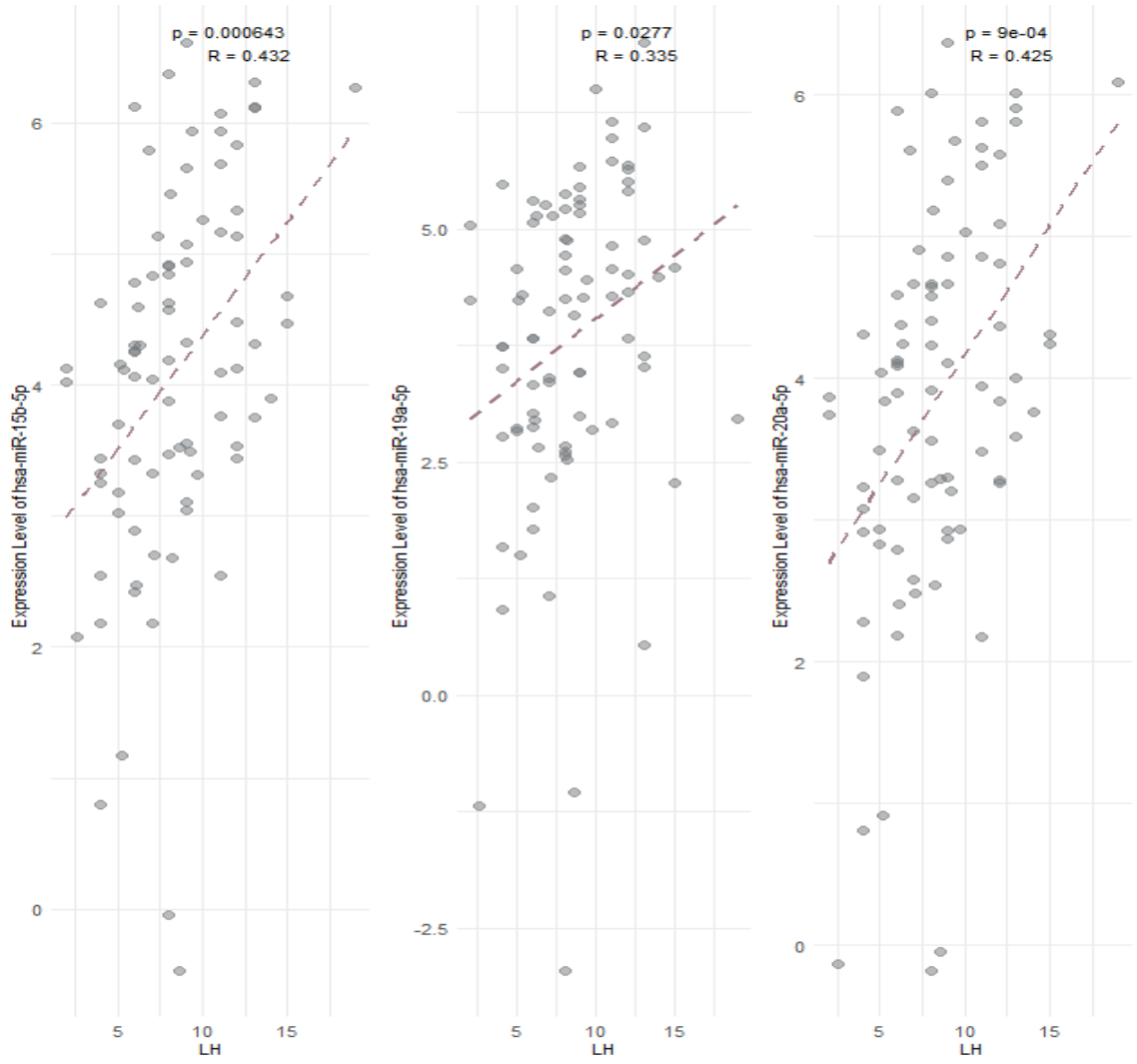

Figure 20. Correlation Between miRNA Expression and Serum Luteinizing Hormone (LH) Concentrations.
Scatter plots demonstrating the correlation between miRNA expression levels (*Δ*Ct values) and serum LH concentrations (mIU/mL) across 85 semen samples. Only miRNAs with statistically significant Spearman correlation coefficients (*r*) and adjusted *p*-values ≤ 0.05 are demonstrated. Each dot shows an individual sample, and the dashed line denotes the linear trend.

3.9.3 Key miRNAs Linked to Sperm Count, Motility, and Morphology

While many miRNAs showed weak or non-significant associations, a specific subset of miRNAs, namely hsa-miR-15b-5p, hsa-miR-19a-5p, and hsa-miR-20a-5p, consistently demonstrated strong and statistically significant correlations across all examined parameters, according to a thorough correlation analysis among miRNA expression levels and core semen quality parameters. These correlations were observed in both the screening and validation datasets and remained significant when multiple comparisons were corrected ($p < 0.001$).

Additionally, the expression of all three miRNAs demonstrated a positive association with the proportion of IM and a negative correlation with sperm count, PM, and normal morphology (M). Each of these miRNAs had a consistent directional trend across the four semen variables, as demonstrated in **Figure 21**.

- hsa-miR-15b-5p demonstrated significant inverse correlations with:
  - Sperm count ($r = –0.668$, $p = 3.82 \times 10^{-12}$),
  - PM ($r = –0.761$, $p = 4.74 \times 10^{-17}$),
  - Morphology ($r = –0.444$, $p = 2.37 \times 10^{-5}$),
  - and a positive correlation with IM ($r = 0.636$, $p = 7.91 \times 10^{-11}$).
- hsa-miR-19a-5p demonstrated:
  - Strong negative correlations with sperm count ($r = –0.704$), PM ($r = –0.794$), and morphology ($r = –0.434$),
  - Positive correlation with IM ($r = 0.578$), all with adjusted p-values well below 10^{-8}.
- hsa-miR-20a-5p mirrored these trends with:
  - Negative correlations with sperm count ($r = –0.675$), PM ($r = –0.766$), and morphology ($r = –0.425$),
  - Positive correlation with IM ($r = 0.645$), all statistically significant ($p < 10^{-5}$).

Overall, our results indicate a direct negative correlation between high levels of these miRNAs and fundamental sperm quality measures. These relationships' constant strength and directionality lend credence to the possibility that hsa-miR-15b-5p, hsa-miR-19a-5p, and hsa-miR-20a-5p are negative regulatory indicators of spermatogenesis or sperm function.

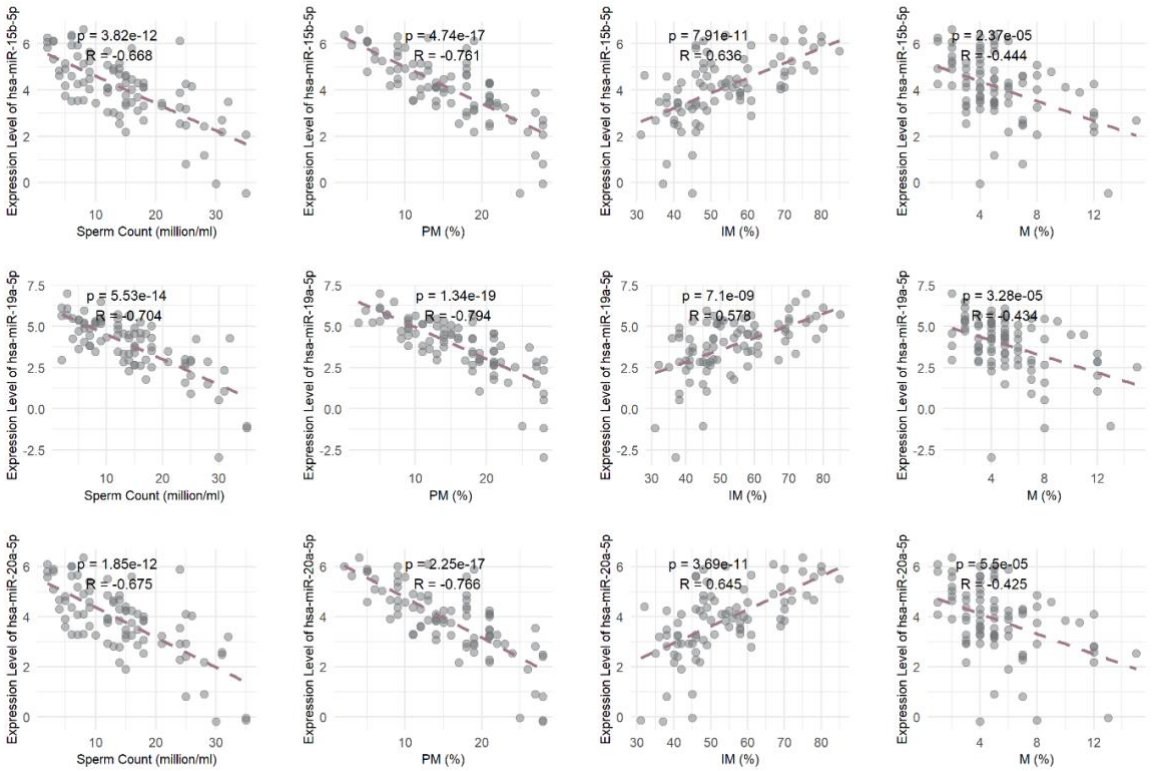

Figure 21. Correlation of key miRNAs with Sperm Concentration, Motility, and Morphology. Scatter plots demonstrating the inverse expression levels (*Δ*Ct values) of three miRNAs — hsa-miR-15b-5p, hsa-miR-19a-5p, and hsa-miR-20a-5p — in relation to four semen parameters: sperm count (million/mL), progressive motility (PM, %), immotile sperm (IM, %), and normal morphology (M, %) across 85 semen samples. The dashed line represents the linear regression trend, whereas each point represents a distinct sample. Each connection that is demonstrated is statistically significant (adjusted $p \leq 0.05$).

3.10 miRNA Expression and Its Association with Embryo Development and Pregnancy Outcomes

We evaluated the expression levels of particular miRNAs in connection to pregnancy markers and embryo morphology in order to gain insight into the clinical significance of these miRNAs in ART.

3.10.1 Association Between miRNA Expression and Embryo Morphological Quality

Samples were organized by embryo grade in order to assess the correlation between sperm-derived miRNA expression and embryo morphological quality. MiRNA expression was evaluated between G1 and G2 embryos, which correspond to the top two groups in a standardized four-grade system (G1–G4). Due to their low engagement in the cohort, grades G3 and G4 were eliminated.

Two of the examined miRNAs, hsa-miR-15b-5p and hsa-miR-20a-5p, showed noticeably lower expression levels in G1 embryos than in G2. Reduced miRNA expression in embryos of superior morphological grade was demonstrated by higher ΔCt values in the G1 group (**Figure 22**). Specifically:

- hsa-miR-15b-5p showed a statistically significant reduction in expression in G1 embryos (adjusted $p = 0.0151$, $\log_2FC = 1.21$).
- hsa-miR-20a-5p displayed a similar pattern (adjusted $p = 0.0158$, $\log_2FC = 1.21$).

These results support their potential function as molecular markers of decreased developmental competence by indicating that increased expression of hsa-miR-15b-5p and hsa-miR-20a-5p may be adversely correlated with embryo morphological quality.

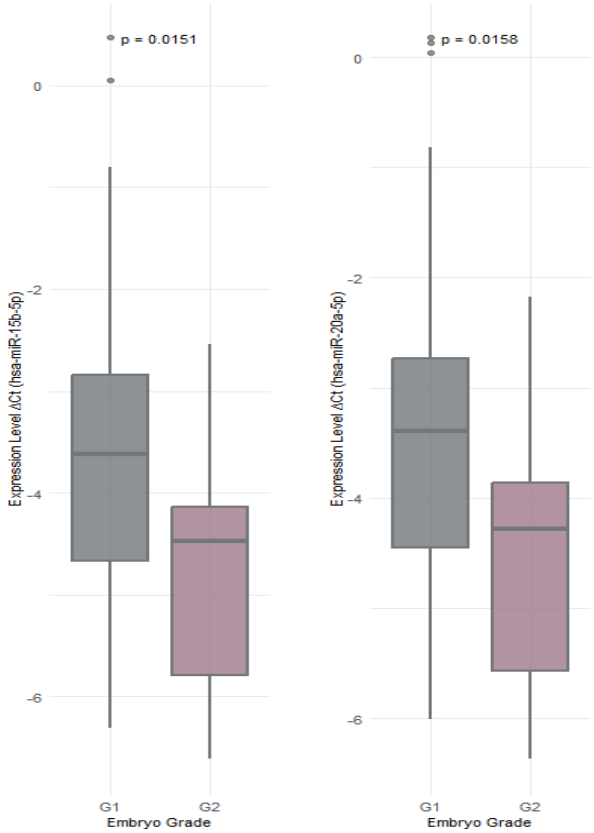

Figure 22. Association Between miRNA Expression and Embryo Morphological Grade.
Boxplots demonstrating the relative expression levels (*ΔCt* values) of two sperm-expressed miRNAs (hsa-miR-15b-5p and hsa-miR-20a-5p) in high-quality (G1) versus lower-quality (G2) groups of embryos. Expression was analyzed by utilizing the Mann–Whitney U test, with statistical significance defined as an adjusted *p*-value < 0.05. Higher values of *ΔCt* show lower miRNA expression. Boxes show interquartile ranges (IQR), medians are implied by horizontal lines, and whiskers extend to 1.5× IQR. G1 embryos showed significant decreases in expression.

3.10.2 miRNA Expression and Association with Early Pregnancy Outcome (β-hCG Status)

We assessed the expression levels of 16 specific miRNAs across individuals who had positive and negative β-hCG values after embryo transfer in order to investigate the connection between sperm-derived miRNA expression and early pregnancy outcomes.

Four of the 16 miRNAs that were examined—hsa-miR-15b-5p, hsa-miR-19a-5p, hsa-miR-20a-5p, and hsa-miR-449b-5p—showed statistically significant differences in expression across the groups (**Figure 23**). In comparison to those who had successful implantation, these miRNAs exhibited increased expression in the β-hCG negative group, which was demonstrated by lower ΔCt values. This adverse connection raises the possibility that increased miRNA expression and pregnancy success are negatively correlated.

The following corrected p-values and related $\log_2$ fold changes ($\log_2$FC) were obtained after expression levels were evaluated:

- hsa-miR-15b-5p: $p = 5.3 \times 10^{-3}$, $\log_2$FC = 1.21
- hsa-miR-19a-5p: $p = 4.86 \times 10^{-2}$, $\log_2$FC = 1.10
- hsa-miR-20a-5p: $p = 7.62 \times 10^{-3}$, $\log_2$FC = 1.21
- hsa-miR-449b-5p: $p = 4.42 \times 10^{-2}$, $\log_2$FC = 1.25

These results imply that elevated expression of these particular sperm-expressed miRNAs may function as unfavorable indicators of implantation success, providing possible therapeutic significance in the context of ART.

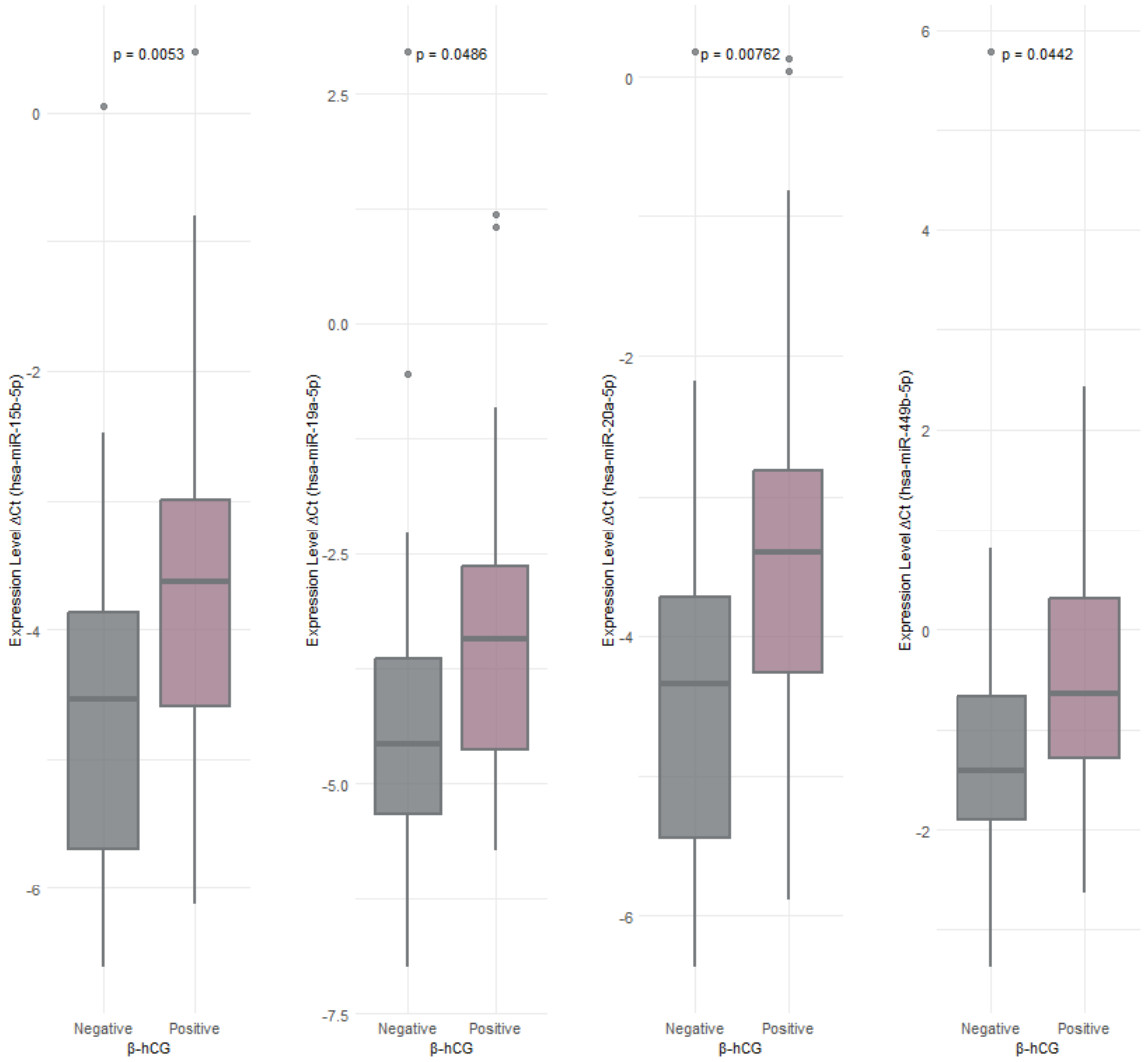

Figure 23. Association of miRNA Expression with Early Pregnancy Outcome.
Boxplots demonstrating the relative expression levels (*Δ*Ct values) of sperm-expressed miRNAs in individuals with negative and positive β-hCG results. The Mann-Whitney U test was employed to assess expression differences, and all comparisons exceeded the significance level (adjusted $p < 0.05$). A miRNA that is strongly linked to the outcome of pregnancy is displayed in each panel. Lower expression levels are correlated with higher *Δ*Ct values. Whiskers extend to 1.5× IQR, medians are shown as horizontal lines, and boxes represent the interquartile range (IQR).

3.10.3 miRNA Expression in Relation to IVF Outcome (Live Birth)

We examined miRNA levels in a cohort of 85 individuals in order to investigate the relationship between sperm-derived miRNA expression and IVF success rate. Among them, 14 samples with missing clinical outcomes were removed from the study, 41 samples were categorized as failed IVF outcomes (negative β-hCG), and 30 samples were associated with successful live births (as shown in **Table 12**).

Three miRNAs—hsa-miR-15b-5p, hsa-miR-19a-5p, and hsa-miR-20a-5p—of the 16 miRNAs examined exhibited noticeably lower ΔCt values in the unsuccessful IVF group, suggesting that their expression levels were higher than those of the group that had a successful live birth (**Figure 24**). The following outcomes demonstrated that the differences in expression were statistically significant:

- hsa-miR-15b-5p: $p = 2.92 \times 10^{-3}$, $\log_2 FC = 1.22$
- hsa-miR-19a-5p: $p = 4.11 \times 10^{-2}$, $\log_2 FC = 1.10$
- hsa-miR-20a-5p: $p = 5.83 \times 10^{-3}$, $\log_2 FC = 1.22$

The found lower ΔCt values in the failed IVF group represent greater expression of these miRNAs in people who did not achieve a live birth. This is significant since higher ΔCt values indicate decreased miRNA expression.

These results imply that elevated expression of hsa-miR-15b-5p, hsa-miR-19a-5p, and hsa-miR-20a-5p is adversely correlated with successful IVF outcomes and might be utilized as non-invasive biomarkers to predict the success of live birth in ART.

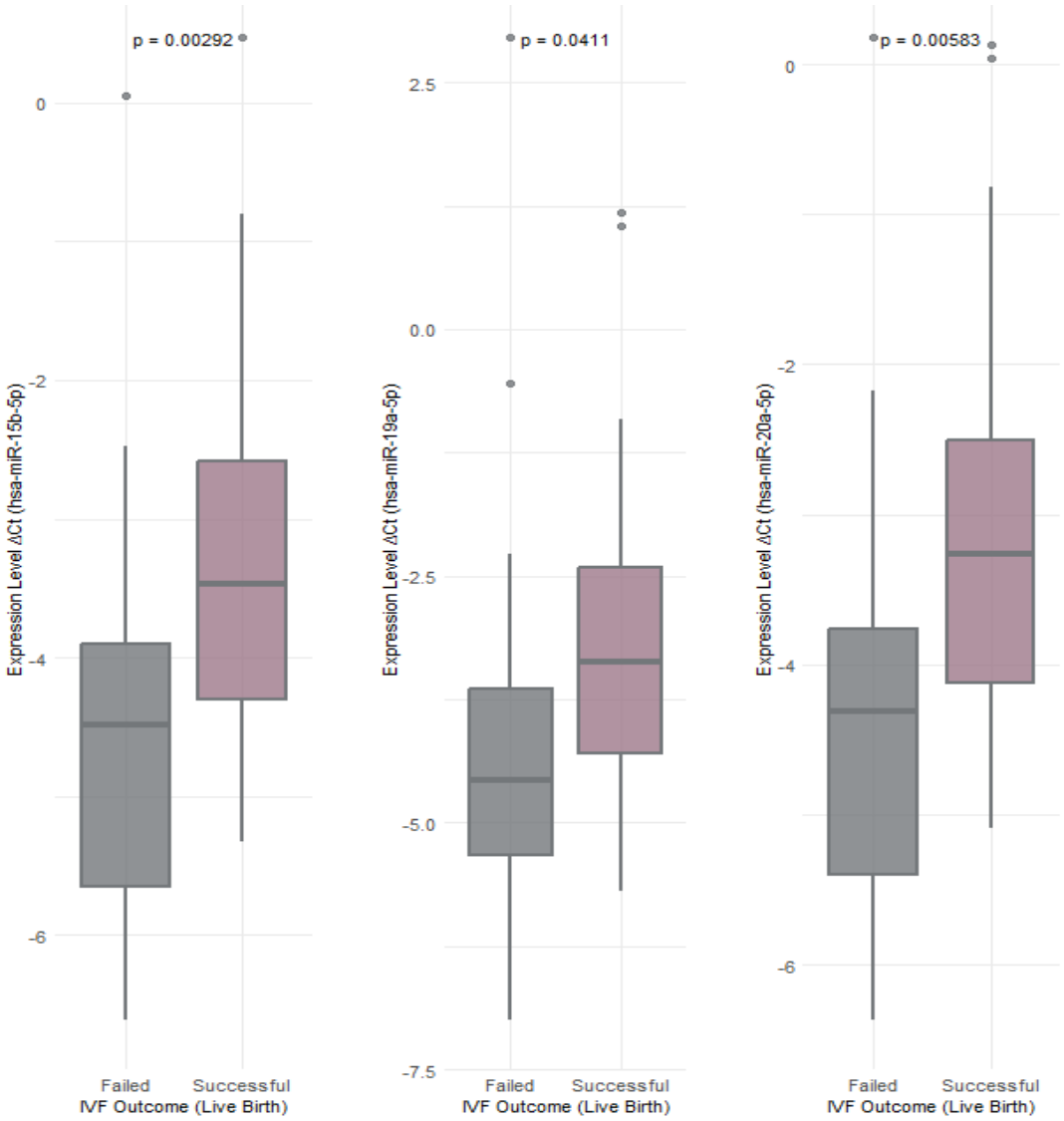

Figure 24. Association of miRNA Expression with IVF Outcomes (Live Birth).
Boxplots demonstrating the relative expression levels (*Δ*Ct values) of sperm-expressed miRNAs in individuals with failed and successful IVF results (live birth). Statistical significance was assessed using the Mann–Whitney U test (adjusted $p < 0.05$). One miRNA that is substantially linked to the prognosis of IVF can be seen in each panel. Lower miRNA expression is correlated with higher *Δ*Ct values. Whiskers extend to 1.5× IQR, horizontal lines indicate the median, and boxes indicate interquartile ranges (IQR).

3.11 Diagnostic Performance of Sperm-Expressed miRNAs in Predicting IVF Outcomes

In order to investigate the clinical value of sperm-expressed miRNAs as predictive biomarkers for the outcomes of IVF treatment (live birth), we evaluated the diagnostic performance of three miRNAs that have been related to sperm quality and implantation success: hsa-miR-15b-5p, hsa-miR-19a-5p, and hsa-miR-20a-5p.

The investigation comprised 71 semen samples with verified clinical results (30 live births and 41 unsuccessful IVF cycles). Logistic regression models were employed to analyze Receiver Operating Characteristic (ROC) curves, and the Area Under the Curve (AUC) was computed to evaluate diagnostic accuracy.

All three miRNAs demonstrated statistically significant AUC values, showing prognostic usefulness for IVF results, as shown in **Figure 25**:

- hsa-miR-15b-5p: AUC = 0.76, 95% CI: 0.64–0.87; $p = 9.11 \times 10^{-5}$
- hsa-miR-20a-5p: AUC = 0.74, 95% CI: 0.63–0.86; $p = 0.0002$
- hsa-miR-19a-5p: AUC = 0.71, 95% CI: 0.59–0.83; $p = 0.0013$

We developed a multivariate logistic regression model using all three miRNAs to determine if combinatorial expression patterns may improve prediction. Although somewhat different from individual performance, the combined model produced an AUC of 0.75 (95% CI: 0.63–0.86; $p = 0.0001$), indicating that the combined use of these markers possesses complementary diagnostic value.

Overall, our results demonstrate the diagnostic potential of hsa-miR-19a-5p, hsa-miR-15b-5p, and hsa-miR-20a-5p as non-invasive sperm-based biomarkers for predicting the outcome of IVF. These miRNAs, whether used alone or in a panel, might be beneficial tools for improving ART and individualized reproductive options for treatment.

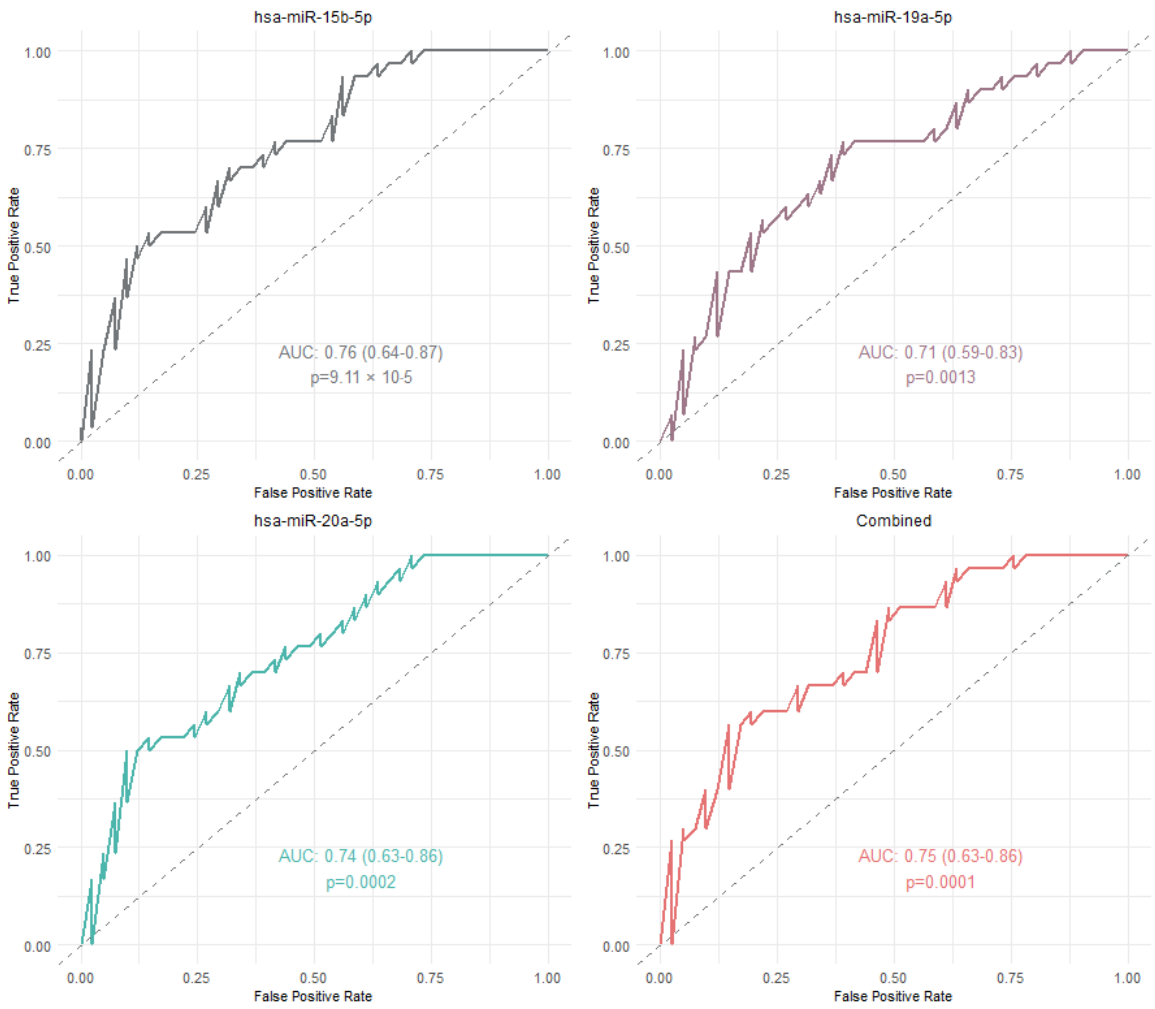

Figure 25. Diagnostic Performance of Individual and Combined miRNAs**.**
Receiver Operating Characteristic (ROC) curves demonstrating the diagnostic performance of three sperm-expressed miRNAs—hsa-miR-15b-5p, hsa-miR-19a-5p, and hsa-miR-20a-5p, and their combined expression profile. The AUC values, 95% CI, and adjusted p-values are shown for each curve. Diagnostic accuracy was determined by utilizing logistic regression, with statistical significance defined as adjusted $p < 0.05$.

4. Discussion

We performed a validation study on 85 male partners of couples receiving infertility therapy for this thesis. Samples of semen were taken from people without any previous individual selection, and they were then purified in compliance with WHO guidelines [1]. According to Al Samdi et al., this independent cohort served as a foundation for RT-qPCR validation of the miRNA candidates found by small RNA sequencing (**Table 2**) [167].

Our results are in line with earlier research demonstrating that abnormal sperm motility and morphology might have a detrimental effect on embryo growth and viability, reducing ART success rates [164,168]. These findings underline the necessity of molecular-based biomarkers, such as particular miRNA signatures, that can supplement and improve the predictive ability of traditional semen analysis in clinical evaluation of male fertility potential and support the significance of male gamete quality in determining IVF outcomes.

Higher semen quality, as indicated by higher sperm count, progressive motility, and normal morphology, was significantly linked to better embryo morphological grades and higher pregnancy success rates, according to analyses conducted across both screening and validation cohorts [167,169,170]. For instance, the proportion of normal morphology was considerably greater in G1-associated samples than in G2 embryos (p = 0.0017), and sperm counts among embryos of the best morphological grade (G1) showed a strong positive connection with motility ($r \approx 0.80$, $p < 0.0001$). Lower-grade embryos (G3–G4) tended to be connected to lower sperm counts, decreased motility, and inadequate morphology, whereas G1 embryos, which reflect the highest level of developmental quality, were most often linked to semen profiles within the top quartile for these parameters.

Reduced serum levels of FSH and LH in female partners were also linked to favorable reproductive outcomes, such as biochemical pregnancy (i.e., β-hCG positive) and live birth [169-171]. Baseline FSH and LH levels were significantly lower in women in the β-hCG positive group (~2–6 mIU/mL in the pregnant group vs. >10–

15 mIU/mL in the non-pregnant group, $p < 0.001$). On the other hand, deficient morphology, increased gonadotropin levels, and decreased motility were more often associated with negative outcomes, including miscarriage, abnormal hormone levels, or implantation failure. The effect of poor sperm quality on embryo viability may be exacerbated by elevated FSH and LH in the female partner, which may be a sign of decreased ovarian reserve or changed folliculogenesis. These results highlight the fact that both couples' combined reproductive health is essential to the effectiveness of ART [172,173].

Our results and those of others indicate that traditional semen analysis is still the predominant diagnostic method for male infertility, although it is not a complete explanation for negative reproductive outcomes [174,175]. Males with WHO-defined normal sperm parameters yet had poor embryo development or failed implantation in a number of cases, suggesting the existence of subtle or idiopathic male variables that are not picked up by standard testing. Even when fundamental sperm metrics seem normal, they might include molecular-level defects, including abnormal chromatin packaging, DNA damage, or dysregulated RNA or small RNA expression that could impair embryo development [30,158,165,176,177]. In comparison to the non-pregnant group, male partners of women with positive β-hCG findings demonstrated substantially higher normal morphology (4–12% vs. <4%, $p < 0.001$), progressive motility (15–25% vs. <10%, $p < 0.001$), and median sperm concentration ($p < 0.001$). These results highlight the need for tests that more accurately represent the molecular integrity of sperm and go beyond standard semen analysis. Normal WHO semen standards do not rule out the occurrence of abnormalities that might negatively impact embryo development or implantation, as shown by our thesis and other investigations. The present thesis examines sperm-derived miRNAs as a biologically pertinent method of identifying such subclinical defects in spermatogenesis or sperm function. In the context of IVF and ICSI, using miRNA-based biomarkers in male fertility evaluation might increase diagnostic accuracy.

It is becoming increasingly acknowledged that small non-coding RNAs, especially miRNAs, are important regulators of male fertility, sperm function, and pregnancy outcomes [132,149,150,155,156,165,176-183]. In this thesis, we verified a panel of

16 miRNAs that showed differences in expression between sperm samples of good and poor quality, as determined by progressive motility and sperm morphology [167].

The idea that sperm-borne small RNAs directly influence male reproductive capacity is supported by these findings [167,184,185]. This is in line with increasing evidence showing that sperm RNAs, including miRNAs, actively participate in regulatory mechanisms throughout spermatogenesis, sperm maturation, and even activities that occur after fertilization [126,131]. The varied and functionally relevant repertoire of small RNAs carried by mature spermatozoa, despite their transcriptional inactivity, is becoming more well acknowledged for its functions in fertilization, the acrosome response, capacitation, and early embryonic development [126,131,184,185].

Our results demonstrate that dysregulated expression of key sperm miRNAs was consistently connected to inferior fertilization and embryo development outcomes, as well as decreased semen quality, namely decreased motility, abnormal morphology, and increased immotile sperm [177-181]. Strong positive correlations between semen parameters (progressive sperm count, motility, and morphology) and embryo quality were found in correlation analyses, which are consistent with other studies. Higher motility and a higher percentage of morphologically normal sperm predicted high-grade (G1) embryos [183]. On the other hand, lower-grade embryos were linked to ejaculates with limited motility and high rates of morphological defects. This correlation persisted throughout ICSI cycles. Even though ICSI may fertilize sperm with less-than-ideal morphology, the resulting embryos frequently demonstrated lower developmental competence, lower implantation rates, and a higher frequency of chromosomal abnormalities [186,187]. This implies that spermatozoa's molecular and structural integrity is essential for maintaining embryogenesis, promoting successful implantation, and starting fertilization. The evidence for the use of molecular biomarkers in addition to standard semen analysis to allow earlier diagnosis of subclinical sperm abnormalities that may otherwise jeopardize the effectiveness of IVF or ICSI is strengthened by the connections found between miRNA dysregulation and negative ART results.

Numerous studies have demonstrated that prolonged paternal age may have a detrimental impact on semen quality, reproductive success, and even the long-term health of children, underscoring the growing recognition of paternal age as a significant determinant of male reproductive ability [188]. Numerous sperm characteristics have been shown to vary with age, including decreased motility and morphology, increased DNA fragmentation, and changes in molecular and epigenetic profiles. Additionally, research using miRNA profiling has demonstrated that a significant portion of human miRNAs have expression variations impacted by both sex and age [189], indicating a possible mechanistic connection between reductions in reproductive function and age-related molecular changes.

Our research revealed no statistically significant relationship between paternal age and the expression levels of any of the validated miRNAs, which is in contrast to these previous results. None of the 16 miRNAs that were analyzed—including those that were most strongly linked to sperm quality and ART results in our cohort—exhibited a significant relationship with age ($r \leq 0.17$, $p > 0.1$). This suggests that in our young cohort (mean male age ~25.5 years), age-related miRNA alterations, if any, were negligible. Instead, these variations in expression were more closely associated with endocrine indicators, including serum FSH, LH, and β-hCG levels as well as clinical criteria that represent sperm function, such as sperm count, progressive motility, and normal morphology. The dysregulated miRNA patterns found in the thesis are more likely to represent continuing pathophysiological processes impacting spermatogenesis or sperm maturation than age-related decrease, as shown by their lack of relationship with paternal age.

Additionally, it is possible that reproductive endpoints like ART results, fertilization rates, and embryo morphological grade had a greater impact on the expression patterns that were found than age. Therefore, variation in sperm-borne miRNA expression seems to be more strongly associated with semen quality and reproductive outcome measures than with age within the relatively young age range of our cohort (21–30 years), indicating their potential utility as age-independent indicators of fertility status.

Several noteworthy patterns were identified by differential expression analysis of additional miRNAs in the cohort under study, many of which are consistent with previously documented relationships between certain miRNAs and reproductive outcomes in both natural and assisted conception situations. For instance, reduced hsa-miR-223 expression in embryo culture media has been demonstrated to be a possible risk factor for unfavorable IVF/ICSI results, underscoring its prognostic significance in ART settings [190]. This thesis provides further evidence for the possible significance of hsa-miR-223 as a predictive biomarker by showing that changed miR-223 expression was linked to inferior semen quality. Similarly, males with increased sperm DNA fragmentation—a measure closely associated with lower fertilization and pregnancy rates—have been demonstrated to have dysregulation of hsa-miR-424 [191]. The expression of *SPAG7*, a gene linked to sperm motility and function, has been shown to strongly correlate with this miRNA [177]. Both hsa-miR-424 and *SPAG7* levels have been found to be altered in seminal plasma and sperm from males with oligoasthenozoospermia, indicating the same molecular mechanism involving compromised motility [177].

Additionally, there was differential expression of hsa-miR-199a-5p and hsa-miR-99a-5p, which have both been identified as potential biomarkers for predicting pregnancy failure after Day 5 embryo development [192]. Defective flagellar formation during spermiogenesis has been experimentally linked to elevated hsa-miR-199a-5p expression, resulting in abnormal sperm morphology. This relationship has been confirmed in male allotriploid crucian carp [193] and is consistent with the negative correlations between hsa-miR-199a-5p expression and sperm morphology that we found in our dataset.

The highly conserved miRNA family miR-449 is essential for germ cell function because it stabilizes mRNAs needed for cilium formation [194]. Deletion of miR-449 loci causes oligoasthenoteratozoospermia in mice, highlighting its vital role in spermatogenesis [194]. Our results strengthen the relationship as lower progressive motility and lower embryo grades were associated with altered hsa-miR-449 expression in our sample.

In line with previous findings indicating a more extensive function for these miRNAs in the pathophysiology of male infertility, other miRNAs, including hsa-miR-16, hsa-miR-19a, and hsa-miR-15b, were also increased in our cohort's asthenozoospermia and oligoasthenozoospermia patients [149,150,155]. Additionally, it has been demonstrated that hsa-miR-106b-5p stimulates the proliferation of spermatogonial stem cells, suggesting possible therapeutic use in regenerative methods for male infertility [195].

Furthermore, hsa-miR-146a-5p exhibited expression patterns in our dataset that were in line with earlier research demonstrating greater abundance in testicular and/or epididymal tissue in obstructive azoospermia as opposed to secretory azoospermia, indicating its usefulness in distinguishing between azoospermia subtypes [196]. Finally, early embryonic gene expression, epigenetic modifications, and embryo development have all been associated with hsa-miR-16, a miRNA that is prevalent in both mature spermatozoa and embryo culture media [149,150,155,197]. It is an excellent candidate for more research in both diagnostic and mechanistic settings due to its prevalence throughout many reproductive compartments.

Furthermore, the polycistronic miR-17–92 cluster, a well-known regulator of germ cell proliferation, differentiation, and death, includes hsa-miR-19a-5p and hsa-miR-20a-5p [198]. Male infertility has been associated with dysregulation of this cluster; for instance, rodents with germline deletion of miR-17-92 exhibit oligozoospermia and severe motility abnormalities [199]. Our research found that low-quality sperm had higher levels of hsa-miR-19a and hsa-miR-20a, which might be a compensatory reaction to spermatogenic stress, impaired germ cell maturation, or changed post-testicular sperm remodeling processes that could affect embryogenesis and implantation competence.

Similar to this, abnormal sperm and male infertility have been connected to hsa-miR-15b-5p, a recognized regulator of apoptosis that directly targets anti-apoptotic genes like *BCL2*. According to Tomic et al., males with teratozoospermia had sperm with its downregulation [200], in line with its function in promoting the formation of healthy germ cells. On the other hand, our findings indicated that hsa-miR-15b-5p

was significantly upregulated in sperm of low quality. This disparity can be the result of variations in patient groups, underlying causes of infertility, or therapeutic settings. Overexpression in the samples we analyzed may indicate increased germ cell death, testicular stress, or abnormal post-meiotic regulatory mechanisms that are detrimental to the survival of the embryo.

These findings support and expand on earlier research that connected sperm miRNA patterns to the quality of embryos and the success of pregnancies. For instance, Abu-Halima et al. (2020) found that successful pregnancies were linked to reduced sperm levels of hsa-miR-19b-3p [183], an outcome consistent with our data for its paralog, hsa-miR-19a-5p. Some sperm-borne miRNAs may function as positive fertility indicators, while others, like those presented here, may function as negative predictors. Other research has associated particular miRNAs, such as miR-191-5p, with the development of top-grade embryos [201].

Our results are consistent with previous research showing a well-established correlation between miRNA expression and traditional semen quality metrics. According to Tomic et al., spermatozoa from males with teratozoospermia revealed substantially lower levels of nine miRNAs, including miR-15b-5p, than controls. These miRNAs were positively correlated with normal sperm morphology [200]. Our cohort exhibited the opposite pattern of overexpression in poor-quality sperm, whereas their study found decreased hsa-miR-15b-5p in abnormal sperm. This suggests that the direction of dysregulation may vary depending on the patient population, underlying pathology, or the stage at which miRNA alterations propagate their impact. Representatives of the polycistronic miR-17 family, miR-19a-5p and miR-20a-5p, are recognized regulators of stem cell differentiation and early mammalian development [202]. Additionally, hsa-miR-20a-5p, which comes from trophectoderm cells, has been found in spent blastocyst culture media, indicating a function in post-fertilization developmental processes and its possible use as a non-invasive biomarker of embryo competence [133]. The evidence supporting these miRNAs' transgenerational importance in reproductive capacity is strengthened by the fact that they are present in both sperm and embryo culture media.

A subgroup of sperm miRNAs, hsa-miR-15b-5p, hsa-miR-19a-5p, and hsa-miR-20a-5p, have also been demonstrated to be consistently overexpressed in samples with abnormal morphology, increased immotile sperm fractions, and decreased progressive motility. These miRNAs demonstrated substantial connections with less favorable embryo morphological grades, lower pregnancy success rates, and lower live birth outcomes. They also demonstrated strong negative correlations with traditional semen quality indicators and positive correlations with the fraction of immotile sperm. Importantly, even in the presence of ART, these three miRNAs continued to have predictive significance.

Our results also give credibility to the possibility of using miRNAs linked to seminal plasma and sperm as predictive indicators of successful pregnancies in assisted reproduction. Consistent with previous research, we found that, depending on the overall miRNA profile, hsa-miR-19a-5p expression levels varied considerably across sperm samples and were highly related to both successful and unsuccessful pregnancy outcomes [183]. Increased hsa-miR-19a-5p expression was associated with decreased progressive motility, abnormal morphology, inferior embryo grades, and lower live birth rates in our cohort, indicating that greater levels of this miRNA may function as a negative prognostic sign in ART.

Furthermore, hsa-miR-19b and hsa-miR-15b-5p have both been suggested as non-invasive indicators for identifying spermatogenesis impairment [150,182]. Our findings support previous studies by demonstrating that greater levels of hsa-miR-15b-5p and hsa-miR-19a-5p were linked to inferior semen parameters, such as lower sperm counts and motility, as well as larger percentages of immotile sperm. Interestingly, hsa-miR-19b-3p, a paralog of hsa-miR-19a-5p found in seminal plasma and spermatozoa, has been demonstrated to have decreased expression in samples associated with favorable pregnancy outcomes, which is consistent with our discovery that elevated hsa-miR-19a-5p levels were connected to less favorable clinical results [183].

Their expression levels may act as negative prognostic indicators, identifying sperm samples with a decreased capacity to support fertilization, normal embryonic

development, and implantation success. Receiver operating characteristic (ROC) analyses exhibited moderate-to-high diagnostic accuracy for IVF outcome prediction (AUC = 0.71–0.76). In order to increase predictive accuracy in ART and facilitate more individualized, evidence-based reproductive treatment planning, our results highlight the therapeutic significance of combining genetic biomarkers with traditional semen analysis.

Additionally, another member of the miR-17 family, hsa-miR-20a-5p, has been linked to the grading of embryos in spent culture media, exhibiting higher AUC values when differentiating between Grade 2 (G2) and Grade 3 (G3) embryos [183]. This supports our findings that lower pregnancy success rates and inferior embryo morphology (e.g., greater proportions of G2 over G1 embryos) were linked to increased hsa-miR-20a-5p expression in sperm. These results together support the idea that hsa-miR-20a-5p is a useful indicator of sperm quality and embryonic developmental potential.

These genetic markers, in particular hsa-miR-15b-5p, hsa-miR-19a/b, and hsa-miR-20a-5p, may improve the prediction of ART results and allow for personalized treatment approaches by including sperm-derived miRNA profiling into regular clinical assessment. Even when traditional semen characteristics seem acceptable, this method may be especially helpful in identifying couples who have a greater likelihood of experiencing poor embryo development or implantation failure.

Our sperm-borne small RNAs were discovered, and we conducted ROC curve studies for hsa-miR-15b-5p, hsa-miR-19a-5p, and hsa-miR-20a-5p to evaluate their diagnostic value. With AUC values ranging from 0.71 to 0.76, all three exhibited promising discriminative performance, showing strong sensitivity and specificity for differentiating successful from unsuccessful IVF cycles. These results are particularly significant considering our small sample size (n = 71 with verified outcomes), indicating that short RNA profiling has quantifiable predictive value for ART even at this early stage. Chen et al.'s recent study supports our findings by showing that combining miRNA expression patterns with traditional clinical criteria increased the accuracy of pregnancy outcome prediction (AUC ~0.85) when

compared to clinical data alone (~0.75) [203]. Similarly, Huang et al.'s meta-analysis found that small RNA biomarkers had a pooled AUC of 0.81 for predicting embryo implantation across many separate cohorts [204]. Furthermore, hsa-miR-20a was one of the most often found markers in research, which is consistent with our findings demonstrating its significant correlation with live birth rates, pregnancy outcome, and embryo morphology.

From a clinical standpoint, the development of a high-throughput diagnostic test, such as a RT-qPCR panel that targets harmful miRNAs (including hsa-miR-15b-5p, hsa-miR-19a/b, and hsa-miR-20a-5p), may mark a substantial breakthrough in the evaluation of male fertility. In actuality, such a panel may provide a composite "small RNA risk score," in which higher concentrations of certain miRNAs linked to poor semen would indicate a decreased likelihood of successful IVF. Individualized treatment plans, such as selecting ICSI over traditional IVF, putting preimplantation genetic testing into practice, or starting focused therapies like antioxidant supplements, might then be guided by this score. This approach is supported by our findings, which indicated that samples with reduced progressive motility, abnormal morphology, and higher immotile sperm fractions had significantly higher levels of hsa-miR-15b-5p, hsa-miR-19a-5p, and hsa-miR-20a-5p. These elevated levels were associated with lower embryo morphological grades, lower β-hCG positivity rates, and decreased live birth outcomes. AUC values of 0.71 to 0.76 indicated that ROC analysis exhibited moderate-to-high predictive accuracy for IVF success, underscoring their potential as prognostic indicators.

However, further validation will be necessary for clinical use. Variations in patient demographics, analytical tools, and RNA extraction techniques continue to be significant obstacles. To verify repeatability and clinical value, large-scale, multicenter studies and laboratory standardization will be crucial. Furthermore, whereas our correlation analyses indicate a high relationship between miRNA dysregulation and poor ART results and reduced semen characteristics, these correlations do not prove causality. To find out whether modifying sperm small RNA expression may directly improve embryonic development and pregnancy success,

mechanistic research like CRISPR-mediated gene editing or miRNA knockdown experiments in animal models will be required.

5. Conclusion

This research offers fresh perspectives on the connection between ART pregnancy outcomes, embryo development, and semen quality. We demonstrate that there is a high correlation between embryo developmental competence and clinical success rates and standard semen criteria, especially progressive motility and normal morphology. Top-grade embryos, higher implantation rates, and better pregnancy and live birth outcomes were consistently associated with higher sperm concentration, stronger progressive motility, and a larger percentage of morphologically normal sperm. On the other hand, reduced embryo quality, implantation failure, and miscarriage were correlated with decreased motility, abnormal morphology, and higher immotile sperm levels.

Additionally, we discovered three sperm-borne miRNAs whose expression levels were consistently linked to important reproductive parameters: hsa-miR-15b-5p, hsa-miR-19a-5p, and hsa-miR-20a-5p. Reduced β-hCG positive rates, inferior embryo morphology, decreased semen quality, and lower live birth outcomes were all associated with elevated levels of these miRNAs. Their prognostic potential was validated by ROC analysis, which revealed a moderate-to-high prediction accuracy for IVF success. These results underline their potential incorporation into reproductive evaluations to supplement conventional semen analysis and validate their function as negative prognostic indicators.

The findings provide additional evidence for the idea that sperm-borne miRNAs transport regulatory information outside of the paternal genome. Reduced developmental competence and compromised ART results may result from dysregulated expression of particular miRNAs (i.e., hsa-miR-15b-5p, hsa-miR-19a-5p, and hsa-miR-20a-5p), which may affect post-fertilization gene regulation in the early embryo. These findings are in line with mounting evidence that sperm contain molecular regulators that might affect early embryonic development and implantation potential in addition to the paternal genome, which they contribute to reproduction. This underlines the need of expanding the examination of male fertility

beyond routine semen analysis to include molecular-level tests that might identify subclinical abnormalities that could otherwise go undiagnosed.

Clinically, incorporating miRNA-based biomarkers into fertility assessments could improve prognostic accuracy for IVF and ICSI outcomes, detect subtle male-factor infertility in men with normal conventional semen parameters, and guide customized treatment plans, such as antioxidant therapy, ICSI selection, or preimplantation genetic testing when necessary.

Although the results of this research are convincing, standardization of analytical procedures throughout laboratories and validation in larger and more varied cohorts will be necessary for broader clinical applicability. Furthermore, mechanistic research is required to ascertain if altering the expression of these miRNAs might directly enhance the quality of embryos and reproductive outcomes.

This research concludes by highlighting the significance of molecular biomarkers and traditional semen characteristics in predicting the effectiveness of ART. By combining these complementary methods, medical professionals may evaluate male reproductive potential more precisely and individually, which will eventually benefit couples undergoing assisted reproduction.

6. References

1 World Health Organization. WHO laboratory manual for the examination and processing of human semen. Geneva, Switzerland: WHO; 2021.

2 Jungwirth, A. *et al.* European Association of Urology guidelines on Male Infertility: the 2012 update. *Eur Urol* **62**, 324-332, doi:10.1016/j.eururo.2012.04.048 (2012).

3 Minhas, S. *et al.* European Association of Urology Guidelines on Male Sexual and Reproductive Health: 2025 Update on Male Infertility. *Eur Urol* **87**, 601-616, doi:10.1016/j.eururo.2025.02.026 (2025).

4 Salonia, A. European Association of Urology Guidelines on Sexual and Reproductive Health-2021 Update: Male Sexual Dysfunction. *Eur Urol* **80**, 333–357, doi:10.1016/j.eururo.2021.06.007 (2021).

5 Corsini, C. *et al.* Is There a Relevant Clinical Impact in Differentiating Idiopathic versus Unexplained Male Infertility? *World J Mens Health* **41**, 354-362, doi:10.5534/wjmh.220069 (2023).

6 Vander Borght, M. & Wyns, C. Fertility and infertility: Definition and epidemiology. *Clin Biochem* **62**, 2-10, doi:10.1016/j.clinbiochem.2018.03.012 (2018).

7 Carson, S. A. & Kallen, A. N. Diagnosis and Management of Infertility: A Review. *JAMA* **326**, 65-76, doi:10.1001/jama.2021.4788 (2021).

8 Schmelz, H. U. S., Weidner, C. & W. *Facharztwissen Urologie*. Vol. 3 (Springer, 2014).

9 Jiao, S. Y., Yang, Y. H. & Chen, S. R. Molecular genetics of infertility: loss-of-function mutations in humans and corresponding knockout/mutated mice. *Hum Reprod Update* **27**, 154-189, doi:10.1093/humupd/dmaa034 (2021).

10 Pokhrel, G. *et al.* The impact of sociodemographic characteristics, lifestyle, work exposure and medical history on semen parameters in young Chinese men: A cross-sectional study. *Andrologia* **51**, e13324, doi:10.1111/and.13324 (2019).

11 Fronczak, C. M., Kim, E. D. & Barqawi, A. B. The insults of illicit drug use on male fertility. *J Androl* **33**, 515-528, doi:10.2164/jandrol.110.011874 (2012).

12 Nargund, V. H. Effects of psychological stress on male fertility. *Nat Rev Urol* **12**, 373-382, doi:10.1038/nrurol.2015.112 (2015).

13 Alahmar, A. T. Role of Oxidative Stress in Male Infertility: An Updated Review. *J Hum Reprod Sci* **12**, 4-18, doi:10.4103/jhrs.JHRS_150_18 (2019).

14 Miller, A. C. Vol. 117 1621–1627.

15 Sharma, A., Minhas, S., Dhillo, W. S. & Jayasena, C. N. Male infertility due to testicular disorders. *J Clin Endocrinol Metab* **106**, e442-e459, doi:10.1210/clinem/dgaa781 (2021).

16 Sharma, A. Male Infertility; Evidences, Risk Factors, Causes, Diagnosis and Management in Human. *Annals of Clinical and Laboratory Research* **5**, 5180 1000188–1005180 1000188.

17 Agarwal, A., Durairajanayagam, D. & du Plessis, S. S. Utility of antioxidants during assisted reproductive techniques: an evidence based review. *Reprod Biol Endocrinol* **12**, 112, doi:10.1186/1477-7827-12-112 (2014).

18 Houston, B. J. A systematic review of the validated monogenic causes of human male infertility: 2020 update and a discussion of emerging gene–disease relationships. *Human Reproduction Update* **00**, 1–15, doi:10.1093/HUMUPD/DMAB030.

19 Sharpe, R. M. & Irvine, D. S. How strong is the evidence of a link between environmental chemicals and adverse effects on human reproductive health? *Bmj* **328**, 447–451.

20 Skakkebaek, N. E., Rajpert-De Meyts, E. & Main, K. M. Testicular dysgenesis syndrome: an increasingly common developmental disorder with environmental aspects. *Human reproduction* **16**, 972–978.

21 Tuttelmann, F., Ruckert, C. & Ropke, A. Disorders of spermatogenesis: Perspectives for novel genetic diagnostics after 20 years of unchanged routine. *Med Genet* **30**, 12–20, doi:10.1007/s11825-018-0181-7 (2018).

22 Yu, X. W., Wei, Z. T., Jiang, Y. T. & Zhang, S. L. Y chromosome azoospermia factor region microdeletions and transmission characteristics in azoospermic and severe oligozoospermic patients. *Int J Clin Exp Med* **8**, 14634-14646 (2015).

23 Houston, B. J. *et al.* A systematic review of the validated monogenic causes of human male infertility: 2020 update and a discussion of emerging gene–disease relationships. *Human Reproduction Update* **00**, 1-15, doi:10.1093/HUMUPD/DMAB030.

24 Ferlin, A., Arredi, B. & Foresta, C. Genetic causes of male infertility. *Reprod Toxicol* **22**, 133-141, doi:10.1016/j.reprotox.2006.04.016 (2006).

25 Tuttelmann, F., Ruckert, C. & Ropke, A. Disorders of spermatogenesis: Perspectives for novel genetic diagnostics after 20 years of unchanged routine. *Med Genet* **30**, 12-20, doi:10.1007/s11825-018-0181-7 (2018).

26 Gatimel, N., Moreau, J., Parinaud, J. & Leandri, R. D. Sperm morphology: assessment, pathophysiology, clinical relevance, and state of the art in 2017. *Andrology* **5**, 845-862, doi:10.1111/andr.12389 (2017).

27 Guzick, D. S. *et al.* Sperm morphology, motility, and concentration in fertile and infertile men. *N Engl J Med* **345**, 1388-1393, doi:10.1056/NEJMoa003005 (2001).

28 Inaba, K. Molecular architecture of the sperm flagella: molecules for motility and signaling. *Zoolog Sci* **20**, 1043-1056, doi:10.2108/zsj.20.1043 (2003).

29 Gunes, S. & Esteves, S. C. Role of genetics and epigenetics in male infertility. *Andrologia* **53**, e13586, doi:10.1111/and.13586 (2021).

30 Khan, M. R. *et al.* Identifying potential genetic biomarkers for sperm dysfunction through whole-genome sequencing. *Sci Rep* **15**, 36476, doi:10.1038/s41598-025-23897-w (2025).

31 Krausz, C. & Riera-Escamilla, A. Genetics of male infertility. *Nat Rev Urol* **15**, 369-384, doi:10.1038/s41585-018-0003-3 (2018).

32 Wu, H. F. Ejaculatory duct obstruction. *Zhonghua Nan Ke Xue*.

33 Jarow, J. P., Espeland, M. A. & Lipshultz, L. I. Evaluation of the azoospermic patient. *The Journal of urology* **142**, 62–65.

34 Modgil, V., Rai, S., Ralph, D. J. & Muneer, A. An update on the diagnosis and management of ejaculatory duct obstruction. *Nat Rev Urol*, doi:10.1038/nrurol.2015.276.

35 Wosnitzer, M., Marc, G. & and Hardy, M. P. Review of Azoospermia. *Spermatogenesis* **4**, e28218-e28218, doi:10.4161/spmg.28218 (2014).

36 Paick, J., Kim, S. H. & Kim, S. W. Ejaculatory duct obstruction in infertile men. *BJU Int*, doi:10.1046/j.1464-410x.2000.00600.x.

37 Xu, B. *et al.* Novel methods for the diagnosis and treatment of ejaculatory duct obstruction. *BJU Int* **Jul;108(2):263-6**, doi:10.1111/j.1464-410X.2010.09775.x.

38 Palermo, G., Joris, H., Devroey, P. & Steirteghem, A. C. Pregnancies after intracytoplasmic injection of single spermatozoon into an oocyte. *Lancet* **340**, 8-8.

39 Sharlip, I. D. *et al.* Best practice policies for male infertility. *Fertil Steril* **77**, 873-882, doi:10.1016/s0015-0282(02)03105-9 (2002).

40 Tharakan, T., Luo, R., Jayasena, C. N. & Minhas, S. Non-obstructive azoospermia: current and future perspectives. *Fac Rev*, doi:10.12703/r/10-7.

41 Cerilli, L. A., Kuang, W. & Rogers, D. A practical approach to testicular biopsy interpretation for male infertility. *Archives of pathology & laboratory medicine* **134**, 1197–1204.

42 Gat, Y. *et al.* Azoospermia and Sertoli-cell-only syndrome: hypoxia in the sperm production site due to impairment in venous drainage of male reproductive system. *Andrologia* **42**, 314-321.

43 Vicdan, A. *et al.* Genetic aspects of human male infertility: the frequency of chromosomal abnormalities and Y chromosome microdeletions in severe male factor infertility. *European journal of obstetrics*.

44 Alkandari, M. H. & Zini, A. Medical management of non-obstructive azoospermia: A systematic review. *Arab Journal of Urology* **19**, 215–220, doi:10.1080/2090598X.2021.1956233 (2021).

45 Matzuk, M. M. & Lamb, D. J. The biology of infertility: research advances and clinical challenges. *Nat Med* **14**, 1197-1213, doi:10.1038/nm.f.1895 (2008).

46 Hamada, A. J., Esteves, S. C. & Agarwal, A. A comprehensive review of genetics and genetic testing in azoospermia. *Clinics (Sao Paulo)* **68 Suppl 1**, 39-60, doi:10.6061/clinics/2013(sup01)06 (2013).

47 Hotaling, J. & Carrell, D. T. Clinical genetic testing for male factor infertility: current applications and future directions. *Andrology* **2**, 339-350, doi:10.1111/j.2047-2927.2014.00200.x (2014).

48 Anguiano, A. *et al.* Congenital bilateral absence of the vas deferens. A primarily genital form of cystic fibrosis. *JAMA* **267**, 1794-1797 (1992).

49 Oud, M. S. *et al.* A systematic review and standardized clinical validity assessment of male infertility genes. *Hum Reprod* **34**, 932-941, doi:10.1093/humrep/dez022 (2019).

50 Bashamboo, A. *et al.* Human male infertility associated with mutations in NR5A1 encoding steroidogenic factor 1. *Am J Hum Genet* **87**, 505-512, doi:10.1016/j.ajhg.2010.09.009 (2010).

51 Ropke, A. *et al.* Comprehensive sequence analysis of the NR5A1 gene encoding steroidogenic factor 1 in a large group of infertile males. *Eur J Hum Genet* **21**, 1012-1015, doi:10.1038/ejhg.2012.290 (2013).

52 Yang, F. *et al.* TEX11 is mutated in infertile men with azoospermia and regulates genome-wide recombination rates in mouse. *EMBO Mol Med* **7**, 1198-1210, doi:10.15252/emmm.201404967 (2015).

53 Yatsenko, A. N. *et al.* X-linked TEX11 mutations, meiotic arrest, and azoospermia in infertile men. *N Engl J Med* **372**, 2097-2107, doi:10.1056/NEJMoa1406192 (2015).

54 Frainais, C. *et al.* RHOXF2 gene, a new candidate gene for spermatogenesis failure. *Basic Clin Androl* **24**, 3, doi:10.1186/2051-4190-24-3 (2014).

55 Borgmann, J. *et al.* The human RHOX gene cluster: target genes and functional analysis of gene variants in infertile men. *Hum Mol Genet* **25**, 4898-4910, doi:10.1093/hmg/ddw313 (2016).

56 Dieterich, K. *et al.* Homozygous mutation of AURKC yields large-headed polyploid spermatozoa and causes male infertility. *Nat Genet* **39**, 661-665, doi:10.1038/ng2027 (2007).

57 Pierre, V. *et al.* Absence of Dpy19l2, a new inner nuclear membrane protein, causes globozoospermia in mice by preventing the anchoring of the acrosome to the nucleus. *Development* **139**, 2955-2965, doi:10.1242/dev.077982 (2012).

58 Zuccarello, D. *et al.* Mutations in dynein genes in patients affected by isolated non-syndromic asthenozoospermia. *Hum Reprod* **23**, 1957-1962, doi:10.1093/humrep/den193 (2008).

59 Avenarius, M. R. *et al.* Human male infertility caused by mutations in the CATSPER1 channel protein. *Am J Hum Genet* **84**, 505-510, doi:10.1016/j.ajhg.2009.03.004 (2009).

60 Cooper, T. G. World Health Organization reference values for human semen characteristics. *Human Reproduction Update* **16**, 231–245, doi:10.1093/HUMUPD/DMP048.

61 Agarwal, A., Makker, K. & Sharma, R. Clinical relevance of oxidative stress in male factor infertility: An update. *American Journal of Reproductive Immunology* **59**, 2–11, doi:10.1111/J.1600-0897.2007.00559.X.

62 Abu-Halima, M. Altered microRNA expression profiles of human spermatozoa in patients with different spermatogenic impairments. *Fertility and sterility* **99**, 1249–1255 1216–1249–1255 1216, doi:10.1016/j.fertnstert.2012.11.054.

63 Abu-Halima, M. MicroRNA expression profiles in human testicular tissues of infertile men with different histopathologic patterns. *Fertility and Sterility* **101**, doi:10.1016/J.FERTNSTERT.2013.09.009.

64 Guyton, A. C. & Hall, J. E. *Textbook of Medical Physiology*. 11 edn, (Elsevier Saunders, 2006).

65 Suede, S. H., Malik, A. & Sapra, A. in *StatPearls* (2025).

66 de Kretser, D. M., Loveland, K. L., Meinhardt, A., Simorangkir, D. & Wreford, N. Spermatogenesis. *Hum Reprod* **13 Suppl 1**, 1-8, doi:10.1093/humrep/13.suppl_1.1 (1998).

67 Encyclopaedia Britannica, Inc. *Schematic representation of the male reproductive tract and spermatogenesis*. Encyclopaedia Britannica (2013). https://www.britannica.com

68 Cannarella, R., Condorelli, R. A., Mongioì, L. M., Vignera, S. & Calogero, A. E. Molecular biology of spermatogenesis: Novel targets of apparently idiopathic male infertility. *International Journal of Molecular Sciences* **21**, doi:10.3390/IJMS21051728.

69 Bergmann, M. Spermatogenese. Physiologie und pathophysiologie. *Urologe - Ausgabe A* **44**, 1131-1138, doi:10.1007/s00120-005-0909-2.

70 Misell, L. M. *et al.* A stable isotope-mass spectrometric method for measuring human spermatogenesis kinetics in vivo. *J Urol* **175**, 242-246; discussion 246, doi:10.1016/S0022-5347(05)00053-4 (2006).

71 Muciaccia, B. *et al.* Novel stage classification of human spermatogenesis based on acrosome development. *Biol Reprod* **89**, 60, doi:10.1095/biolreprod.113.111682 (2013).

72 Santi, D. *et al.* Clinical Medicine Follicle-Stimulating Hormone (FSH) Action on Spermatogenesis: A Focus on Physiological and Therapeutic Roles. *Journal of Clinical Medicine*, doi:10.3390/jcm9041014.

73 Servier Medical Art (https://smart.servier.com), licensed under CC BY 4.0 (https://creativecommons.org/licenses/by/4.0/)

74 Mattick, J. S. RNA regulation: a new genetics? *Nature reviews. Genetics* **5**, 316-323, doi:10.1038/nrg1321 (2004).

75 Krawetz, S. A. Paternal contribution: new insights and future challenges. *Nat Rev Genet* **6**, 633-642, doi:10.1038/nrg1654 (2005).

76 Ostermeier, G. C., Miller, D., Huntriss, J. D., Diamond, M. P. & Krawetz, S. A. Reproductive biology: delivering spermatozoan RNA to the oocyte. *Nature* **429**, 154, doi:10.1038/429154a (2004).

77 Kramer, J. A. & Krawetz, S. A. RNA in spermatozoa: implications for the alternative haploid genome. *Mol Hum Reprod* **3**, 473-478, doi:10.1093/molehr/3.6.473 (1997).

78 Miller, D. RNA in the ejaculate spermatozoon: a window into molecular events in spermatogenesis and a record of the unusual requirements of haploid gene expression and post-meiotic equilibration. *Mol Hum Reprod* **3**, 669-676, doi:10.1093/molehr/3.8.669 (1997).

79 Sendler, E. *et al.* Stability, delivery and functions of human sperm RNAs at fertilization. *Nucleic acids research* **41**, 4104-4117, doi:10.1093/nar/gkt132 (2013).

80 Ren, X., Chen, X., Wang, Z. & Wang, D. Is transcription in sperm stationary or dynamic? *J Reprod Dev* **63**, 439-443, doi:10.1262/jrd.2016-093 (2017).

81 Krawetz, S. A. *et al.* A survey of small RNAs in human sperm. *Hum Reprod* **26**, 3401-3412, doi:10.1093/humrep/der329 (2011).

82 Lalancette, C., Miller, D., Li, Y. & Krawetz, S. A. Paternal contributions: new functional insights for spermatozoal RNA. *J Cell Biochem* **104**, 1570-1579, doi:10.1002/jcb.21756 (2008).

83 Yan, W. *et al.* Birth of mice after intracytoplasmic injection of single purified sperm nuclei and detection of messenger RNAs and MicroRNAs in the sperm nuclei. *Biol Reprod* **78**, 896-902, doi:10.1095/biolreprod.107.067033 (2008).

84 Kutter, C. & Svoboda, P. miRNA, siRNA, piRNA: Knowns of the unknown. *RNA Biol* **5**, 181-188, doi:10.4161/rna.7227 (2008).

85 Bartel, D. P. MicroRNAs: target recognition and regulatory functions. *Cell* **136**, 215-233, doi:10.1016/j.cell.2009.01.002 (2009).

86 Lee, R. C., Feinbaum, R. L. & Ambros, V. The C. elegans heterochronic gene lin-4 encodes small RNAs with antisense complementarity to lin-14. *Cell* **75**, 843-854, doi:10.1016/0092-8674(93)90529-y (1993).

87 Wightman, B., Ha, I. & Ruvkun, G. Posttranscriptional regulation of the heterochronic gene lin-14 by lin-4 mediates temporal pattern formation in C. elegans. *Cell* **75**, 855-862, doi:10.1016/0092-8674(93)90530-4 (1993).

88 Pasquinelli, A. E. *et al.* Conservation of the sequence and temporal expression of let-7 heterochronic regulatory RNA. *Nature* **408**, 86-89, doi:10.1038/35040556 (2000).

89 Lagos-Quintana, M., Rauhut, R., Lendeckel, W. & Tuschl, T. Identification of novel genes coding for small expressed RNAs. *Science* **294**, 853-858, doi:10.1126/science.1064921 (2001).

90 Lau, N. C., Lim, L. P., Weinstein, E. G. & Bartel, D. P. An abundant class of tiny RNAs with probable regulatory roles in Caenorhabditis elegans. *Science* **294**, 858-862, doi:10.1126/science.1065062 (2001).

91 Kozomara, A., Birgaoanu, M. & Griffiths-Jones, S. miRBase: from microRNA sequences to function. *Nucleic Acids Res* **47**, D155-D162, doi:10.1093/nar/gky1141 (2019).

92 Alles, J. *et al.* An estimate of the total number of true human miRNAs. *Nucleic Acids Res* **47**, 3353-3364, doi:10.1093/nar/gkz097 (2019).

93 Saliminejad, K., Khorram Khorshid, H. R., Soleymani Fard, S. & Ghaffari, S. H. An overview of microRNAs: Biology, functions, therapeutics, and analysis methods. *J Cell Physiol* **234**, 5451-5465, doi:10.1002/jcp.27486 (2019).

94 Etheridge, A., Lee, I., Hood, L., Galas, D. & Wang, K. Extracellular microRNA: a new source of biomarkers. *Mutat Res* **717**, 85-90, doi:10.1016/j.mrfmmm.2011.03.004 (2011).

95 Bartel, D. P. MicroRNAs: genomics, biogenesis, mechanism, and function. *Cell* **116**, 281-297, doi:10.1016/s0092-8674(04)00045-5 (2004).

96 Ambros, V. *et al.* A uniform system for microRNA annotation. *RNA* **9**, 277-279, doi:10.1261/rna.2183803 (2003).

97 Ruby, J. G., Jan, C. H. & Bartel, D. P. Intronic microRNA precursors that bypass Drosha processing. *Nature* **448**, 83-86, doi:10.1038/nature05983 (2007).

98 Garzon, R., Calin, G. A. & Croce, C. M. MicroRNAs in Cancer. *Annu Rev Med* **60**, 167-179, doi:10.1146/annurev.med.59.053006.104707 (2009).

99 Wang, Z. MicroRNA: A matter of life or death. *World J Biol Chem* **1**, 41-54, doi:10.4331/wjbc.v1.i4.41 (2010).

100 O'Donnell, K. A., Wentzel, E. A., Zeller, K. I., Dang, C. V. & Mendell, J. T. c-Myc-regulated microRNAs modulate E2F1 expression. *Nature* **435**, 839-843, doi:10.1038/nature03677 (2005).

101 Ozsolak, F. *et al.* Chromatin structure analyses identify miRNA promoters. *Genes Dev* **22**, 3172-3183, doi:10.1101/gad.1706508 (2008).

102 Bartel, D. P. Metazoan MicroRNAs. *Cell* **173**, 20-51, doi:10.1016/j.cell.2018.03.006 (2018).

103 Lee, Y. *et al.* MicroRNA genes are transcribed by RNA polymerase II. *EMBO J* **23**, 4051-4060, doi:10.1038/sj.emboj.7600385 (2004).

104 Lee, Y. *et al.* The nuclear RNase III Drosha initiates microRNA processing. *Nature* **425**, 415-419, doi:10.1038/nature01957 (2003).

105 Lund, E., Guttinger, S., Calado, A., Dahlberg, J. E. & Kutay, U. Nuclear export of microRNA precursors. *Science* **303**, 95-98, doi:10.1126/science.1090599 (2004).

106 Bernstein, E., Caudy, A. A., Hammond, S. M. & Hannon, G. J. Role for a bidentate ribonuclease in the initiation step of RNA interference. *Nature* **409**, 363-366, doi:10.1038/35053110 (2001).

107 Grishok, A. *et al.* Genes and mechanisms related to RNA interference regulate expression of the small temporal RNAs that control C. elegans developmental timing. *Cell* **106**, 23-34, doi:10.1016/s0092-8674(01)00431-7 (2001).

108 Hutvagner, G. *et al.* A cellular function for the RNA-interference enzyme Dicer in the maturation of the let-7 small temporal RNA. *Science* **293**, 834-838, doi:10.1126/science.1062961 (2001).

109 Iwasaki, S. *et al.* Hsc70/Hsp90 chaperone machinery mediates ATP-dependent RISC loading of small RNA duplexes. *Mol Cell* **39**, 292-299, doi:10.1016/j.molcel.2010.05.015 (2010).

110 Kawamata, T. & Tomari, Y. Making RISC. *Trends Biochem Sci* **35**, 368-376, doi:10.1016/j.tibs.2010.03.009 (2010).

111 Frank, F., Sonenberg, N. & Nagar, B. Structural basis for 5'-nucleotide base-specific recognition of guide RNA by human AGO2. *Nature* **465**, 818-822, doi:10.1038/nature09039 (2010).

112 Suzuki, H. I. *et al.* Small-RNA asymmetry is directly driven by mammalian Argonautes. *Nat Struct Mol Biol* **22**, 512-521, doi:10.1038/nsmb.3050 (2015).

113 Ameres, S. L. *et al.* Target RNA-directed trimming and tailing of small silencing RNAs. *Science* **328**, 1534-1539, doi:10.1126/science.1187058 (2010).

114 Bail, S. *et al.* Differential regulation of microRNA stability. *RNA* **16**, 1032-1039, doi:10.1261/rna.1851510 (2010).

115 Gantier, M. P. *et al.* Analysis of microRNA turnover in mammalian cells following Dicer1 ablation. *Nucleic Acids Res* **39**, 5692-5703, doi:10.1093/nar/gkr148 (2011).

116 Meister, G. *et al.* Human Argonaute2 mediates RNA cleavage targeted by miRNAs and siRNAs. *Mol Cell* **15**, 185-197, doi:10.1016/j.molcel.2004.07.007 (2004).

117 Yekta, S., Shih, I. H. & Bartel, D. P. MicroRNA-directed cleavage of HOXB8 mRNA. *Science* **304**, 594-596, doi:10.1126/science.1097434 (2004).

118 Shirai, Y. T., Suzuki, T., Morita, M., Takahashi, A. & Yamamoto, T. Multifunctional roles of the mammalian CCR4-NOT complex in physiological phenomena. *Front Genet* **5**, 286, doi:10.3389/fgene.2014.00286 (2014).

119 Jonas, S. & Izaurralde, E. Towards a molecular understanding of microRNA-mediated gene silencing. *Nat Rev Genet* **16**, 421-433, doi:10.1038/nrg3965 (2015).

120 Chen, C. Y. & Shyu, A. B. Mechanisms of deadenylation-dependent decay. *Wiley Interdiscip Rev RNA* **2**, 167-183, doi:10.1002/wrna.40 (2011).

121 Eichhorn, S. W. *et al.* mRNA destabilization is the dominant effect of mammalian microRNAs by the time substantial repression ensues. *Mol Cell* **56**, 104-115, doi:10.1016/j.molcel.2014.08.028 (2014).

122 Djuranovic, S., Nahvi, A. & Green, R. miRNA-mediated gene silencing by translational repression followed by mRNA deadenylation and decay. *Science* **336**, 237-240, doi:10.1126/science.1215691 (2012).

123 Lewis, B. P., Burge, C. B. & Bartel, D. P. Conserved seed pairing, often flanked by adenosines, indicates that thousands of human genes are microRNA targets. *Cell* **120**, 15-20, doi:10.1016/j.cell.2004.12.035 (2005).

124 Salomon, W. E., Jolly, S. M., Moore, M. J., Zamore, P. D. & Serebrov, V. Single-Molecule Imaging Reveals that Argonaute Reshapes the Binding Properties of Its Nucleic Acid Guides. *Cell* **162**, 84-95, doi:10.1016/j.cell.2015.06.029 (2015).

125 Parker, J. S., Roe, S. M. & Barford, D. Structural insights into mRNA recognition from a PIWI domain-siRNA guide complex. *Nature* **434**, 663-666, doi:10.1038/nature03462 (2005).

126 Gapp, K. *et al.* Implication of sperm RNAs in transgenerational inheritance of the effects of early trauma in mice. *Nature neuroscience* **17**, 667-669, doi:10.1038/nn.3695 (2014).

127 Amanai, M., Brahmajosyula, M. & Perry, A. C. A restricted role for sperm-borne microRNAs in mammalian fertilization. *Biol Reprod* **75**, 877-884, doi:10.1095/biolreprod.106.056499 (2006).

128 Rassoulzadegan, M. *et al.* RNA-mediated non-mendelian inheritance of an epigenetic change in the mouse. *Nature* **441**, 469-474, doi:10.1038/nature04674 (2006).

129 Ostermeier, G. C., Goodrich, R. J., Moldenhauer, J. S., Diamond, M. P. & Krawetz, S. A. A suite of novel human spermatozoal RNAs. *J Androl* **26**, 70-74 (2005).

130 Giraldez, A. J. *et al.* Zebrafish MiR-430 promotes deadenylation and clearance of maternal mRNAs. *Science* **312**, 75-79, doi:10.1126/science.1122689 (2006).

131 Wang, J. Y., Lan, J., Zhao, J., Chen, L. & Liu, Y. Molecular characterization, polymorphism and association of porcine SPATA19 gene. *Mol Biol Rep* **39**, 9741-9746, doi:10.1007/s11033-012-1839-x (2012).

132 Abu-Halima, M. *et al.* Micro-ribonucleic acids and extracellular vesicles repertoire in the spent culture media is altered in women undergoing In Vitro Fertilization. *Sci Rep* **7**, 13525, doi:10.1038/s41598-017-13683-8 (2017).

133 Capalbo, A. *et al.* MicroRNAs in spent blastocyst culture medium are derived from trophectoderm cells and can be explored for human embryo reproductive competence assessment. *Fertil Steril* **105**, 225-235 e221-223, doi:10.1016/j.fertnstert.2015.09.014 (2016).

134 Kropp, J. & Khatib, H. mRNA fragments in in vitro culture media are associated with bovine preimplantation embryonic development. *Frontiers in genetics* **6**, 273, doi:10.3389/fgene.2015.00273 (2015).

135 Kropp, J., Salih, S. M. & Khatib, H. Expression of microRNAs in bovine and human pre-implantation embryo culture media. *Front Genet* **5**, 91, doi:10.3389/fgene.2014.00091 (2014).

136 Rosenbluth, E. M., Shelton, D. N., Wells, L. M., Sparks, A. E. & Van Voorhis, B. J. Human embryos secrete microRNAs into culture media--a potential biomarker for implantation. *Fertil Steril* **101**, 1493-1500, doi:10.1016/j.fertnstert.2014.01.058 (2014).

137 Batiha, O. *et al.* Gene expression alterations in testicular biopsies from males with spermatogenesis arrest identified by transcriptome analysis. *PLoS One* **20**, e0332025, doi:10.1371/journal.pone.0332025 (2025).

138 Lian, J. *et al.* Altered microRNA expression in patients with non-obstructive azoospermia. *Reprod Biol Endocrinol* **7**, 13, doi:10.1186/1477-7827-7-13 (2009).

139 Wang, C. *et al.* Altered profile of seminal plasma microRNAs in the molecular diagnosis of male infertility. *Clin Chem* **57**, 1722-1731, doi:10.1373/clinchem.2011.169714 (2011).

140 Wu, W. *et al.* Seminal plasma microRNAs: potential biomarkers for spermatogenesis status. *Mol Hum Reprod* **18**, 489-497, doi:10.1093/molehr/gas022 (2012).
141 Wu, W. *et al.* Genome-wide microRNA expression profiling in idiopathic non-obstructive azoospermia: significant up-regulation of miR-141, miR-429 and miR-7-1-3p. *Hum Reprod* **28**, 1827-1836, doi:10.1093/humrep/det099 (2013).
142 Liu, T., Cheng, W., Gao, Y., Wang, H. & Liu, Z. Microarray analysis of microRNA expression patterns in the semen of infertile men with semen abnormalities. *Mol Med Rep* **6**, 535-542, doi:10.3892/mmr.2012.967 (2012).
143 Zhou, Q. Z. *et al.* Expressions of miR-525-3p and its target gene SEMG1 in the spermatozoa of patients with asthenozoospermia. *Andrology*, doi:10.1111/andr.12573 (2018).
144 Zhou, J. H. *et al.* MicroRNA-27a-mediated repression of cysteine-rich secretory protein 2 translation in asthenoteratozoospermic patients. *Asian J Androl* **19**, 591-595, doi:10.4103/1008-682X.185001 (2017).
145 Zhou, J. H. *et al.* The expression of cysteine-rich secretory protein 2 (CRISP2) and its specific regulator miR-27b in the spermatozoa of patients with asthenozoospermia. *Biol Reprod* **92**, 28, doi:10.1095/biolreprod.114.124487 (2015).
146 Ji, Z. *et al.* Expressions of miR-15a and its target gene HSPA1B in the spermatozoa of patients with varicocele. *Reproduction* **147**, 693-701, doi:10.1530/REP-13-0656 (2014).
147 Vojtech, L. *et al.* Exosomes in human semen carry a distinctive repertoire of small non-coding RNAs with potential regulatory functions. *Nucleic acids research* **42**, 7290-7304, doi:10.1093/nar/gku347 (2014).
148 Belleannee, C. Extracellular microRNAs from the epididymis as potential mediators of cell-to-cell communication. *Asian J Androl* **17**, 730-736, doi:10.4103/1008-682X.155532 (2015).
149 Abu-Halima, M. *et al.* Altered micro-ribonucleic acid expression profiles of extracellular microvesicles in the seminal plasma of patients with oligoasthenozoospermia. *Fertil Steril* **106**, 1061-1069 e1063, doi:10.1016/j.fertnstert.2016.06.030 (2016).
150 Abu-Halima, M. *et al.* Altered microRNA expression profiles of human spermatozoa in patients with different spermatogenic impairments. *Fertil Steril* **99**, 1249-1255 e1216, doi:10.1016/j.fertnstert.2012.11.054 (2013).
151 Kosaka, N. *et al.* Secretory mechanisms and intercellular transfer of microRNAs in living cells. *J Biol Chem* **285**, 17442-17452, doi:10.1074/jbc.M110.107821 (2010).
152 Valadi, H. *et al.* Exosome-mediated transfer of mRNAs and microRNAs is a novel mechanism of genetic exchange between cells. *Nat Cell Biol* **9**, 654-659, doi:10.1038/ncb1596 (2007).

153 Wang, K., Zhang, S., Weber, J., Baxter, D. & Galas, D. J. Export of microRNAs and microRNA-protective protein by mammalian cells. *Nucleic acids research* **38**, 7248-7259, doi:10.1093/nar/gkq601 (2010).

154 Salas-Huetos, A. *et al.* The role of miRNAs in male human reproduction: a systematic review. *Andrology*, doi:10.1111/andr.12714 (2019).

155 Abu-Halima, M. *et al.* MicroRNA expression profiles in human testicular tissues of infertile men with different histopathologic patterns. *Fertil Steril* **101**, 78-86 e72, doi:10.1016/j.fertnstert.2013.09.009 (2014).

156 Abu-Halima, M. *et al.* Panel of five microRNAs as potential biomarkers for the diagnosis and assessment of male infertility. *Fertil Steril* **102**, 989-997 e981, doi:10.1016/j.fertnstert.2014.07.001 (2014).

157 Abu-Halima, M. *et al.* Differential expression of miR-23a/b-3p and its target genes in male patients with subfertility. *Fertil Steril*, doi:10.1016/j.fertnstert.2019.03.025 (2019).

158 Abu-Halima, M. *et al.* Single Sperm RNA signatures reveal MicroRNA biomarkers for male subfertility. *J Assist Reprod Genet* **41**, 3119-3132, doi:10.1007/s10815-024-03264-w (2024).

159 Abu-Halima, M. *et al.* Altered micro-ribonucleic acid expression profiles of extracellular microvesicles in the seminal plasma of patients with oligoasthenozoospermia. *Fertility and sterility*, doi:10.1016/j.fertnstert.2016.06.030 (2016).

160 Jin, X. *et al.* Survey of the situation of infertile women seeking in vitro fertilization treatment in China. *Biomed Res Int* **2013**, 179098, doi:10.1155/2013/179098 (2013).

161 Bühler K, B.-P. M., Blumenauer V, Dahncke W, Felberbaum R, Fiedler K, Gnoth C, Happel L, Krüssel JS, Kupka MS, Wendelken M. DIR Annual 2011. *Journal für Reproduktionsmedizin und Endokrinologie* **9**, 453-484 (2012).

162 Beyer, D. A. a. K. D. *Bewertung von Eizellen und Embryonen, in Reproduktionsmedizin*. 225-231 (Springer, 2013).

163 Blumenauer V, C. U., Fiedler K, Gnoth C, Happel L, Krüssel JS, Kupka MS, Tandler-Schneider A. DIR Annual 2013 - German IVF-Registry. *J Reproduktionsmed Endokrinol* **11**, 236-273 (2014).

164 Yuan, S. *et al.* Sperm-borne miRNAs and endo-siRNAs are important for fertilization and preimplantation embryonic development. *Development* **143**, 635-647, doi:10.1242/dev.131755 (2016).

165 Mohammad A. Al Smadi, H. H., Albert Salas-Huetos , Ulrike Fischer, Hashim Abdul-Khaliq , Eckart Meese , Masood Abu-Halima. Small RNA sequencing in individually selected sperm: Biomarkers for male subfertility and predictors of pregnancy success. *Non-coding RNA Research* **16**, 126-143, doi:https://doi.org/10.1016/j.ncrna.2025.09.008 (2025).

166 Benjamini, Y. & Hochberg, Y. Controlling the False Discovery Rate: A Practical and Powerful Approach to Multiple Testing. *Journal of the Royal Statistical Society: Series B (Methodological)* **57**, 289–300, doi:10.1111/j.2517-6161.1995.tb02031.x (1995).

167 Al Smadi, M. A. *et al.* Small RNA sequencing in individually selected sperm: Biomarkers for male subfertility and predictors of pregnancy success. *Noncoding RNA Res* **16**, 126-143, doi:10.1016/j.ncrna.2025.09.008 (2026).

168 Naghi, P. *et al.* Teratozoospermia and Embryo Development: The Significance of Sperm Selection in In Vitro Fertilization Success. *J Clin Med* **14**, doi:10.3390/jcm14113763 (2025).

169 Villani, M. T. *et al.* Are sperm parameters able to predict the success of assisted reproductive technology? A retrospective analysis of over 22,000 assisted reproductive technology cycles. *Andrology* **10**, 310-321, doi:10.1111/andr.13123 (2022).

170 Dcunha, R. *et al.* Current Insights and Latest Updates in Sperm Motility and Associated Applications in Assisted Reproduction. *Reprod Sci* **29**, 7-25, doi:10.1007/s43032-020-00408-y (2022).

171 Liu, Z. *et al.* Associations between male reproductive characteristics and the outcome of assisted reproductive technology (ART). *Biosci Rep* **37**, doi:10.1042/BSR20170095 (2017).

172 Sahin, G. *et al.* In-Vitro Fertilization Outcome Predictors in Women With High Baseline Follicle-Stimulating Hormone Levels: Analysis of Over 1000 Cycles From A Tertiary Center. *JBRA Assist Reprod* **25**, 235-241, doi:10.5935/1518-0557.20200088 (2021).

173 Ocal, P. *et al.* Recurrent implantation failure is more frequently seen in female patients with poor prognosis. *Int J Fertil Steril* **6**, 71-78 (2012).

174 Agarwal, A., Majzoub, A., Parekh, N. & Henkel, R. A Schematic Overview of the Current Status of Male Infertility Practice. *World J Mens Health* **38**, 308-322, doi:10.5534/wjmh.190068 (2020).

175 Lewis, S. E. Is sperm evaluation useful in predicting human fertility? *Reproduction* **134**, 31-40, doi:10.1530/REP-07-0152 (2007).

176 Abu-Halima, M. *et al.* Sperm Motility Annotated Genes: Are They Associated with Impaired Fecundity? *Cells* **12**, doi:10.3390/cells12091239 (2023).

177 Abu-Halima, M. *et al.* Expression of SPAG7 and its regulatory microRNAs in seminal plasma and seminal plasma-derived extracellular vesicles of patients with subfertility. *Sci Rep* **13**, 3645, doi:10.1038/s41598-023-30744-3 (2023).

178 Abu-Halima, M. *et al.* Differential expression of miR-23a/b-3p and its target genes in male patients with subfertility. *Fertil Steril* **112**, 323-335 e322, doi:10.1016/j.fertnstert.2019.03.025 (2019).

179 Abu-Halima, M., Becker, L. S., Ayesh, B. M. & Meese, E. MicroRNA-targeting in male infertility: Sperm microRNA-19a/b-3p and its spermatogenesis related transcripts content in men with oligoasthenozoospermia. *Front Cell Dev Biol* **10**, 973849, doi:10.3389/fcell.2022.973849 (2022).

180 Abu-Halima, M. *et al.* MicroRNA-targeting in spermatogenesis: Over-expressions of microRNA-23a/b-3p and its affected targeting of the genes ODF2 and UBQLN3 in spermatozoa of patients with oligoasthenozoospermia. *Andrology*, doi:10.1111/andr.13004 (2021).

181 Abu-Halima, M. *et al.* Single Sperm RNA signatures reveal MicroRNA biomarkers for male subfertility. *J Assist Reprod Genet*, doi:10.1007/s10815-024-03264-w (2024).

182 Abu-Halima, M. *et al.* MicroRNA signature in spermatozoa and seminal plasma of proven fertile men and in testicular tissue of men with obstructive azoospermia. *Andrologia* **52**, e13503, doi:10.1111/and.13503 (2020).

183 Abu-Halima, M. *et al.* MicroRNAs in combined spent culture media and sperm are associated with embryo quality and pregnancy outcome. *Fertil Steril* **113**, 970-980 e972, doi:10.1016/j.fertnstert.2019.12.028 (2020).

184 Sharma, U. *et al.* Biogenesis and function of tRNA fragments during sperm maturation and fertilization in mammals. *Science* **351**, 391-396, doi:10.1126/science.aad6780 (2016).

185 Joshi, M., Sethi, S., Mehta, P., Kumari, A. & Rajender, S. Small RNAs, spermatogenesis, and male infertility: a decade of retrospect. *Reprod Biol Endocrinol* **21**, 106, doi:10.1186/s12958-023-01155-w (2023).

186 Vallet-Buisan, M., Mecca, R., Jones, C., Coward, K. & Yeste, M. Contribution of semen to early embryo development: fertilization and beyond. *Hum Reprod Update* **29**, 395-433, doi:10.1093/humupd/dmad006 (2023).

187 Castillo, J., Jodar, M. & Oliva, R. The contribution of human sperm proteins to the development and epigenome of the preimplantation embryo. *Hum Reprod Update* **24**, 535-555, doi:10.1093/humupd/dmy017 (2018).

188 Jimbo, M. *et al.* Fertility in the aging male: a systematic review. *Fertil Steril* **118**, 1022-1034, doi:10.1016/j.fertnstert.2022.10.035 (2022).

189 Meder, B. *et al.* Influence of the confounding factors age and sex on microRNA profiles from peripheral blood. *Clin Chem* **60**, 1200-1208, doi:10.1373/clinchem.2014.224238 (2014).

190 Song, Q. *et al.* Prognostic value of miR-223 for pregnancy outcomes in patients with in vitro fertilisation and intracytoplasmic sperm injection. *J Obstet Gynaecol* **44**, 2368773, doi:10.1080/01443615.2024.2368773 (2024).

191 Zhao, K. *et al.* miR-424/322 is downregulated in the semen of patients with severe DNA damage and may regulate sperm DNA damage. *Reprod Fertil Dev*, doi:10.1071/RD15052 (2015).

192 Wang, S., Chen, L., Zhu, Y. & Jiang, W. Characterization of microRNAs in spent culture medium associated with human embryo quality and development. *Ann Transl Med* **9**, 1648, doi:10.21037/atm-21-5029 (2021).

193 Li, S. *et al.* miR-199-5p regulates spermiogenesis at the posttranscriptional level via targeting Tekt1 in allotriploid crucian carp. *J Anim Sci Biotechnol* **13**, 44, doi:10.1186/s40104-022-00693-4 (2022).

194 Comazzetto, S. *et al.* Oligoasthenoteratozoospermia and infertility in mice deficient for miR-34b/c and miR-449 loci. *PLoS Genet* **10**, e1004597, doi:10.1371/journal.pgen.1004597 (2014).

195 Hasani Fard, A. H., Valizadeh, M., Mazaheri, Z. & Hosseini, S. J. miR-106b-5p Intensifies the Proliferative Potential of Spermatogonial Stem Cells as a

Prerequisite for Male Infertility Treatment. *Reprod Sci* **29**, 3394-3403, doi:10.1007/s43032-022-00884-4 (2022).

196 Larriba, S. *et al.* Seminal extracellular vesicle sncRNA sequencing reveals altered miRNA/isomiR profiles as sperm retrieval biomarkers for azoospermia. *Andrology* **12**, 137-156, doi:10.1111/andr.13461 (2024).

197 Kiani, M., Salehi, M., Mogheiseh, A., Mohammadi-Yeganeh, S. & Shahidi, S. The Effect of Increased miR-16-1 Levels in Mouse Embryos on Epigenetic Modification, Target Gene Expression, and Developmental Processes. *Reprod Sci* **27**, 2197-2210, doi:10.1007/s43032-020-00240-4 (2020).

198 Hurtado, A. *et al.* Deficiency of the onco-miRNA cluster, miR-106b approximately 25, causes oligozoospermia and the cooperative action of miR-106b approximately 25 and miR-17 approximately 92 is required to maintain male fertility. *Mol Hum Reprod* **26**, 389-401, doi:10.1093/molehr/gaaa027 (2020).

199 Tong, M. H., Mitchell, D. A., McGowan, S. D., Evanoff, R. & Griswold, M. D. Two miRNA clusters, Mir-17-92 (Mirc1) and Mir-106b-25 (Mirc3), are involved in the regulation of spermatogonial differentiation in mice. *Biol Reprod* **86**, 72, doi:10.1095/biolreprod.111.096313 (2012).

200 Tomic, M. *et al.* Association between Sperm Morphology and Altered Sperm microRNA Expression. *Biology (Basel)* **11**, doi:10.3390/biology11111671 (2022).

201 Xu, H. *et al.* MicroRNA expression profile analysis in sperm reveals hsa-mir-191 as an auspicious omen of in vitro fertilization. *BMC Genomics* **21**, 165, doi:10.1186/s12864-020-6570-8 (2020).

202 Foshay, K. M. & Gallicano, G. I. miR-17 family miRNAs are expressed during early mammalian development and regulate stem cell differentiation. *Dev Biol* **326**, 431-443, doi:10.1016/j.ydbio.2008.11.016 (2009).

203 Chen, L., Jiang, R., Jiang, Y., Su, Y. & Wang, S. A validated model for individualized prediction of pregnancy outcome in woman after fresh cycle of Day 5 single blastocyst transfer. *Sci Rep* **13**, 10016, doi:10.1038/s41598-023-36824-8 (2023).

204 Huang, W., Chen, A. C. H., Ng, E. H. Y., Yeung, W. S. B. & Lee, Y. L. Non-Coding RNAs as Biomarkers for Embryo Quality and Pregnancy Outcomes: A Systematic Review and Meta-Analysis. *Int J Mol Sci* **24**, doi:10.3390/ijms24065751 (2023).

7. Publications

Al Smadi MA, **Haidar H**, Salas-Huetos A, Fischer U, Abdul-Khaliq H, Meese E, Abu-Halima M. Small RNA sequencing in individually selected sperm: Biomarkers for male subfertility and predictors of pregnancy success. Noncoding RNA Res 2026;16:126-43.

8. Acknowledgments

My heartfelt thanks go to **PD Dr. Masood Abu-Halima** for his dedicated supervision and extensive assistance throughout the experimental stages of this thesis. His practical guidance in the laboratory, insightful discussions, continuous support, and valuable input in structuring and writing the thesis greatly contributed to the quality of this work. I am sincerely appreciative of his commitment, patience, and willingness to share his expertise throughout the entire research process.

I would also like to express my sincere gratitude to **Prof. Dr. Eckart Meese** for allowing me access to the laboratory and supporting the use of all necessary facilities required for this research. His support in providing the infrastructure and resources made it possible to successfully conduct the experimental work of this thesis.

I would like to express my sincere thanks to **PD Dr. med. Ralph E. Eckert** at the Center for Urology, Andrology, and Urological Oncology, MVZ GmbH, for his personal and collegial support.

Finally, I am deeply grateful to my wife, my parents, my parents-in-law, and my brothers for their constant encouragement, motivation, and unwavering support. Their understanding and patience, especially during the more challenging phases of this thesis, have been essential, and I am truly thankful for their presence in my life.

Aus datenschutzrechtlichen Gründen wird der Lebenslauf in der elektronischen Fassung der Dissertation nicht veröffentlicht.